



Norwegian University of
Science and Technology

Superstructure Optimization of Early Stage Offshore Oil Field Development with Subsea Processing

Dag Svenningsson Krogstad

Chemical Engineering and Biotechnology

Submission date: June 2018

Supervisor: Johannes Jäschke, IKP

Norwegian University of Science and Technology
Department of Chemical Engineering

Abstract

The oil and gas industry has been subject to a series of challenges during the last couple of decades, including increased water depths, step-out distances and harsher environmental and operational conditions. This has caused a need for new innovative ideas and solutions, which has resulted in increased attention to the development of subsea processing. The main objective of this thesis has been to develop a mixed integer nonlinear programming (MINLP)-model for optimizing the planning and development of offshore oil field infrastructure with an integrated subsea separation system for each field.

First, a MINLP-model was developed for a single field connected to a floating production storage and offloading (FPSO) unit with subsea processing. The objective of the optimization was to identify the set of subsea processing units that maximized the net present value over the given time horizon. A superstructure including all potentially useful units and interconnections was generated and used as a basis for the optimization model. Binary variables were assigned to each of the potential units to represent the installation of the unit in the optimal solution, while continuous variables were used for the mass flows, pressures, costs and sizing variables. The proposed constraints of the model included mass balances, logical conditions related to the binary variables, as well as sizing and cost estimation equations.

The single-field model was extended to include multiple fields and FPSOs, as well as time scheduling of the installations and drilling over the time horizon. The objectives of this multi-field model included determining the FPSOs to be installed, the fields to be developed, the number of wells to be drilled in each field in each time step, the production rates of the fields, as well as the installation of subsea equipment in each of the fields developed. The superstructure that was developed for the single-field model was used to optimize the configuration of the subsea systems of each of the developed fields in the multi-field model.

Both the single-field and the multi-field model were implemented in the high-level mathematical optimization system GAMS (General Algebraic Modeling System). The models were then solved for different cases on the NEOS-server for numerical optimization problems with two different MINLP-solvers (DICOPT and BARON). The results showed that the single-field model was solved to global optimality by BARON within reasonable computational time. The multi-field model was only solved to global optimality by BARON when the number of time steps was low. For higher number of time steps, the optimality gap was too large to conclude that the global optimal solution was obtained.

Sammendrag

Olje og gassindustrien har i de siste tiårene møtt flere utfordringer, blant annet gjennom økte vanddybder, transportdistanser, og hardere miljø- og operasjonelle forhold. Dette har ført til et behov for nye innovative idéer og løsninger, noe som har økt fokuset på subsea-prosessering. Målet med dette arbeidet har vært å utarbeide en ”mixed integer nonlinear programming” (MINLP)-modell for optimalisering av planlegging og utvikling av offshore oljefelt infrastruktur med integrerte subsea-separasjonssystemer for de utviklede feltene.

En MINLP-modell ble først utviklet for ett enkelt felt med subsea-prosessering koblet til en ”floating production storage and offloading” (FPSO)-enhet. Målet med optimeringen var å identifisere settet med subsea-komponenter som maksimerer netto nåverdien av prosessen over den gitte tidshorizonten. En superstruktur for prosessen som inkluderte alle potensielt nyttige prosesseringsenheter og tilkoblinger ble brukt som en basis for optimaliseringsmodellen. Installasjonen av prosesseringskomponentene i den optimale løsningen ble representert ved binære variabler, mens kontinuerlige variabler ble brukt for driftsbetingelser som massestrømmer og trykk, i tillegg til variabler for kapasiteter og kostnader. Beskrankingene for optimeringsmodellen inkluderte blant annet massebalanser, logiske betingelser relatert til de binære variablene, og likninger for beregning av kapasiteter og kostnader.

Modellen ble utvidet til å inkludere flere potensielle felt og FPSO-er, samt tidsplanlegging av installasjonene og brønnboringen over tidshorizonten. Målet bak optimeringen var å bestemme hvilke FPSO-er som skulle installeres, hvilke felt som skulle utvikles, antallet brønner boret i hvert felt i hvert tidssteg, produksjonsratene for feltene og konfigurasjonen av subsea-separasjonssystemet for hvert av de utviklede feltene. Superstrukturen som ble utviklet for enkeltfeltmodellen ble brukt til å optimere konfigurasjonen av subsea-separasjonssystemet til hvert av de utviklede feltene.

Både enkeltfeltsmodellen og multifeltsmodellen ble implementert i høy-nivå språket GAMS (General Algebraic Modeling System) for matematisk optimering. Modellene ble deretter løst for forskjellige case-studier på NEOS-serveren for numerisk optimering ved bruk av to forskjellige løsere (DICOPT og BARON). Resultatene viste at enkeltfeltsmodellen ble løst til global optimalitet av BARON innen rimelige beregningstider. Multifeltsmodellen ble kun løst til global optimalitet av BARON for problemer med få steg i tidshorizonten. Dersom antallet steg i tidshorizonten var høyt, ble optimalitetsgapet for høyt til å konkludere med at den globale løsningen var funnet.

Preface

This thesis was written as the final part of the master program in chemical engineering at the Norwegian University of Science and Technology.

I would like to express my gratitude and appreciation to my supervisor Associate Professor Johannes Jäschke for all his support and guidance during my work. I am grateful for the valuable discussion, useful critiques and advice guiding me throughout the process.

Table of Contents

Abstract	i
Sammendrag	iii
Preface	v
Table of Contents	ix
List of Tables	xii
List of Figures	xiii
Abbreviations	xv
1 Introduction	1
2 Background and Theory	5
2.1 Oil and Gas Exploration and Production	5
2.2 Subsea Technology	7
2.2.1 Subsea Separation and Injection	8
2.2.2 Subsea Boosting and Compression	10
2.3 Superstructure Optimization	11
2.3.1 Generating the Superstructure	12
2.3.2 Optimization Methods	13
3 Optimization of a Single-Field with Subsea Processing	23
3.1 Problem Statement	23
3.2 Model	27
3.2.1 Objective Function	27
3.2.2 Mass Balances and Pressure Decline	28

TABLE OF CONTENTS

3.2.3	Logical Conditions	31
3.2.4	Compressor and Pump Duties	32
3.2.5	Sizing and Equipment Cost	33
3.3	Case Studies	36
3.3.1	Case I	37
3.3.2	Case II	37
3.4	Results	38
3.4.1	Case I	38
3.4.2	Case II	40
3.5	Discussion	41
4	Optimization of Multi-Field Structure and Scheduling	45
4.1	Problem Statement	45
4.2	Model	47
4.2.1	Objective Function	47
4.2.2	Mass Balances and Pressure Decline	48
4.2.3	Logical Conditions	51
4.2.4	Compressor and Pump Duties	53
4.2.5	Sizing and Cost Estimation	54
4.3	Case Studies	56
4.3.1	Case I	57
4.3.2	Case II	58
4.4	Results	59
4.4.1	Case I	59
4.4.2	Case II	61
4.5	Discussion	62
5	Conclusion	67
5.1	Future Work	68
	List of Symbols	69
	Bibliography	73
A	Cost Estimation of Separators	i
A.1	Topside Separator	i
A.2	Subsea Separator	iii

TABLE OF CONTENTS

B Simulation Parameters	v
B.1 Single-Field Model	vi
B.2 Multi-Field Model	vi
C Simulation Output Data	ix
C.1 Single-Field Model	ix
C.2 Multi-Field Model	x
D GAMS Code	xiii
D.1 Single-Field Model	xiii
D.2 Multi-Field Model	xxi

List of Tables

3.1	Binary variables for single-field model	26
3.2	Qualitative description of constraints in equation set 3.14	30
3.3	Cost data for subsea flowline and risers	36
3.4	Size of single-field model for 10 time steps	36
3.5	Simulation parameters of case I	37
3.6	Simulation parameters of case II	38
3.7	Best solutions found by DICOPT and BARON for case I	38
3.8	Optimal set of binary variables for case I	39
3.9	Best solutions found for DICOPT and BARON case II	40
3.10	Optimal set of binary variables for case II	40
4.1	Binary and integer variables for multi-field model	47
4.2	Reservoir data for the base case of the multi-field model	57
4.3	Distances between the proposed locations of the FPSOs and the fields of the base case	57
4.4	Fixed costs for FPSOs and water depths	58
4.5	Size of multi-field model for 3 FPSOs, 3 fields and 5 time steps	58
4.6	Number of potential wells for the fields of case II	58
4.7	Size of multi-field model for 3 FPSOs, 3 fields and 10 time steps	59
4.8	Best solutions found by DICOPT and BARON for case I	59
4.9	Scheduling of drilling and installation of FPSOs for case I	60
4.10	Installed subsea equipment for the fields of case I	60
4.11	Best solutions found by DICOPT and BARON for case II	61
4.12	Scheduling of drilling and installation of FPSOs for case II	61
4.13	Installed subsea equipment for the fields of case II	62
B.1	Simulation parameters common for all cases	v
B.2	Coefficients for oil deliverability and pressure decline for case I & II (single-field model)	vi

LIST OF TABLES

B.3	Cost coefficients for separators case I & II (single-field model)	vi
B.4	Coefficients for oil deliverability and pressure decline for case I & II (multi-field model)	vii
B.5	Cost coefficients for separators case I & II (multi-field model)	vii
C.1	Installed equipment costs for the single-field model (case I & case II)	ix
C.2	Installed equipment capacities for the single-field model (case I & case II) . .	x
C.3	Installed equipment costs for the multi-field model (case I & case II)	x
C.4	Installed equipment capacities for the multi-field model (case I & case II) . .	xi

List of Figures

2.1	Main steps of development of an offshore oil field	6
2.2	Oil deliverability as a function of recovered oil	7
2.3	Reservoir pressure maintenance by water and gas injection.	9
2.4	General procedure of superstructure optimization	11
2.5	Generation of superstructure by combining flowsheets	12
2.6	Superstructure representations	13
2.7	Optimum of LP-problems	15
2.8	Branch and bound search tree	16
2.9	Graphical illustration of outer approximation algorithm	19
2.10	Graphical illustration of spatial branch and bound	21
3.1	Subsea separation flowsheet: alternative 1	24
3.2	Subsea separation flowsheet: alternative 2	25
3.3	Subsea separation flowsheet: alternative 3	25
3.4	Superstructure for single oil field with subsea processing	27
3.5	Optimal flowsheet for case I	39
3.6	Optimal flowsheet for case II	41
4.1	General superstructure for multi-field system with subsea processing	46
4.2	Superstructure for base case of multi-field model with three FPSOs and three fields	56
A.1	Cost of topside separator as a function of mass flow	iii
A.2	Cost of subsea separator as a function of mass flow	iv

Abbreviations

FPSO	=	Floating production storage and offloading
GBD	=	Generalized Benders decomposition
GOR	=	Gas oil ratio
LP	=	Linear programming
MIP	=	Mixed integer programming
MILP	=	Mixed integer linear programming
MINLP	=	Mixed integer nonlinear programming
MP	=	Multiphase
NLP	=	Nonlinear program
NPV	=	Net present value
OA	=	Outer approximation
QP	=	Quadratic programming
SEN	=	State equipment network
STN	=	State task network
SQP	=	Sequential quadratic programming

Chapter 1

Introduction

A fundamental problem of chemical engineering is the process of identifying the best possible flowsheet structure for a given process. This often involves a series of decisions regarding flows, interconnections and units. These decisions can generally be divided into two categories: structural and operational decisions. The former deals with the selection of equipment and units as well as the interconnection between them and the flows of the system. Examples of the latter category include flow rates, temperatures and pressures. The complexity of such combinatorial problems can become quite high, and for a process synthesis problem, it is not uncommon to have as many as 10^{15} alternatives [1]. This illustrates the importance of developing good models for process design and optimization of flowsheet configurations.

Development of offshore oil and gas fields represent a problem where the need for optimization of structural and operational decisions is especially crucial. Decisions in such projects have a high level of complexity and can involve multibillion dollar investments and profits [2]. Therefore, careful consideration must be taken in order to ensure a high return on investment over the time horizon considered. Several alternatives for the installation of the units as well as the interconnections between them, give rise to problems of considerable sizes. The complexity is further increased by the scheduling of installations and well drilling, which forces the problem to include time as a variable. In addition, the decisions are subject to a number of physical considerations and limitations, such as the nonlinear flow profiles from which the flow-rates of oil and gas are determined, the number of wells that can be drilled in each time step, and logical constraints regarding the installations and connections.

The complexity of the oilfield operation and planning problem has lead to a number of quantitative methods for determining the optimal way of developing oil and gas-reserves.

These methods take the form of mathematical programming models. One of the earliest models was developed by A. S Lee and J.S Aronofsky in 1958 [3]. Based on a number of assumptions, they formulated a linear programming (LP) problem for maximizing the total profit from a collection of oil reservoirs located in the same area. The decision variables were the average production rates of oil from the respective fields. L. S Frair developed a mixed integer linear programming (MILP) problem in 1973, for optimizing the economics of oil field development. [4]. The model accounted for the number of platforms to be developed, the number of wells to be drilled, the location and size of the platforms, the scheduling for the installations of the units, and the production rate of each reservoir. The decision variables were chosen to maximize the total discounted after tax cash flow. Due to the size of the problem the model was decomposed into sub-problems to make it computationally tractable. A nonlinear model similar to the one developed by L.S Frair was developed by Vijay Gupta and Ignacio E. Grossmann in 2011 [2]. This model also accounted for installation and scheduling, but used third and higher order polynomials in order to approximate the nonlinear nature of the reservoir profiles.

During the last couple of decades, the oil and gas industry has been subject to a series of new challenges. Tie-back distances are increasing, design conditions are harsher and stricter environmental conditions have forced the industry to come up with new innovative ideas and technology. As a result, subsea technology has gained increased focus by both the scientific community and the industry. By placing central components and processes at the seafloor, a number of advantages can be gained including; increased hydrocarbon recovery factors, less environmental impact and increased flow assurance [5] [6]. There are however, different alternatives to evaluate when designing a subsea system. Depending on the reservoir characteristics, different sets of equipment and flow-interconnections can be used. This give rise to the question of which alternative of the subsea flowsheet would give the most profitable operation. Superstructure optimization provides a powerful approach that could be utilized in order to optimize the flowsheet. First, all potential useful equipment and interconnections are included in a process diagram, referred to as the superstructure. From the superstructure, a mathematical optimization model is formulated where the constraints include mathematical models for all the units as well as logical constraints. By solving the mathematical optimization model, the optimal configuration of the flow sheet is identified.

This thesis is a continuation of the specialization project completed in 2017, where an optimization model for the configuration of a subsea separation system was formulated for constant flow rates and pressures. In this thesis, the previous work done in optimization

of oilfield operation and planning is extended by incorporating the optimization of a subsea system for each of the fields developed in the system. In addition, the model will account for varying production rates and pressure decline over the time horizon.

The master thesis is organized as follows: Chapter 2 deals with some of the theoretical concepts and background for the models. Chapter 3 presents a model for optimization of a single field with subsea processing. The model is expanded to include multiple fields and scheduling of the installations and production in Chapter 4. Finally, the work is concluded in Chapter 5 with some suggestions for further work.

Chapter 2

Background and Theory

This chapter gives some insight in the basic concepts of oil and gas field development to give an indication of the practical significance of the developed models. A brief description is also given for the most central theoretical concepts of optimization required for the development and solution of the models.

2.1 Oil and Gas Exploration and Production

The offshore oil and gas industry dates back to 1945 when the first offshore installation took place in the gulf of Mexico [7]. This occasion symbolizes an important milestone in petroleum industry, opening up a new door for production of crude oil and natural gas. However, there were several challenges to be overcome, as experienced by the early pioneers [8]. Since then, major improvements have been made in all aspects of the process, including computerization and automatization of the equipment for production and drilling. The realizable step-out distances and sea depths have increased, shifting the main issue from the feasibility of operation to the economic potential of the production.

Today, the process of offshore development consists of several steps, requiring competence on a variety of fields. The initial phase is primarily focused around using geological criteria to identify general areas where accumulations of hydrocarbons may have developed at some period in geological time [9]. This step is subject to a considerable degree of uncertainty despite the spectacular advances and breakthroughs that have taken place since oil and gas exploration first started. To this date, drilling is still the only way that can guarantee the

presence or absence of hydrocarbons, but due to the high cost of drilling, geological studies are an essential part to the overall process. After the potential areas have been identified, further investigation is carried out by the use of magnetic surveys and sonic readings. The resulting information is used to construct a detailed map of the subsurface area, which again allows geologists to locate the sites where the probability of finding hydrocarbon reserves are relatively high. At this point, the existence of a deposit is still uncertain, and based on the collected data, a decision of whether or not to drill an exploration well can be made. If the drilling provides positive results, step-out wells are drilled in order to determine physical reservoir characteristics like pressure, temperature, volume, porosity, etc. The optimization models presented in this thesis are useful once the data from the test wells have been gathered, and decisions regarding the development and production strategy should be taken. The main steps of the exploration and development process are summarized in figure 2.1.

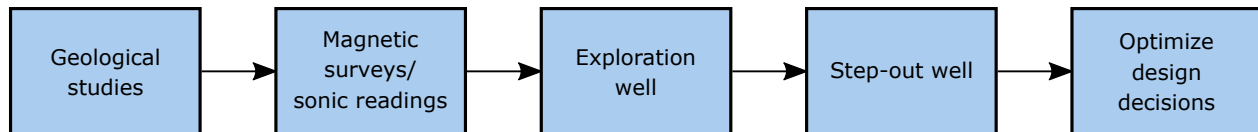


Figure 2.1: Main steps of development of an offshore oil field.

The infrastructure of an offshore installation is made up of several different parts, including fields, wells, pipelines and floating production storage and offloading (FPSO) units. The oil fields consist of a number of potential wells that are drilled using drilling ships. These wells are connected to the installed facilities by pipelines. During the course of production, the reservoir pressure decreases, which lowers the maximum production rate of oil. Furthermore, the relative amounts of oil, gas and water will vary nonlinearly in time. There exist different methods to model these effects. A commonly used approach is to calculate the maximum production rate from decline-curves, where the production rate decreases exponentially in time [4]. Another alternative is to approximate the maximum production rate by third order polynomials in terms of fractional oil recovered [2]. In this thesis, the latter method is used to estimate the maximum production rate of oil per well. Figure 2.2 illustrates how the maximum production rate typically varies with the fraction of recovered oil for an oil well. The way the reservoir pressure declines over time is dependent on the drive mechanism of the field. The pressure in a water drive reservoir will for example have a slower decline than a solution gas drive reservoir, as the water in the aquifer can move into the reservoir and displace the oil. In this thesis, it is assumed that the reservoir pressure declines linearly with the fraction of oil recovered.

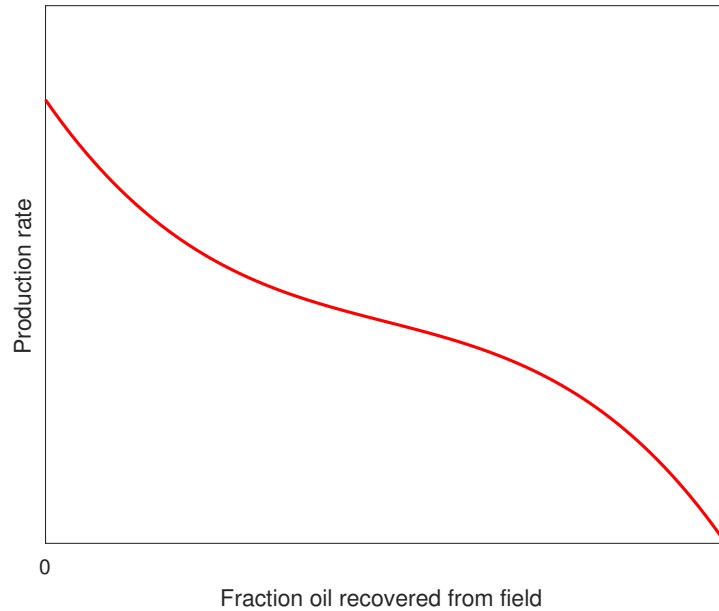


Figure 2.2: Oil deliverability as a function of recovered oil.

2.2 Subsea Technology

During the last couple of decades, subsea processing has gained increased attention due to its promising potential, and is currently one of the most attractive technologies utilized by the oil and gas industry. The term subsea processing can be defined as any handling or treatment of the produced fluids below or at the seabed [10] and include several applications such as single phase/multiphase boosting, gas compression, separation systems and water injection systems [11]. One of the main driving factors behind the development of subsea technology is the fact that the oil industry is running out of the oil that is “easy” to produce. New challenges arise from the discoveries of remote fields including increased water depths, increased step-out distances and harsher environmental and operational conditions. Subsea processing opens up the possibility for production from fields that otherwise would be infeasible. However, there are also several operational benefits from carrying out the production with subsea technology, including [12]:

- Increased hydrocarbon recovery
- Accelerated production
- Improved flow assurance

- HSE-benefits

The HSE-benefits include improved energy efficiency, reduced environmental impact as well as reduced fire and explosion risks. There are also benefits related to the flexibility of development through reducing the number of constraints that the topside facilities are faced with.

2.2.1 Subsea Separation and Injection

Technology for produced water separation and reinjection was one of the first subsea processing concepts to be applied [13]. There is usually a considerable amount of water present in most reservoirs, that is transported together with the oil through the pipelines. During the course of the production, the water cut will increase, which requires the topsides facility to have a high capacity for water handling. This could be costly, or serve as a bottleneck for the oil production. By separating the water from the valuable fluids subsea, this problem is avoided and valuable space is saved at the FPSO. In addition, the separation will lower the cost of fluid transportation and reduce the risk of hydrate formation in the pipelines.

After the separation, the produced water can be reinjected into the reservoir. This maintains the reservoir pressure, which again increases the flow rate and the hydrocarbon recovery factor. In Norway, the Troll C pilot project follows the model of water separation and reinjection. The separation station is located at a water depth of 310 m at a distance of 3.5 km from the Troll C production platform [14]. The water is separated from the rest of the well stream by the use of a gravitational separator and reinjected into the reservoir by the use of a centrifugal pump. It is also possible to inject external seawater into the reservoir in order to maintain the pressure levels. This often requires the water to be processed in advance to ensure continued safe and efficient production of hydrocarbons. By filtering the water, the risk of blocking the formation pores is lowered. The oxygen levels of the water can also be lowered in order to reduce the corrosion of equipment and pipes [15]. Tyrihans is a field operated by Equinor that applies subsea pumps to inject unprocessed seawater into the reservoir. Around 14 000 Sm³ seawater is injected each day without filtration or chemical treatment [12]. However, the seawater is sourced from the seabed rather than near the surface, which ensures lower particular content as well as reduced levels of dissolved oxygen. It is estimated that the injection of seawater has increased the amount of recovered oil with 10 Sm³. This corresponds to a 10 % increase in the overall recovery factor. Figure 2.3 illustrates the principle of gas/water-injection for maintaining the reservoir pressure.

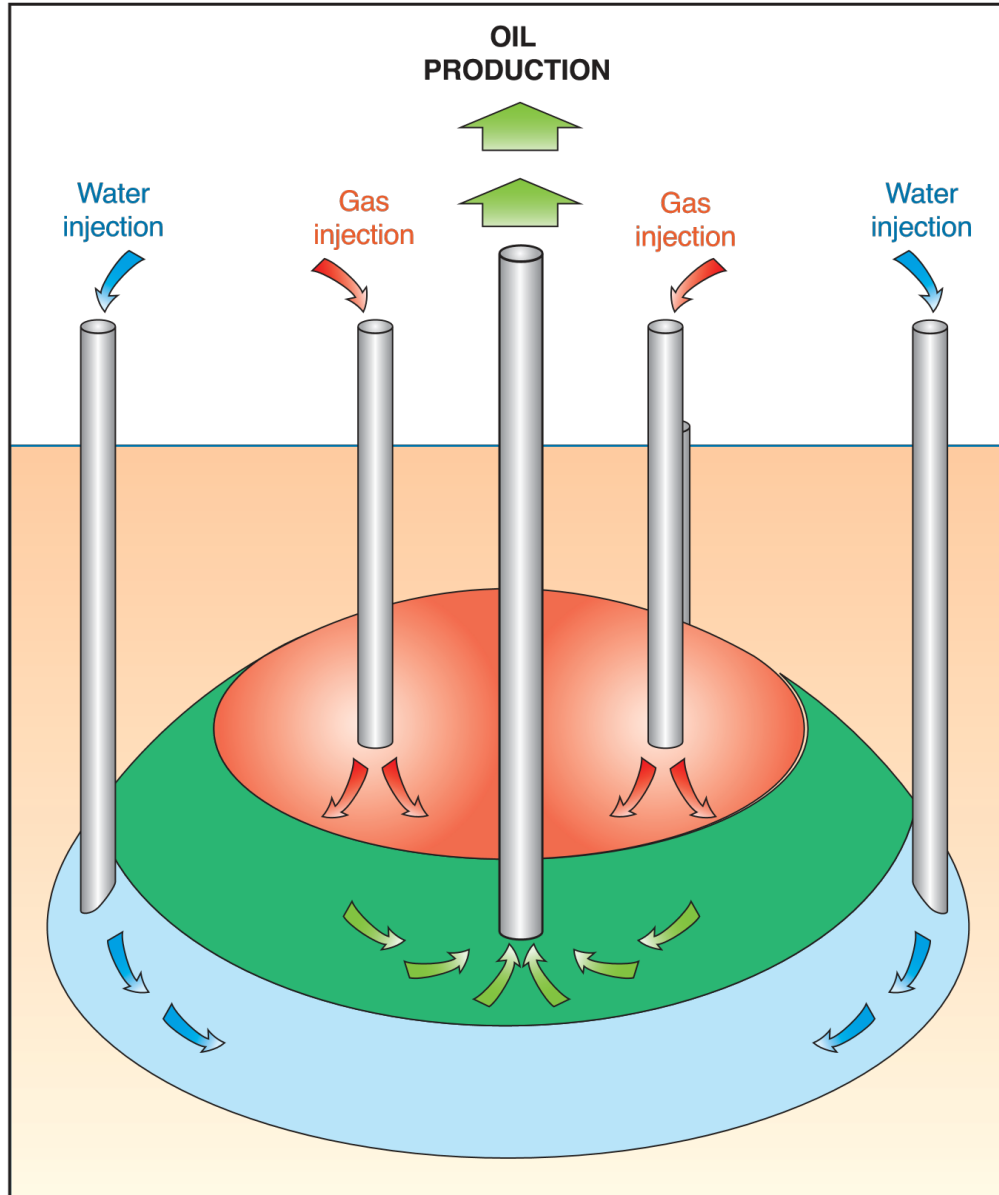


Figure 2.3: Reservoir pressure maintenance by water and gas injection [9]

2.2.2 Subsea Boosting and Compression

Subsea boosting technology started its development in the 1980's and is one of the most commonly used subsea processing methods. The technology was developed as a result of declining natural production rates suffered by oil fields due to reduced reservoir pressures. By installing a pump close to the well, the backpressure of the well and the reservoir is lowered, giving increased flow assurance as well as higher recovery factors. The increase in kinetic energy also allows for transport over greater distances. During the life of the field, subsea boosting can result in an additional 5-15 % increase of recovered hydrocarbons [5]. The technology is especially useful for low energy fields with low initial reservoir pressure and fields with long tie-back distances. Such fields could in many cases be deemed uneconomical based on the production rates generated by the natural flow. However, by applying subsea boosting, development of these fields can be enabled. The first electrically driven subsea pumping system was constructed at the Lufeng field in 1997 [12]. There were initially made two unsuccessful attempts to find economically feasible solutions to the operation. However, by incorporating the subsea boosting system, the field was finally brought online. The boosting system consisted of five single phase pumps with a motor power of 400 kW each. The water depth was at 330 m, which was considered relatively deep water at the time. Another field that applies subsea boosting technology is the Tordis field located in the North Sea. The field began production in 1994. As the field matured, the amount of produced water increased, and the topside water handling capacity acted as a bottleneck for the production. In order to increase the economic potential of the field, a subsea processing system consisting of subsea separation, boosting and reinjection was installed. A multiphase pump with capacity of 2.3 MW was installed for the boosting of the reservoir fluids.

The newest development in subsea processing is gas compression. The benefits of this technology are similiar to those for pumping. Current fields operating with this technology are the Gullfaks and Åsgard compression stations. The gullfaks compression station consists of two 5 MW wet gas compressors giving a pressure boost of 32 bar, while the Åsgard compression station consists of two 11.5 MW centrifugal compressors giving a pressure boost of around 50 bar [16]. There are also offshore compression solutions being evaluated to increase production and extend the lifetime of the Ormen Lange field. This field is located more than 120 km from the gas processing facilities onshore. The suggested compression system consists of four identical 12.5 MW compressor trains, which allows maintenance and shutdown of one compressor without impacting the production through the other trains [17].

2.3 Superstructure Optimization

There are two general approaches for identifying the optimal configuration of a flowsheet and its operating conditions. One approach consists of decomposing the problem and solving it in sequential form [18]. Heuristics are used to identify the changes that give improved solutions when a set of the flowsheet elements are held fixed. This method is relatively simple to implement. However, due to the sequential nature of the approach, it may lead to sub-optimal solutions. The main alternative to this method is superstructure optimization. The general procedure for this approach can be broken down into three steps. The first step consists of formulating a superstructure for the process. A superstructure refers to a process flowsheet that includes all potentially useful units and interconnections between them [19]. All competing processing units, or subsystems that can perform the same tasks should be present in this structure and connected. The next step is to formulate an optimization model based on the superstructure. This optimization model should include an objective function that reflects the quantity to be maximized/minimized, usually the profit, or total cost respectively. In addition, mathematical models for each of the processing units should be incorporated in the model as constraints. The final step is to apply an appropriate solver to the optimization problem, which selects the best flowsheet configuration along with the optimal operating variables for each of the selected units. The general steps are illustrated by figure 2.4.

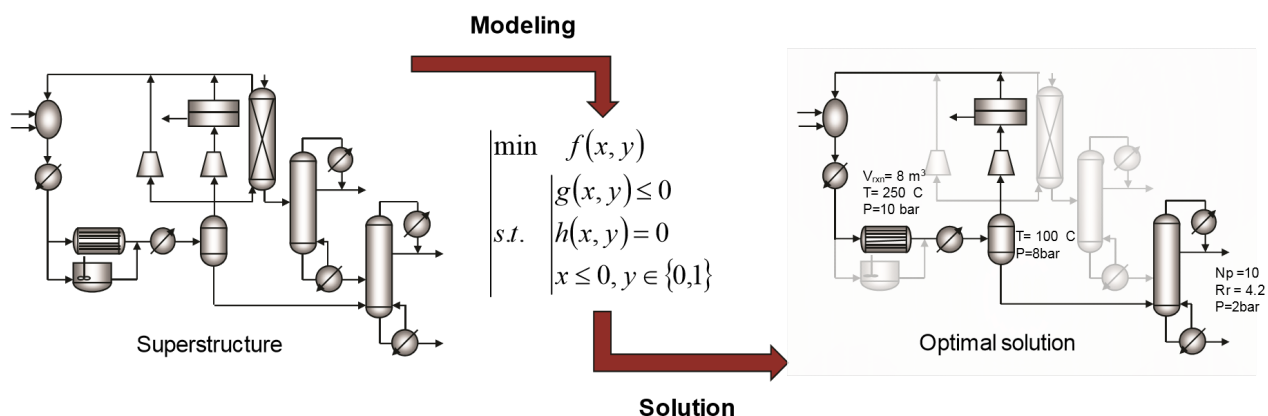


Figure 2.4: General procedure of superstructure optimization [19].

2.3.1 Generating the Superstructure

A significant challenge when generating a superstructure for a process is to find the appropriate degree of complexity for the structure. A simpler design will generally be easier to represent by a mathematical model. In addition, the resulting mathematical model will be easier to solve. However, if the true optimal configuration is not represented in the original superstructure, it can not be identified by solving the model. The superstructure should therefore be as simple as possible without losing the optimal configuration. There are no general methodologies that can guarantee this, and engineering judgment is therefore a central part of the process. An early approach for generating superstructures consisted of combining simple flowsheets for the process [20], as illustrated by figure 2.5. All the potentially useful units and interconnections are then included in the superstructure. The advantage of this method is that it is relatively simple to implement, and the resulting superstructure is based on existing pathways, rooted in engineering judgement. However, the superstructure will be limited by the experience and creativity of the creator, and will therefore not lead to any new or revolutionary designs for the process.

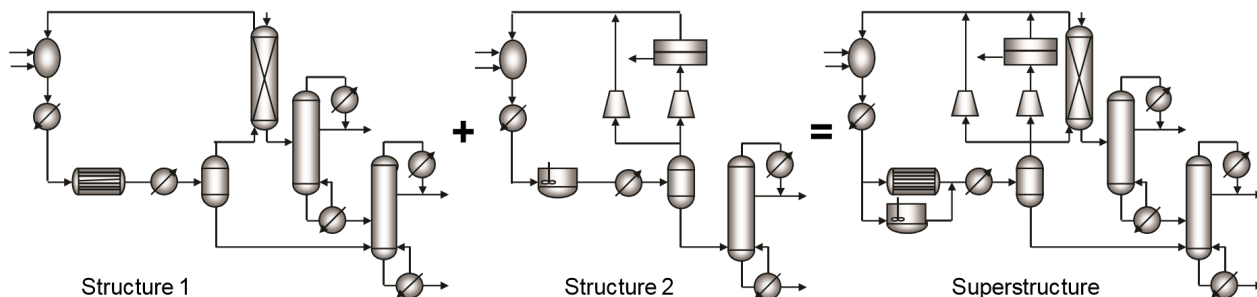


Figure 2.5: Generation of superstructure by combining simpler flowsheets [1].

The way the superstructure is represented plays an important part for both the formulation and solution of the optimization model. There are primarily two common representation forms that are used for superstructures, namely the state task networks (STN) representation and the state equipment network (SEN) representation. The STN representation was originally intended for process scheduling. The main concept behind the STN representation is that the states and the tasks of the process are pre-defined, while the equipment for each task should be assigned by solving the optimization model. Here, states can be defined as the physical and chemical properties that define a process stream (e.g., temperature, pressure, composition etc.) Tasks can be defined as the processes that transform a state into an adja-

cent state in the diagram. Examples include heat transfer, mass transfer and phase changes. Some tasks are conditional, while others are present for all the possible design alternatives that are captured by the superstructure. STN-representations are especially useful for optimization of synthesis processes where several pathways exist for converting a set of raw materials to a set of products.

SEN-representations are more similar to conventional process diagrams, and assume full connectivity among all states and equipment. A set of potentially useful equipment and units for the process is selected and connected by the relevant process streams of the system. The optimization then selects the optimal set of equipment for the process and assigns tasks for each unit. Note however that the state definition is not unique in the SEN-representation, as the properties of the exiting stream will depend on the task assigned to the unit. The main advantage of the SEN-representation is that the combinatorial complexity of the problem generally becomes smaller. The STN and SEN-representations are illustrated in figure 2.6.

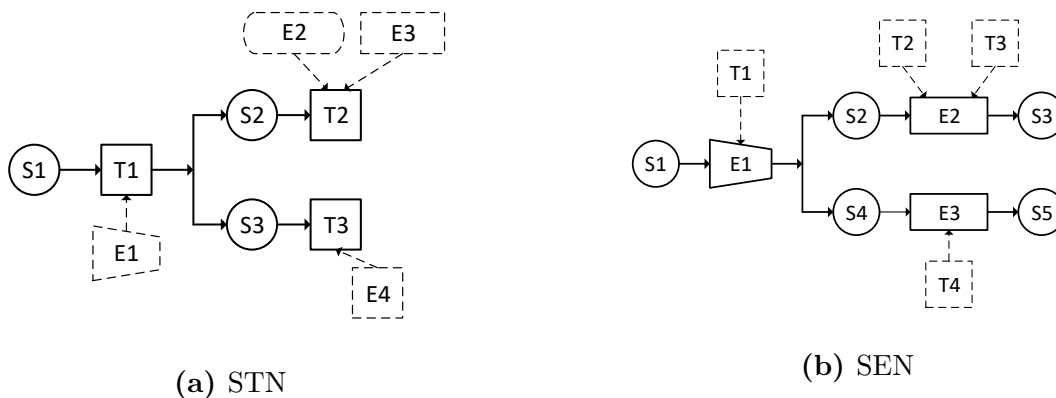


Figure 2.6: Superstructure representations. S, T and E in the diagrams correspond to states, tasks and equipment respectively.

2.3.2 Optimization Methods

An optimization model is formulated based on the superstructure created for the process. The optimization model contains equations for all the equipment and interconnections included in the superstructure, as well as constraints for the operating conditions. The field of optimization is a highly complex and extensive field, and the theory presented in this section is therefore included to give a very brief overview over the most important concepts applied when formulating and solving the optimization models generated from superstructures. This

includes the different types of optimization problems, and the underlying algorithms that are used for their respective solvers. The standard form of a *continuous* optimization problem is given in equation 2.1.

$$\begin{cases} \min f(x) \\ s.t. h(x) = 0 \\ g(x) \leq 0 \\ x \in R^n \end{cases} \quad (2.1)$$

Here, $f(x)$ is the objective function to be minimized over the vector x , $h(x)$ are the equality constraints and $g(x)$ are the inequality constraints of the problem. Note however, that the above formulation assumes that all decision variables are continuous. This is not always the case, which will be explained in further detail. The optimization model can take on several different forms, depending on the properties of the equations and variables that are present in the model.

If all functions are linear, and the decision variables are continuous, the optimization model is referred to as a LP-problem. The development of these problems are regarded as one of the most important scientific advances of the mid 20-th century, and is often considered as the beginning of the modern era of optimization. Especially important was the development of the SIMPLEX algorithm by George Dantzig in the late 1940s [21]. Due to the fact that the functions are linear in the decision variables, LP-problems are always convex, and hence any local minimum is a global minimum. The SIMPLEX algorithm is based on the fact that the optimum will lie on one of the vertices of the feasible region as illustrated by figure 2.7. Here, the black lines represent the constraints defining the feasible region, while the red dashed lines are the contour lines of the objective function. The SIMPLEX algorithm iterates over the vertices of the feasible region, searching for the optimum. The method has been revised several times since it was first formulated, and many modern commercial solvers are based on the method (e.g., CPLEX, LINDO). [22].

Mixed integer linear programming is an extension of linear programming where a subset of the variables are restricted to be integer or binary. Both the objective and the constraints however, are still linear in the decision variables. These types of models are common for superstructure optimization because discrete choices of equipment can be represented by binary variables. In addition, logic conditions for the system can be modeled relatively

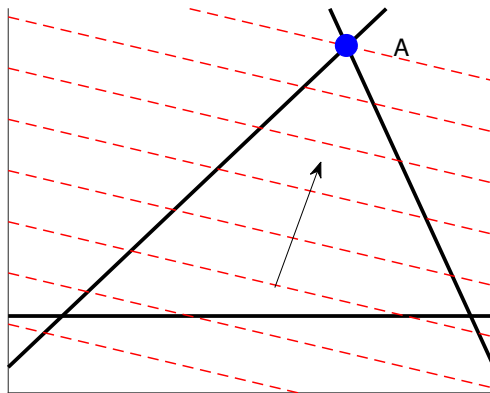


Figure 2.7: Optimum of LP-problems are located at a vertex of the feasible region.

easily, as illustrated by the following examples [23].

$$\sum_j y_j = 1 \tag{2.2a}$$

$$\sum_j y_j \leq 1 \tag{2.2b}$$

$$x - U y_j \leq 0 \tag{2.2c}$$

Here y is restricted to be binary ($y \in 0, 1$), and x is restricted to non-negative values ($x \geq 0$). Equation 2.2a specifies that *exactly one* element y_j should be selected in the set, while equation 2.2b specifies that *at most one* element y_j should be selected in the set. Equation 2.2c ensures that the continuous variable x is set to zero if element y_j is not selected. However, if y_j is selected, x is constrained by some parameter U . Logical conditions like these prove to be very useful when formulating an optimization model from a superstructure.

The general solution technique for MILP problems are based on the branch and bound algorithm, for which the underlying concept is to divide and conquer [24]. The algorithm solves a sequence of LP-relaxations, while dividing and removing parts of the search space based on the bounds obtained from the solutions. The procedure can be represented graphically by a search tree where the first node is the relaxed version of the original problem. This node is called the root node. If the root node provides an integer solution, the search is stopped and the optimal solution is found. If however, one of the decision variables is not integer ($y_j^* = a$), the node is split in to two new nodes separated by the additional constraints

$y_j = \text{floor}(a)$ and $y_j = \text{ceil}(a)$. The solution of the root node represents the lower bound for the problem, given that the objective function is minimized. The new nodes are then solved as relaxed LPs. If one of the nodes provide an integer solution, it is closed and the corresponding solution provides an upper bound for the overall problem. If the solution of a given node is higher than the best upper bound, the node can be closed due to the fact that further branching will not give a better solution. A node is also closed if the corresponding LP-problem is infeasible. The process is repeated as long as there are open nodes.

Figure 2.8 shows an illustration of a branch and bound tree for a minimization problem. The root node does not provide an integer solution, so the node is branched into the sub-problems S_1 and S_2 by discarding the search space that included the solution of the root node. The LP-relaxation of S_2 is infeasible, and the node is closed. S_1 does not provide an integer solution and is branched into subproblems S_{11} and S_{12} . The solution of S_{11} is integer, and thus provides an upper bound for the real problem. The solution of S_{12} is higher than the best upper bound. Because the solution can only get worse by further discarding and partitioning the search space, there is no reason to continue the branching of node S_{12} . Hence, there are no more open nodes and the algorithm terminates with the best solution found in S_{11} .

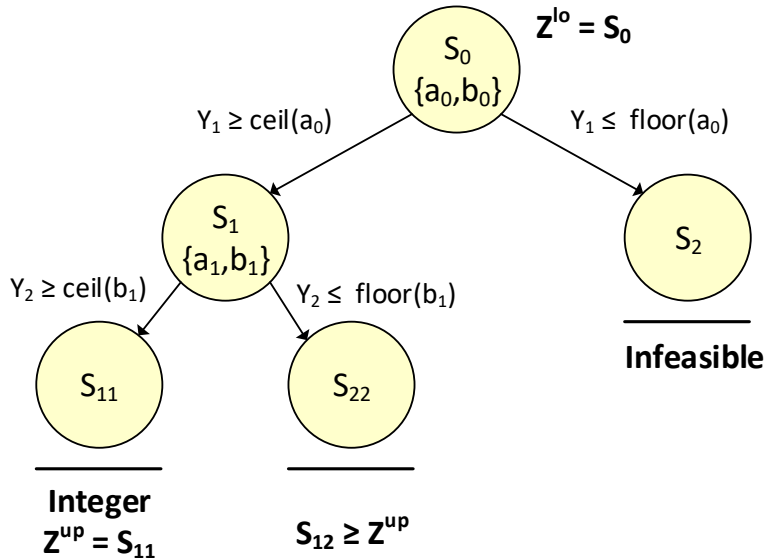


Figure 2.8: Example of a branch and bound search tree for a minimization problem where the optimal solution is found in node S_{11} .

In the case where one or more of the model functions are nonlinear and all variables are

continuous, the optimization problem is referred to as a nonlinear programming (NLP) problem. Unlike linear programming problems, NLP-problems are not necessarily convex. This means that a global minimum can not be guaranteed unless all the nonlinear functions are convex and the equality constraints are linear. There are a couple of different solution strategies for NLP-problems. Two of the most common approaches are sequential quadratic programming (SQP) and interior point methods [21]. The main concept behind SQP is that a sequence of quadratic programming (QP) problems are solved iteratively. The objective of the sub-problems are quadratic approximations of the Lagrangian function, while linear approximations are used for the original constraints as illustrated:

$$\left\{ \begin{array}{l} \min f(x) \\ s.t. \ c_i(x) = 0 \quad i \in \mathcal{I} \\ \quad \quad c_i(x) \geq 0 \quad i \in \mathcal{E} \end{array} \right. \implies \left\{ \begin{array}{l} \min_p \quad f_k + \nabla f_k^\top p + \frac{1}{2} p^\top \nabla_{xx}^2 \mathcal{L}_k p \\ s.t \ \nabla c_i(x_k)^\top p + c_i(x_k) = 0 \quad i \in \mathcal{I} \\ \quad \quad \nabla c_i(x_k)^\top p + c_i(x_k) \geq 0 \quad i \in \mathcal{E} \end{array} \right. \quad (2.3)$$

Here p is the predicted search direction, x_k the current point, and \mathcal{I} and \mathcal{E} are finite sets for inequality and equality constraints respectively. The quadratic sub-problems are solved for each iterate by applying a QP solver, and the search direction p is obtained. The next iterate is then given by $(x_{k+1} = x_k + \alpha p)$, where α is the step length determined by the merit function. The merit function weighs the satisfaction of the constraints against the minimization of the objective. The process is repeated until a convergence test is satisfied. The SQP algorithm can be very effective for many non-linearly constrained optimization problems. The main drawback of the algorithm is the fact that it can be computationally expensive to solve the QP-subproblems if the problem is large. Examples of commercial solvers that apply the SQP algorithm are KNITRO and SNOPT.

Optimization models that include discrete and continuous variables in addition to nonlinear functions in the objective and/or constraints are referred to as mixed integer nonlinear programming (MINLP) problems. These problem types are considered as one of the most general modelling paradigms in optimization and are among the hardest to solve, unless some specific properties of the model structure can be exploited [25]. They are especially important as they often arise from modeling of superstructures and process synthesis problems. The discrete variables are useful for representing choices and implementing logic as previously explained, while the nonlinear functions often arise from operating constraints or cost estimation models. A general formulation for MINLP-problems is:

$$\left\{ \begin{array}{l} \min \quad c^\top y + f(x) \\ s.t. \quad c_i(x, y) = 0 \quad i \in \mathcal{I} \\ \quad \quad c_i(x, y) \geq 0 \quad i \in \mathcal{E} \\ \quad \quad \quad x \in X \\ \quad \quad \quad y \in \{0, 1\} \end{array} \right. \quad (2.4)$$

where it is assumed that the objective function is linear in the discrete variables. This is often the case since the discrete variables are used to represent fixed costs in the objective function. Solution strategies for MINLP-problems borrow principles from MILP, NLP and LP-methods. The branch and bound algorithm described for MILP-problems can in principle also be used to solve MINLP-problems. However, each node now represents a relaxed NLP problem instead of a relaxed LP-problem, which can be computationally demanding. Other important algorithms are based on outer approximation (OA) suggested by Duran and Grossman [26] and generalized Benders decomposition (GDB) [27].

The outer approximation algorithm consists of solving an alternating sequence of master MILP-problems and NLP-subproblems. The NLP-subproblems arise when fixing the discrete variables. The solution of these problems provide upper bounds if the objective is minimized. The original MINLP-problem can then be linearized around the point obtained from the NLP-subproblem, to produce a master MILP-problem. Since the master MILP-problems are relaxations of the original MINLP-problem, their solutions are used as lower bounds. After solving a master MILP-problem, the resulting discrete variables of the solution are held fixed to create the next NLP-subproblem. By accumulating linearizations from the previous iterations, an increasingly better approximation of the feasible region is produced. The algorithm terminates when the upper and lower bounds meet.

Figure 2.9 shows a graphical illustration of the first two iterations of the OA-algorithm. In figure 2.9a, the initial point $y = 5$ is given to create the first NLP-subproblem. Figure 2.9b shows the solution of the first MILP-master problem with the linearization around the point obtained from the NLP subproblem. In the next iteration, y is held fixed from the MILP to create the NLP-subproblem showed in figure 2.9c. The linear approximation from the solution is added to the next MILP to give a better approximation of the feasible region as shown in figure 2.9d. DICOPT is an example of a commercial solver that applies OA together with equality relaxations and augmented penalties to find local solutions of MINLP-problems [22]. The performance of the solver is heavily dependent on the choice of subsolvers for the NLP and MILP-problems.

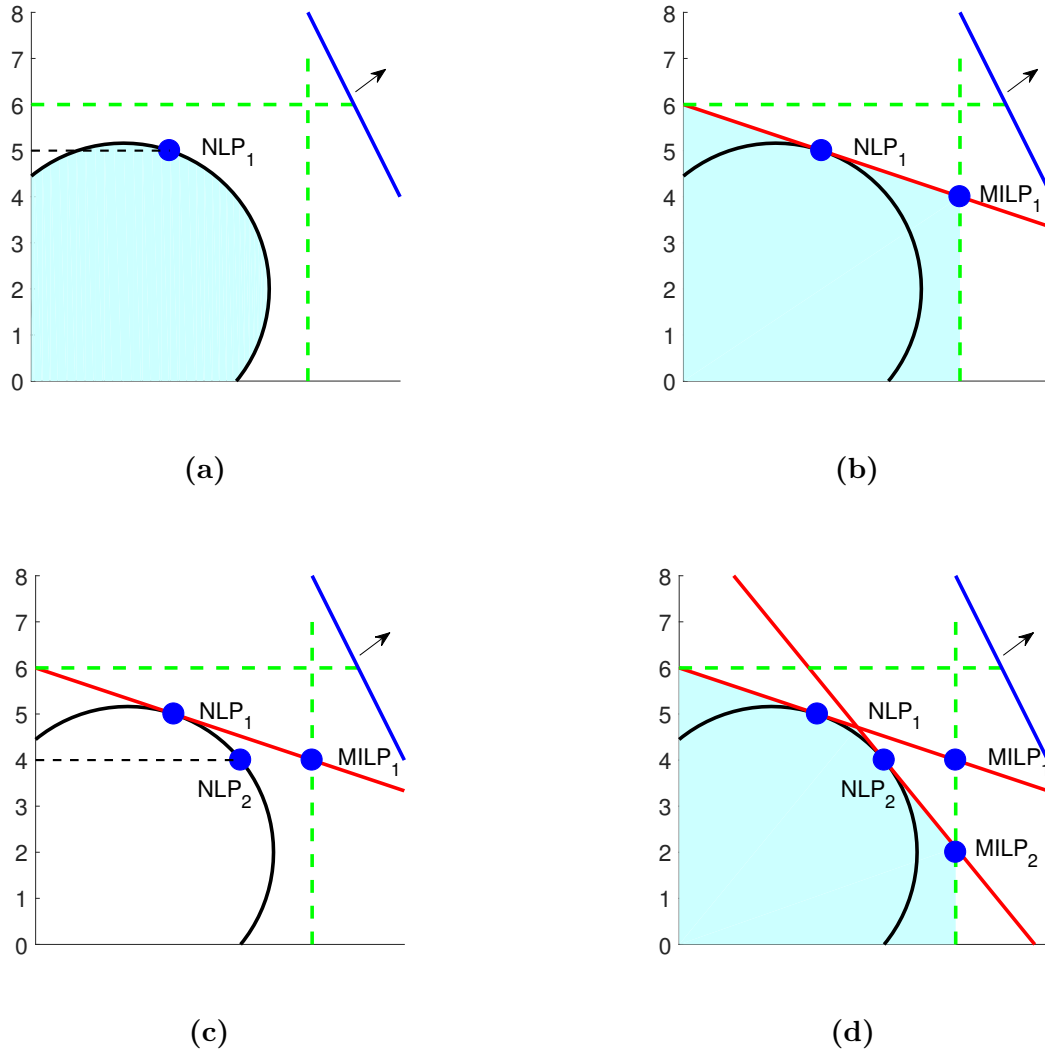
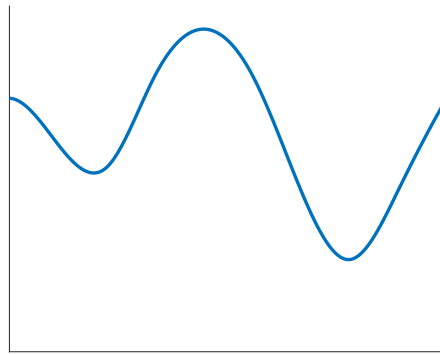


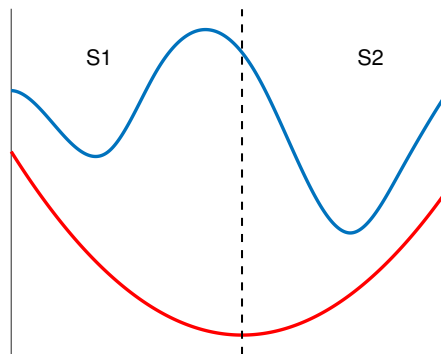
Figure 2.9: Graphical illustration of two iterations of the outer approximation algorithm. The shaded area is the feasible region, the red lines are linearizations, the blue line is the objective function.

Although methods like OA and GBD can provide good integer solutions, they are not guaranteed to find the global optimum. In many cases, non-convex terms are required to model real-world problems, and multiple local solutions complicate the optimization process. This calls for global optimization techniques, that searches for the best possible solution of the entire feasible region. One of the central aspects of global optimization is the spatial branch and bound algorithm [28]. Here, the non-convex terms are replaced with convex envelopes to produce convex relaxations of the original problem. The relaxations are solved to obtain underestimations of the objective. The problem is branched into subproblems, that is relaxed and solved to produce bounds. If the bounds meet, the optimal value of the subproblem is identified. If not, they are branched further. A subregion whose lower bound is higher than an upper bound of another subregion can be discarded, as the optimum can not be located in this subregion.

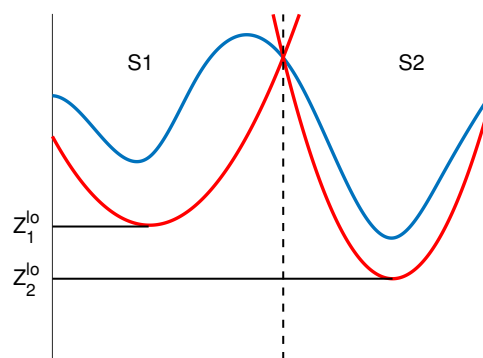
Figure 2.10 illustrates the general concept. The original objective function in 2.10a is replaced with the convex underestimator as shown in 2.10b. The search space is then partitioned, and two new convex underestimators are used to relax the objective of each subproblem. If the lower bound of subregion S1 (Z_1^{lo}) is found to be higher than the upper bound of S2 (any solution of the real problem in the region), there is no need to continue searching for the global minimum in S1 and the region can be discarded. Several other algorithms have been derived from spatial branch and bound, including the branch and reduce algorithm applied by the commercial solver BARON. Although global solvers are equipped to determine the global solution of optimization problems, they can be very resource consuming. If the solver has identified the optimal solution, it will not terminate until all other lower bounds are higher than the solution found, or at an acceptable tolerance. A central part of the process is therefore to increase the lower bound until the gap between the best found solution and the lower bound is so small that the solution can be considered to be globally optimal for all practical purposes. The gap between the best found solution and the lower bound is referred to as the *optimality gap*, and can be used as an indicator for the possibility that the current best obtained solution is the global optimum.



(a) Original objective function



(b) Convex underestimator of objective



(c) Convex underestimators for the two sub-regions

Figure 2.10

Chapter 3

Optimization of a Single-Field with Subsea Processing

This section presents a MINLP model for optimizing the structural configuration of a single oil field with subsea processing. The main goal of the model is to identify the set of subsea equipment that yields the maximum net present value (NPV) over a given time horizon. This includes decisions regarding boosting and transportation of the produced reservoir fluids.

3.1 Problem Statement

There are multiple ways of designing a subsea system. Several factors influence the design and selection of equipment including: reservoir characteristics, geographical location, environmental conditions and existing infrastructure [6]. The model presented in this section requires pre-determined knowledge regarding several of these factors. More specifically, the model requires deterministic values for:

- The initial pressure and temperature of the reservoir
- The size of the reservoir
- The average gas oil ratio (GOR) over the time horizon
- An estimation of the pressure decline of the reservoir
- The oil deliverability as a function of oil recovered

Based on the data provided, the objective of the model is to determine the set of equipment and flow interconnections that optimizes the economics of the field. This entails finding the best configuration of the flowsheet of the subsea system. The model only considers a single oil field producing oil and gas that are transported to a FPSO. It is also given that there will be performed a gas/oil/water-separation subsea, and that the resulting reservoir fluids should be boosted in order to ensure efficient production. This gives the following alternative designs for the subsea separation system:

1. Single phase compression/pumping, transport and rising.
2. Multiphase boosting, transport and rising.
3. Single phase compression/pumping with multiphase transport and rising.

The possible configurations are illustrated in figure 3.1-3.3. Multiphase boosting requires the installation of a multiphase pump with the capacity to handle the combined flow of oil and gas. If multiphase transport and rising is chosen, a separator must be installed topsides at the FPSO. If multiphase boosting is not chosen, the pressure of the phases must be increased separately by installing a pump for the oil and a compressor for the gas. For this case, a cooler is installed to condense out any remaining liquid before the compression. The condensed liquid is then separated from the gas before it is joined with the oil flow to the pump.

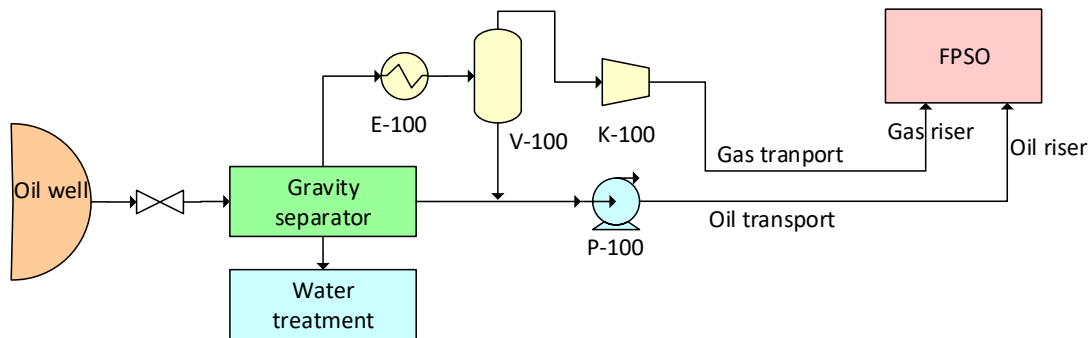


Figure 3.1: Separate phase compression/pumping and separate phase transportation and rising.

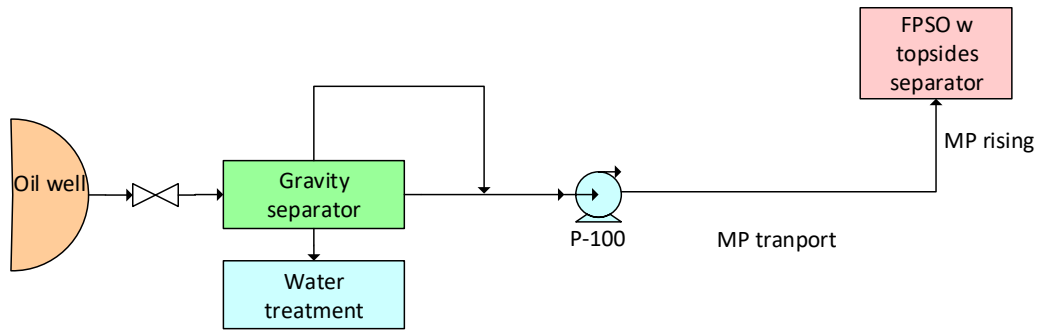


Figure 3.2: Multiphase boosting and multiphase transportation and rising.

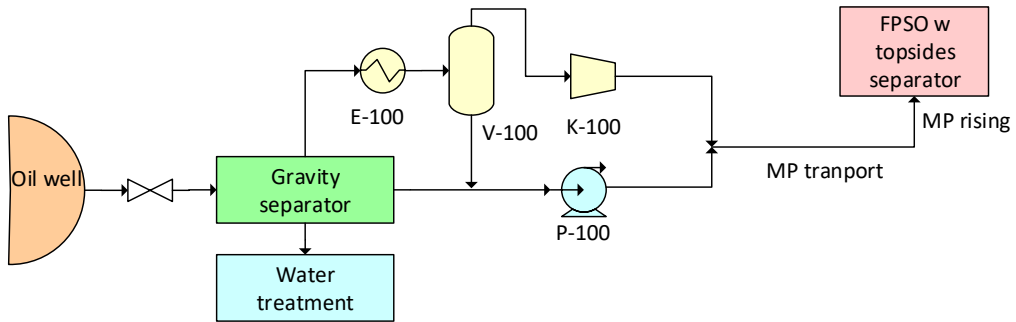


Figure 3.3: Single phase compression/pumping and multiphase transportation and rising.

The possible flowsheet configurations can be combined into a superstructure, that includes all the potentially useful equipment and interconnections of the flows (SEN), as discussed in Chapter 2.3. This superstructure is presented in figure 3.4 and is used as a basis for the MINLP-model presented in section 3.2. The yellow nodes of the diagram symbolizes splitting points, where only one output flow is allowed. The green nodes are potential mixing points for the flows. Each potential piece of equipment is assigned a binary variable to represent its existence in the optimal solution, as shown in table 3.1. If the binary variable takes the value 1, the corresponding piece of equipment is installed. Since no alternative solutions are proposed for the water treatment or the three-phase gravity separator, these processes can be excluded from the optimization model.

Table 3.1: Binary variables for the potential subsea processing equipment.

Binary variable	Unit
y ₁	Cooler
y ₂	Separator
y ₃	Compressor
y ₄	Oil pump
y ₅	Multiphase pump
y ₆	Gas transport line
y ₇	Gas riser
y ₈	Multiphase transport line
y ₉	Multiphase riser
y ₁₀	Topside separator
y ₁₁	Oil transport line
y ₁₂	Oil riser

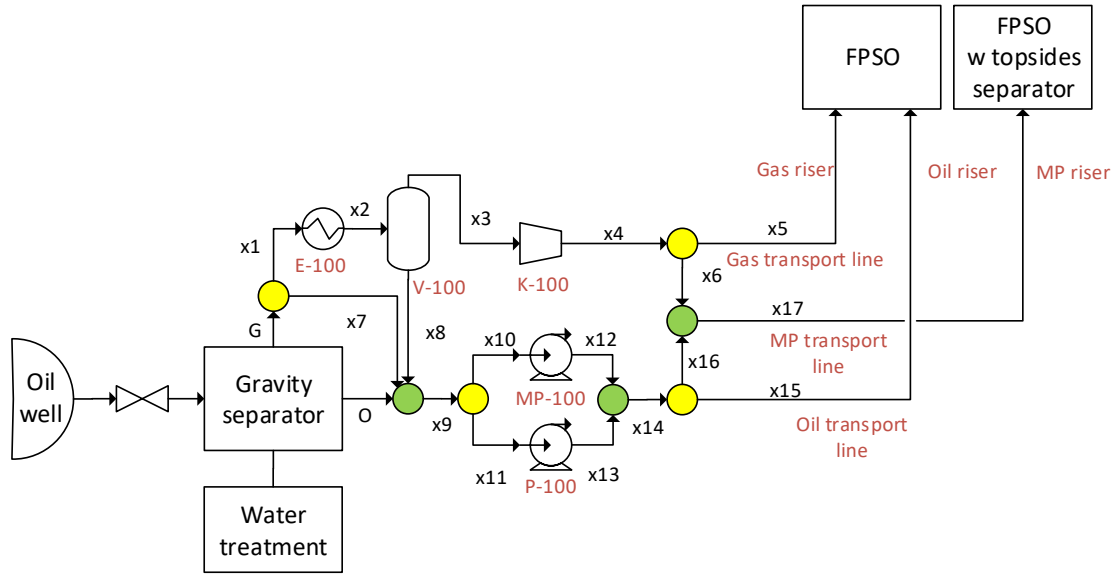


Figure 3.4: Superstructure for single oil field with subsea processing. The total mass flows between the units and nodes are denoted by x .

3.2 Model

3.2.1 Objective Function

The objective function is to maximize the NPV of the project, as presented in equation 3.1.

$$\max \text{ NPV} \quad (3.1)$$

The NPV is defined in equation 3.2.

$$\text{NPV} = -C_0 + \sum_{t=1}^{N_t} \frac{C_t^F}{(1+r)^t} \quad (3.2)$$

Here, C_0 is the initial investment, and C_t^F is the cash flow for time step t . The initial investment is the sum of the costs of the installed equipment, as presented in equation 3.3.

$$C_0 = \sum_{j=1}^{N_j} c_j \quad (3.3)$$

Note, however, that the sum is defined over all of the potential useful pieces of equipment, which requires the cost of the equipment that is not installed to be set to zero. The cost of the equipment will also depend on the capacity, which in turn requires knowledge about the mass flows of the system. The cash flow for time step t is defined as the difference between the revenue and operating cost as illustrated by equation 3.4.

$$C_t^F = (O_t p^{oil} + G_t p^{gas}) \alpha - (P_t^k + P_t^p + P_t^{MP}) \alpha p^{el}, \quad \forall t = 1, 2, \dots, N_t \quad (3.4)$$

Here, O_t and G_t are the flowrates of oil and gas in time step t , respectively. p^{oil} is the oil price, p^{gas} is the price of natural gas, p^{el} is the price of electricity and α is the number of operating hours per time step. P_t^k , P_t^p and P_t^{MP} are the power consumption rates of the compressor, oil pump and multiphase pump respectively.

3.2.2 Mass Balances and Pressure Decline

The flow rate of oil is constrained by the maximum deliverability of oil, as illustrated by equation 3.5. Equation 3.6 gives the flow rate of gas as the product of the oil flowrate and the gas-oil-ratio.

$$O_t \leq Q_t \quad \forall t = 1, 2, \dots, N_t \quad (3.5)$$

$$G_t = GOR \times O_t \quad \forall t = 1, 2, \dots, N_t \quad (3.6)$$

The maximum deliverability of oil is approximated by a third order polynomial in the fraction of oil recovered from the field, as given in equation 3.7

$$Q_t = k_1^q f_{t-1}^3 + k_2^q f_{t-1}^2 + k_3^q f_{t-1} + k_4^q \quad \forall t = 2, 3, \dots, N_t \quad (3.7a)$$

$$Q_1 = k_4^q \quad (3.7b)$$

Here, k_1^q - k_4^q are constants that need to be determined by preliminary studies of the field. These factors will naturally have a considerable degree of uncertainty. However, for the purpose of this model, the constants are treated as deterministic parameters. The fraction of oil that is recovered from the field up until the end of time step t is given by equation 3.8.

$$f_t = \frac{\sum_{\tau=1}^t O_\tau \alpha}{O_{rec}} \quad \forall t = 1, 2, \dots, N_t \quad (3.8)$$

O^{rec} is the total amount of recoverable oil from the field. The numerator of equation 3.8 is the total amount of oil produced from the field up until the end of time step t . Naturally, this quantity can not be greater than the total amount of recoverable oil, which is ensured by equation 3.9.

$$\sum_{\tau=1}^t O_{\tau} \alpha \leq O^{rec} \quad \forall t = 1, 2, \dots, N_t \quad (3.9)$$

The pressure of the reservoir is assumed to decline linearly with the fraction of recovered oil, as illustrated by equation 3.10.

$$p_t^{res} = p^{init} - \beta f_t \quad \forall t = 1, 2, \dots, N_t \quad (3.10)$$

p^{init} is the initial pressure of the reservoir and β is the proportionality constant. In order to estimate the required capacity for the subsea equipment, the mass balances of figure 3.4 must be solved for each time step. By formulating the balances in total mass form, the flows of figure 3.4 can be determined by solving a set of linear equations illustrated by equation 3.11.

$$\underline{\underline{\mathbf{A}}} \underline{\mathbf{x}}_t = \underline{\mathbf{b}}_t \quad \forall t = 1, 2, \dots, N_t \quad (3.11)$$

$\underline{\mathbf{x}}_t$ is here a vector containing all the mass flows of the subsea system as labeled in figure 3.4. The $\underline{\underline{\mathbf{A}}}$ -matrix takes the following form:

$$\underline{\underline{\mathbf{A}}} = \begin{bmatrix} 1 & 0 & 0 & 0 & 0 & 0 & 1 & 0 & 0 & 0 & 0 & 0 & 0 & 0 & 0 & 0 \\ 1 & -1 & 0 & 0 & 0 & 0 & 0 & 0 & 0 & 0 & 0 & 0 & 0 & 0 & 0 & 0 \\ 0 & 0.05 & 0 & 0 & 0 & 0 & 0 & -1 & 0 & 0 & 0 & 0 & 0 & 0 & 0 & 0 \\ 0 & -1 & 1 & 0 & 0 & 0 & 0 & 1 & 0 & 0 & 0 & 0 & 0 & 0 & 0 & 0 \\ 0 & 0 & -1 & 1 & 0 & 0 & 0 & 0 & 0 & 0 & 0 & 0 & 0 & 0 & 0 & 0 \\ 0 & 0 & 0 & -1 & 1 & 1 & 0 & 0 & 0 & 0 & 0 & 0 & 0 & 0 & 0 & 0 \\ 0 & 0 & 0 & 0 & 0 & 0 & 1 & 1 & -1 & 0 & 0 & 0 & 0 & 0 & 0 & 0 \\ 0 & 0 & 0 & 0 & 0 & 0 & 0 & 0 & -1 & 1 & 1 & 0 & 0 & 0 & 0 & 0 \\ 0 & 0 & 0 & 0 & 0 & 0 & 0 & 0 & 0 & -1 & 0 & 1 & 0 & 0 & 0 & 0 \\ 0 & 0 & 0 & 0 & 0 & 0 & 0 & 0 & 0 & 0 & -1 & 0 & 1 & 0 & 0 & 0 \\ 0 & 0 & 0 & 0 & 0 & 0 & 0 & 0 & 0 & 0 & 0 & 1 & 1 & -1 & 0 & 0 \\ 0 & 0 & 0 & 0 & 0 & 0 & 0 & 0 & 0 & 0 & 0 & 0 & 0 & -1 & 1 & 1 \\ 0 & 0 & 0 & 0 & 0 & 1 & 0 & 0 & 0 & 0 & 0 & 0 & 0 & 0 & 1 & -1 \end{bmatrix} \quad (3.12)$$

It is here assumed that 5% of the gas stream is condensed in the cooler, in order to avoid complex thermodynamic calculations in the model constraints. The $\underline{\mathbf{b}}_t$ -vector is given by:

$$\underline{\mathbf{b}}_t = \left[G_t \ 0 \ 0 \ 0 \ 0 \ 0 \ 0 \ -O_t \ 0 \ 0 \ 0 \ 0 \ 0 \ 0 \ 0 \ 0 \right]^T \quad \forall t = 1, 2, \dots, N_t \quad (3.13)$$

where G_t and O_t are determined from equation 3.5, 3.6, and 3.7 for each time step. When solving the mass balances of the subsea system, the flows of the unused units should be set to zero for each time step in the time horizon. This is achieved through including the constraints in equation set 3.14.

$$\left. \begin{aligned} x_{1,t} - U y_1 &\leq 0 & (3.14a) \\ x_{2,t} - U y_2 &\leq 0 & (3.14b) \\ x_{7,t} - U y_5 &\leq 0 & (3.14c) \\ x_{10,t} - U y_5 &\leq 0 & (3.14d) \\ x_{11,t} - U y_4 &\leq 0 & (3.14e) \\ x_{5,t} - U y_6 &\leq 0 & (3.14f) \\ x_{6,t} - U y_8 &\leq 0 & (3.14g) \\ x_{15,t} - U y_{11} &\leq 0 & (3.14h) \\ x_{16,t} - U y_8 &\leq 0 & (3.14i) \end{aligned} \right\} \quad \forall t = 1, 2, \dots, N_t$$

From equation 3.14a it can be seen that if the cooler is not installed ($y_1 = 0$), the mass flow to the cooler (x_1) must be zero in order to satisfy the constraint. However, if the cooler is installed ($y_1 = 1$), the mass flow to the cooler must be smaller than some parameter U . This parameter acts as the maximum mass flow or total capacity of the system and must be determined before attempting to solve the model. By the mass balances in equation 3.11, the flow out of the cooler will naturally also be zero when $y_1 = 0$. The remaining constraints in equation set 3.14 follow similar logic. The significance of each of these constraints are summarized in table 3.2.

Table 3.2: Qualitative description of constraints in equation set 3.14.

Equation	Description
3.14a	Mass flow to cooler is zero when it is not installed

- 3.14b Mass flow to separator is zero when it is not installed
 - 3.14c Phases are not mixed if multiphase pump is not installed
 - 3.14d Mass flow to multiphase pump is zero when it is not installed
 - 3.14e Mass flow to oil pump is zero when it is not installed
 - 3.14f Gas is not transported single phase to FPSO if no gas transportation line is installed
 - 3.14g Compressed gas is not sent to mixing node if no multiphase transport line is installed
 - 3.14h Oil is not transported single phase to FPSO if no oil transportation line is installed
 - 3.14i Boosted oil is not sent to mixing node if no multiphase transport line is installed
-

3.2.3 Logical Conditions

There are also several logical restrictions between the binary variables that must be taken into consideration when formulating the model. Since the pressure of the reservoir fluids should be increased, the system requires the installation of either the multiphase pump, or the combined installation of both the compressor and the oil pump. In logic notation:

$$y_5 \vee (y_3 \wedge y_4)$$

Similiarly, the fluids must be transported to the FPSO by pipelines, which requires the installation of either the multiphase transportation line or the combined installation of the gas and oil transportation lines:

$$y_8 \vee (y_6 \wedge y_{11})$$

However, if multiphase boosting is chosen, there is no other alternative than to transport the phases together by installing the multiphase pipe line. This gives the following implication:

$$y_5 \Rightarrow y_8$$

The installation of a transportation pipe naturally requires the corresponding riser to be installed. In addition, if the phases are transported together, they must be separated by a

topside separator. This produces the following equivalence conditions:

$$y_8 \Leftrightarrow y_9 \Leftrightarrow y_{10}$$

$$y_6 \Leftrightarrow y_7$$

$$y_{11} \Leftrightarrow y_{12}$$

These logic conditions are incorporated in the model by reformulation to algebraic constraints as presented in equation set 3.16

$$y_3 + y_5 - 1 = 0 \tag{3.16a}$$

$$y_4 + y_5 - 1 = 0 \tag{3.16b}$$

$$y_6 + y_8 - 1 = 0 \tag{3.16c}$$

$$y_{11} + y_8 - 1 = 0 \tag{3.16d}$$

$$y_5 - y_8 \leq 0 \tag{3.16e}$$

$$y_8 = y_9 = y_{10} \tag{3.16f}$$

$$y_6 = y_7 \tag{3.16g}$$

$$y_{11} = y_{12} \tag{3.16h}$$

3.2.4 Compressor and Pump Duties

The duty of the compressor, oil pump and the multiphase pump depends on the mass flows through the system and the reservoir pressure. The power consumption rate of the compressor in time step t is given by equation 3.17.

$$P_t^k = \frac{x_{3,t}}{\eta_k} \frac{R T}{M_m} \frac{\gamma}{3.6} \frac{\gamma}{\gamma - 1} \left(\frac{p_2}{p_t^{res}} \frac{\gamma-1}{\gamma} - 1 \right) \quad \forall t = 1, 2, \dots, N_t \tag{3.17}$$

Here, it is assumed that the compression is isothermal. R is the universal gas constant, M_m is the molar mass of the natural gas, η_k is the compressor efficiency, γ is the dimensionless heat capacity ratio of the gas, and p_2 is the outlet pressure. The power consumption rate of the oil pump for time step t , is given by equation 3.18 [29].

$$P_t^p = x_{11,t} \frac{p_2 - p_t^{res}}{\rho^{oil} 3600 \eta_p} \quad \forall t = 1, 2, \dots, N_t \tag{3.18}$$

where ρ^{oil} is the density of the oil and η_p is the pump efficiency. It is assumed that the oil density is constant and independent of the reservoir pressure. The power consumption of the multiphase pump in time step t is given by equation 3.19 [30].

$$P_t^{MP} = x_{10,t} \frac{g h_t}{3600 \eta_{MP}} \quad \forall t = 1, 2, \dots, N_t \quad (3.19)$$

where h_t is the head in meters converted from the pressure differential by equation 3.20. Note that if the mass flow to any of the units presented above are zero (as enforced by equation set 3.14), the corresponding power consumption rate will be zero from equation 3.17 - 3.19.

$$\Delta P_t = 0.0981 h_t \frac{\rho_t^{mix}}{\rho_{water}} \quad \forall t = 1, 2, \dots, N_t \quad (3.20)$$

ρ_t^{mix} is the density of the multiphase flow in time step t . This quantity will depend on both the pressure and the gas fraction, as illustrated by equation 3.21

$$\rho_t^{mix} = \frac{O_t + G_t}{\frac{O_t}{\rho^{oil}} + \frac{G_t}{\rho_t^{gas}}} \quad \forall t = 1, 2, \dots, N_t \quad (3.21)$$

where the density of the gas in time step t is approximated by ideal gas law as illustrated by equation 3.22

$$\rho_t^{gas} = \frac{p_t^{res} M_m}{R T} \quad \forall t = 1, 2, \dots, N_t \quad (3.22)$$

3.2.5 Sizing and Equipment Cost

The cost of the installed equipment is estimated from cost correlations on the basic form:

$$C_j = (a_j y_j + b_j S_j^{n_j}) f_1 f_2 \dots \quad \forall j = 1, 2, \dots, N_j$$

C_j is the estimated equipment cost for unit j , S_j is the size parameter and n_j is the cost exponent. a_j acts as a fixed cost, and is hence multiplied with the binary variable for the corresponding piece of equipment. b_j is a cost parameter for the term that is dependent on the installed capacity. The f -factors are factors for additional adjustments of the cost. Note that the installed capacity S_j should be set to zero if the unit is not installed. All cost

correlations presented in this section are from Sinnott&Towler [29] unless otherwise specified. The cost of the compressor is given by equation 3.23

$$C_3 = (490000 y_3 + 16800 (P_{max}^k)^{0.6}) f_{inst} f_{sub} f_I \quad (3.23)$$

f_{inst} , f_{sub} and f_I are additional cost factors for installation, subsea operation and cost changes in time respectively. P_{max}^k is here the maximum power consumption of the compressor, which acts as the size parameter. Naturally, the power consumption rate of any year can not exceed the the maximum capacity which is ensured by equation 3.24

$$P_{max}^k \geq P_t^k \quad \forall t = 1, 2, \dots, N_t \quad (3.24)$$

Similiarly, the cost of the oil pump is approximated by equation 3.25

$$C_4 = C_{pm} + \left(6900 y_4 + 206 \left(\frac{m_{max}^p}{\rho_o 3.6} \right)^{0.9} \right) f_{inst} f_{sub} f_I \quad (3.25)$$

where m_{max}^p is the maximum flow capacity of the pump. The mass flows to the oil pump must therefore be constrained as illustrated in equation 3.26.

$$m_{max}^p \geq x_{11,t} \quad \forall t = 1, 2, \dots, N_t \quad (3.26)$$

C_{pm} is the cost of the pump motor, given by equation 3.27

$$C_{pm} = (-950 y_4 + 1770 (P_{max}^p)^{0.6}) f_{inst} f_{sub} f_I \quad (3.27)$$

P_{max}^p is here the maximum power consumption or capacity of the pump motor, which produces equation 3.28 as an additional constraint for the power consumption of the oil pump.

$$P_{max}^p \geq P_t^p \quad \forall t = 1, 2, \dots, N_t \quad (3.28)$$

There exists very little cost data for multiphase pumps. A technical report done by “Det Norske Veritas” listed the cost to lie roughly between 1 and 3 million USD in 2001 [31]. The ACES cost database, which is based on previous experience on the Norwegian continental shelf, reported the cost to lie around 3 million USD. For the purpose of this model it is

assumed that the multiphase pump can be represented by a fixed cost of 3 million USD, not including installation. The cost equation then takes the form presented in equation 3.29

$$C_5 = 3000000 f_{inst} f_I y_5 \quad (3.29)$$

The cost of the cooler is given by equation 3.30

$$C_1 = (24000 y_1 + 46 A^{1.2}) f_{inst} f_{sub} f_I \quad (3.30)$$

Where A is the heat exchange area needed for the maximum flow, as illustrated by equation 3.31.

$$A = m_{max}^c \frac{Cp_g \Delta T}{3.6 U_h \Delta T_{LM}} \quad \left. \vphantom{A} \right\} \quad \forall t = 1, 2, \dots, N_t \quad (3.31a)$$

$$m_{max}^c \geq x_{1,t} \quad (3.31b)$$

Cp_g is the heat capacity of the gas, ΔT is the temperature difference between the in- and out flow of the gas, U_h is the heat transfer area, and ΔT_{LM} is the logarithmic mean temperature difference. The cost of the separators have a slightly different form from the equipment presented so far. The cost of the subsea separator is approximated by equation 3.32a, while the cost of the topside separator is approximated by equation 3.32b. The cost factors for these equations are dependent on the the reservoir characteristics. This means that the equations for the separators will be unique for each field, and are therefore estimated prior to running the model. The procedure for obtaining the separator cost factors for a field is presented in appendix A.

$$C_2 = (a_{sub} y_2 + b_{sub} m_{max}^{sub}) f_{inst} f_{sub} f_I \quad (3.32a)$$

$$C_{10} = (a_{top} y_{10} + b_{top} m_{max}^{top}) f_{inst} f_I \quad (3.32b)$$

m_{max}^{sub} and m_{max}^{top} represent the maximum capacity of the separators, giving the additional constraints presented in equation 3.33

$$m_{max}^{sub} \geq x_{2,t} \quad \left. \vphantom{m_{max}^{sub}} \right\} \quad \forall t = 1, 2, \dots, N_t \quad (3.33a)$$

$$m_{max}^{top} \geq x_{17,t} \quad (3.33b)$$

The cost of the subsea flowlines and risers are estimated from equation 3.34 [32].

$$C_j = (C_j^b f_j^s + C_j^{coat}) L_j y_j \quad \forall j \in \{6, 7, 8, 9, 11, 12\} \quad (3.34)$$

Here, C^b is the basic cost per unit length, f_s is a cost factor for size, C_{coat} is the cost for coating, and L is the length of the pipe. The length of the transport lines are the distance, d , from the field to the FPSO, while the length of the risers are equal to the water depth, w_d . The cost is multiplied with the binary variable corresponding to the installation of the unit. Each of the cost factors depend on the type and size of the pipes. The data used for cost estimation of the flowlines and risers is presented in table 3.3.

	Size [In.]	Type	C_b [\$/m]	f_s [-]	$C_{coating}$ [\$/m]	L
MP transport line	10	Rigid	230	1.00	360	d
MP riser	10	Flexible	2300	1.70	360	w_d
Oil transport line	8	Rigid	230	0.72	290	d
Oil riser	8	Flexible	2300	1.1	290	w_d
Gas transport line	4	Rigid	230	0.15	150	d
Gas riser	4	Flexible	2300	0.5	150	w_d

Table 3.3: Cost data for subsea flowline and risers [32].

3.3 Case Studies

The single-field model includes equation 3.1-3.34. The model was implemented in GAMS for two cases of varying production rates and pressures. The implementation of case I in GAMS is given in appendix D.1. The models were solved by applying the solvers DICOPT and BARON on the NEOS server [33]. The size of the single-field model for 10 time steps is given in table 3.4. The main findings from the optimization is presented in Chapter 3.4.

Number of equations	772
Number of variables	454
Number of binary variables	12

Table 3.4: Size of single-field model for 10 time steps (case I & II)

3.3.1 Case I

Case I is the optimization of a low energy oil field with medium/small sized production. The size of the reservoir is set equal to that of the Goliat field, which is considered to be relatively small. The field is located close to the FPSO at 8 km, and with a water depth of 200 m. It is assumed that the initial production is low, at around 16 000 bbls/day. The operation is optimized over a time horizon of 10 years. The most significant parameters for the simulation are presented in table 3.5. The remaining parameters essential for the simulation are given in appendix B.

Table 3.5: Simulation parameters of case I.

Parameter	Value	Unit
N_t	10	[-]
p^{init}	9000	[kPa]
O^{rec}	25.5e6	[ton]
Q_0	16 0000	[bbls/day]
T	300	[K]
GOR	0.06	[ton/ton]
d	8	[km]
ρ^{oil}	0.844	[ton/m ³]
W_d	0.2	[km]

3.3.2 Case II

Case II is the optimization of a more remotely located reservoir. The distances and water depths are greater, requiring a higher pressure boost compared to case I. The initial production rate and size of the reservoir is also greater for this case, at 80 000 bbl/day and 50 MSm³ respectively. This is approximately the size and production rate of the Alvheim field [34], which is considered a medium sized field. The operation is optimized over 10 time steps. The most significant parameters for the simulation are presented in table 3.6. The remaining parameters can be found in appendix B.

Table 3.6: Simulation parameters of case II.

Parameter	Value	Unit
N_t	10	[-]
p^{init}	60000	[kPa]
Q^{rec}	42.5e6	[ton]
Q_0	80 000	[bbls/day]
T	300	[K]
GOR	0.06	[ton/ton]
d	70	[km]
ρ^{oil}	0.844	[ton/m ³]
W_d	0.6	[km]

3.4 Results

This chapter presents the most significant results of the optimization of case I and case II for the single field model, including the calculated objective and the optimal configuration of the subsea separation systems. Additional output for the unit costs and capacities is presented in Appendix C. Both cases were run on the NEOS server for numerical optimization with a maximum time limit of eight hours. The cases were solved for two different solvers: DICOPT and BARON. The optimality gap for termination was set to 0.001 % for BARON.

3.4.1 Case I

The best solutions found for case I are given in table 3.7 for the two solvers, with the optimality gap and time usage.

Table 3.7: Best solutions found by DICOPT and BARON for case I.

	DICOPT	BARON
NPV [mill USD]	1572.04	1574.35
Optimality gap [-]	-	$\leq 1e-5$
Time [s]	0.299	6.270

The rest of the data presented is for the best value found by BARON. The optimal values of

the binary variables are given in table 3.8. The selected set of binary variables correspond to the flowsheet presented in figure 3.5.

Table 3.8: Optimal set of binary variables for case I.

Variable	Description	Value in optimal solution
y_1^*	Cooler	1
y_2^*	Separator	1
y_3^*	Compressor	1
y_4^*	Oil pump	1
y_5^*	Multiphase pump	0
y_6^*	Gas transport line	1
y_7^*	Gas riser	1
y_8^*	Multiphase transport line	0
y_9^*	Multiphase riser	0
y_{10}^*	Topside separator	0
y_{11}^*	Oil transport line	1
y_{12}^*	Oil riser	1

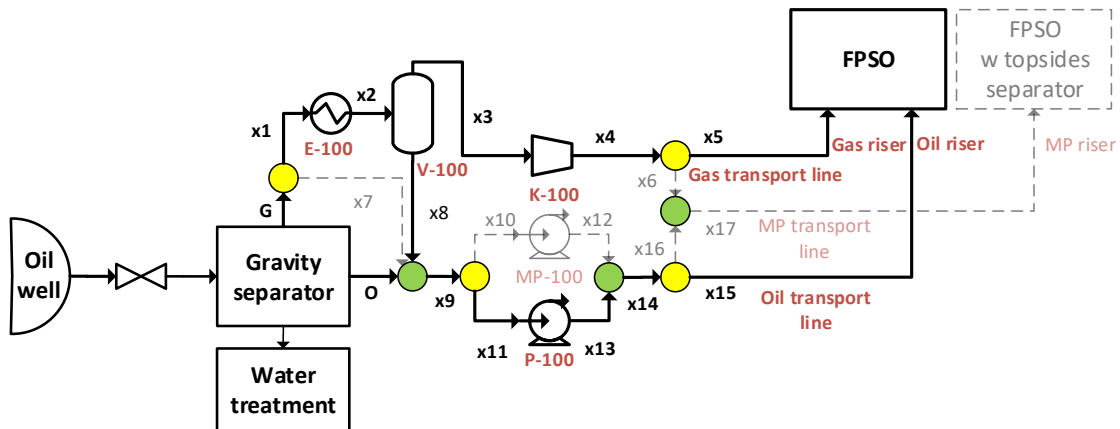


Figure 3.5: Optimal flowsheet for case I.

3.4.2 Case II

The best solutions found for case II by DICOPT and BARON are presented in table 3.9.

Table 3.9: Best solutions found for DICOPT and BARON case II.

	DICOPT	BARON
NPV [mill USD]	6390.31	6390.31
Optimality gap [-]	-	1e-5
Time [s]	0.527	18.860

The binary variables corresponding to the best solution are given in table 3.10.

Table 3.10: Optimal set of binary variables for case II.

Variable	Description	Value in optimal solution
y_1^*	Cooler	0
y_2^*	Separator	0
y_3^*	Compressor	0
y_4^*	Oil pump	0
y_5^*	Multiphase pump	1
y_6^*	Gas transport line	0
y_7^*	Gas riser	0
y_8^*	Multiphase transport line	1
y_9^*	Multiphase riser	1
y_{10}^*	Topside separator	1
y_{11}^*	Oil transport line	0
y_{12}^*	Oil riser	0

The optimal set of binary variables corresponds to the flowsheet in figure 3.6.

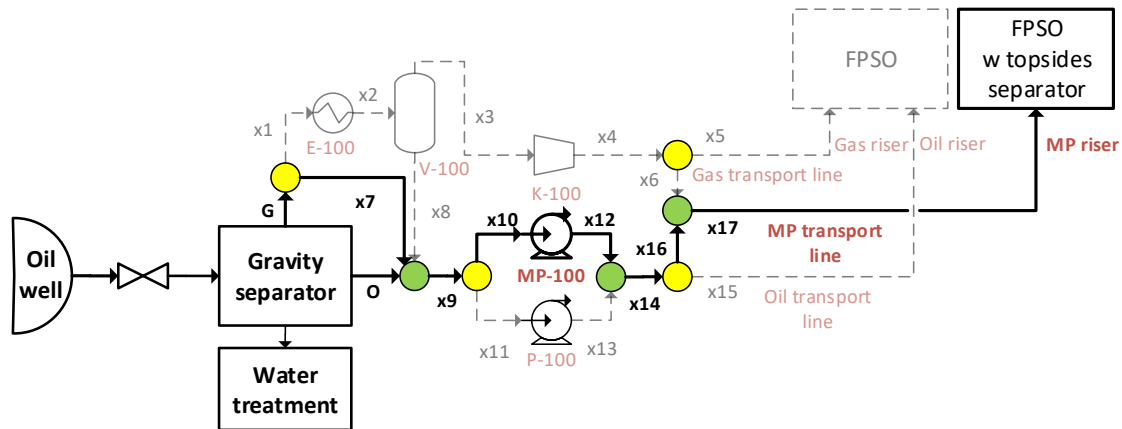


Figure 3.6: Optimal flowsheet for case II.

3.5 Discussion

Table 3.7 shows that DICOPT and BARON find two different solutions for case I. The solution obtained by BARON has an optimality gap under 0.001 %. Since the optimality gap shows the distance between the currently best found solution, and the overestimated upper bound of the problem, it is safe to assume that the solution obtained by BARON is very close to, or at the global maximum of the problem. The solution returned by DICOPT is slightly worse than the solution obtained by BARON. This is not surprising as the single-field model is not convex, which means that DICOPT is not guaranteed to obtain the global solution. Although both solvers terminate fairly quickly for case I, it can be seen that BARON uses over 20 times the computational time that DICOPT uses. This is due to the fact that BARON is a global solver that has to calculate and reduce the optimality gap to the specified limit in order to terminate. Since DICOPT is not classified as a global solver, no optimality gap is returned for the obtained solution.

The NPVs calculated for case II is considerably higher than for case I, as shown by table 3.9. This is due to the increased production and size of the field. The optimality gap calculated by BARON once again gives strong indication that the obtained solution is indeed the global optimum. For this case, however, BARON uses almost 40 times the computational time that DICOPT requires. In addition, it can be seen that DICOPT now gives the same exact solution as BARON. However, DICOPT can not guarantee that the obtained solution is the global maximum for the problem, as shown for case I.

The optimal set of binary variables for case I in table 3.8 indicate that single phase compression/pumping combined with single phase transport and rising is the best configuration of the flowsheet. It is easy to verify that the logical conditions posed in Chapter 3.2.3 are satisfied for the solution. The mass flows of the unused units are also set to zero during the entire time horizon, and the mass flows to the installed equipment do not exceed the installed capacities presented in table C.2 in appendix. This indicates that the model solves as intended. Table 3.10 shows that a different set of optimal variables are selected for case II. Here, multiphase boosting is combined with multiphase transport and rising with the additional installation of a topside separator. The change of the optimal set of binary variables can be explained by the increased production rate from case I to case II. In case I, the limited size of the production allows the installation of a small compressor and a small pump. The costs of these units are lower than the cost of the multiphase pump because of the high fixed cost associated with the installation of the multiphase pump. For case II, the production is considerably higher, and the fixed cost of the multiphase pump is small compared to the cost of a compressor that is capable of handling the gas flow. The choice of using single phase transportation in the optimal solution of case I can be explained by the short tie-back distance and shallow water depth. Since these distances are small, the cost of two separate sets of transport lines and risers are lower than the cost of the multiphase equivalents, with the additional installation of a topside separator. For case II however, the distances are much greater, and the cost of the topside separator is lower than the cost of two separate sets of flow lines and risers.

The validity of the results are strongly dependent on the reliability of the approximations used to estimate the cost of the various subsea equipment. The majority of the equipment cost was calculated from correlations based on a large number of previous installations. These correlations are not as reliable as rigorous cost estimation software, but can give a decent estimate for preliminary design. However, for the multiphase pump, there exists very limited data for cost estimation purposes, which resulted in a fixed cost model for the unit. This might have a substantial effect on the results produced from the optimization model, as the installation cost of the multiphase pump is not properly scaled in accordance with the mass flow or the pressure differential. This causes solutions that features multiphase pumps to be highly favoured for fields with high production and/or low initial reservoir pressure, which is not necessarily the case for actual field development. The model could therefore be improved by including a cost equation for the multiphase pump that properly reflects the capacity dependency of the cost.

It should be noted that several of the operating conditions of the subsea system are entered as

parameters and are held constant during the optimization. These include the boost pressures of the multiphase pump, oil pump and the compressor, the temperature difference over the cooler and the logarithmic mean temperature difference of the cooler. One of the major advantages of superstructure optimization is the ability to simultaneously optimize the process structure and the operating conditions. This feature is lost when the operating conditions are not incorporated as decision variables. This means that the solution identified by the optimization model might only be valid for the given set of operating conditions specified. A possible improvement of the model would therefore be to include a set of equations that allowed the additional optimization of the operating variables for safe and efficient production. The boost pressures could for example be optimized by including models for the friction and pressure loss of the various phases, pipes and risers. This would also give different required boost pressures for the pumps and compressor, which again would affect both the operating costs and the sizing of the equipment. However, in order to optimize these variables, more complex models are needed for each of the units in the flow sheet, which would affect the overall solveability of the model. Especially when the model is extended to include several fields and time scheduling (Chapter 4).

It is important to emphasize that the NPVs calculated by the optimization model in table 3.8 and 3.10 do not provide a valid measure for the overall profitability of the project. The calculated NPV only accounts for the equipment and costs that are essential for the optimization, and does not account for several important costs related to field development such as drilling costs, cost of water handling, cost of the platform/FPSO etc. The NPV is therefore used solely as an objective function for comparing the alternative configurations, and should not be used as an indication for the overall profitability of the project. A more detailed economic evaluation should naturally be performed to ensure that the project truly is profitable from a broader perspective.

Chapter 4

Optimization of Multi-Field Structure and Scheduling

This chapter extends the model presented in chapter 3 to include multiple fields and FPSOs as well as the scheduling of installations and drilling over the time horizon. Several models have been made to optimize decisions in oil production and planning. This chapter merges the single-field model presented in chapter 3 with several concepts from the multiperiod MINLP-model described by Grossmann and Gupta in 2012 [2].

4.1 Problem Statement

While the previous model only considered a single field connected to a single FPSO, the basis for the model presented in this chapter is a set of potential FPSOs with given distances to a set of fields. Each of the fields have a set of potential wells that can be drilled during the time horizon considered. However, there are limitations on both the number of wells that can be drilled in each time step, as well as the number of wells that can be drilled in total in each field. Each of the fields that are developed should have an optimized subsea processing system as implemented by the model in chapter 3. The model presented in this chapter aims to provide answers to the following key aspects of development:

- Which FPSOs should be installed
- Which fields should be developed

- The set of subsea equipment that should be installed in each field
- The capacity of the subsea equipment installed
- How the fields should be connected to the FPSOs
- How many wells should be drilled in each field
- The time scheduling of installing the equipment
- The time scheduling of drilling

These decisions should be made to maximize the NPV of the entire operation over the time horizon considered. A generalized superstructure for the problem is presented in figure 4.1. Each field can potentially be connected to each of the FPSOs in the set, as illustrated by the figure. However, the field can only be connected to one FPSO. The integer and binary variables for the model is presented in table 4.1.

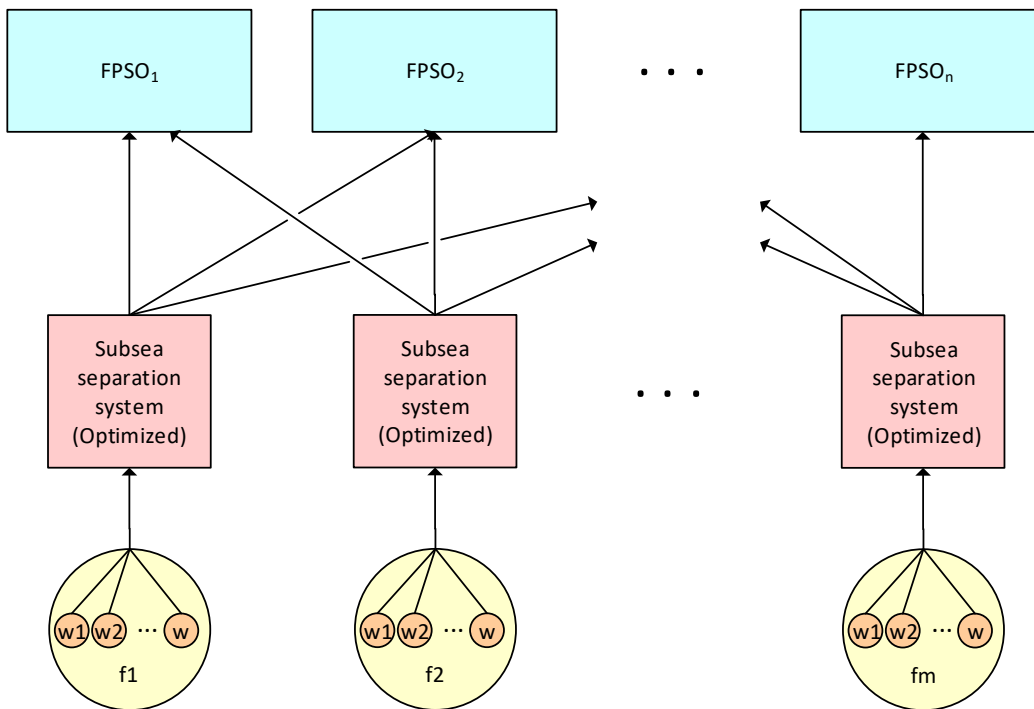


Figure 4.1: General superstructure for multi-field system with subsea processing.

Table 4.1: Binary and integer variables for multi-field model.

Variable	Description
$y_{t,f,j}$	Binary variable for installation of subsea equipment j in field f in time step t
$D_{t,f}$	Integer variable for number of wells drilled in field f in time step t
$N_{t,f}^w$	Integer variable for number of producing wells in field f at time step t
$z_{t,fpso}$	Binary variable for installation of FPSO $fpso$ in time step t
$z_{t,f,fpso}^c$	Binary variable for connecting FPSO $fpso$ to field f in time step t

4.2 Model

4.2.1 Objective Function

The objective of the model is to maximize the NPV of the entire operation over the time horizon.

$$\max \text{NPV} \quad (4.1)$$

The definition of the NPV is given in equation 3.2. The cash flow in time step t , is the difference between the total revenue and expenditures as illustrated by equation 4.2.

$$C_t^F = \text{REV}_t - \text{COST}_t \quad \forall t \quad (4.2)$$

The revenue in time step t is dependent on the production over all FPSOs of both oil and gas as presented in equation 4.3.

$$\text{REV}_t = \left(\sum_{fpso}^{N_{fpso}} O_{t,fpso} p^{oil} + \sum_{fpso}^{N_{fpso}} G_{t,fpso} p^{gas} \right) \alpha \quad \forall t \quad (4.3)$$

Here $O_{t,fpso}$ and $G_{t,fpso}$ are the production rates of oil and gas for FPSO $fpso$ at time step t respectively. The cost in time step t is composed of capital expenditures and operational expenses as illustrated by equation 4.4.

$$\text{COST}_t = \text{CAPEX}_t + \text{OPEX}_t \quad \forall t \quad (4.4)$$

The capital expenditures in time step t are the sum of the subsea equipment cost, the cost of the FPSO installations and the cost of drilling as presented in equation 4.5.

$$\text{CAPEX}_t = \sum_f^{N_f} \sum_j^{N_j} C_{t,f,j} + \sum_{fpso}^{N_{fpso}} C_{fpso}^{FPSO} z_{t,fpso} + \sum_f^{N_f} C_f^{drill} D_{t,f} \quad \forall t \quad (4.5)$$

Here $C_{t,f,j}$ is the cost of installing subsea unit j in field f at time step t , C_{fpso}^{FPSO} is the cost of installing FPSO $fpso$ and C_f^{drill} is the cost of drilling in field f . The operating expenses for time step t is given by equation 4.6.

$$\text{OPEX}_t = \sum_f^{N_f} (P_{t,f}^k + P_{t,f}^p + P_{t,f}^{MP}) \alpha p^{el} \quad \forall t \quad (4.6)$$

$P_{t,f}^k$, $P_{t,f}^p$, and $P_{t,f}^{MP}$ are the power consumption rates of the compressor, pump and multiphase pump for field f in time step t , respectively.

4.2.2 Mass Balances and Pressure Decline

The FPSO production rates of oil and gas can be expressed by equation 4.7.

$$O_{t,fpso} = \sum_f^{N_f} O_{t,f,fpso} \quad \forall t \quad \forall fpso \quad (4.7a)$$

$$G_{t,fpso} = \sum_f^{N_f} G_{t,f,fpso} \quad \forall t \quad \forall fpso \quad (4.7b)$$

Here, $O_{t,f,fpso}$ and $G_{t,f,fpso}$ are the production rates of oil and gas from field f to FPSO $fpso$ in time step t respectively. The production rate of oil is dependent on the number of wells drilled in the field up until time step t as illustrated by equation 4.8a. The gas flow is then calculated by using the gas oil ratio as presented in equation 4.8b.

$$\left. \begin{aligned} O_{t,f,fpso} &= N_{t,f}^w O_{t,f,fpso}^w \\ G_{t,f,fpso} &= GOR_f O_{t,f,fpso} \end{aligned} \right\} \quad \forall t \quad \forall f \quad \forall fpso \quad (4.8a)$$

$$(4.8b)$$

$O_{t,f,fpso}^w$ is here the oil flow rate from field f to FPSO $fpso$ in time step t per well. The well flow is constrained by the maximum deliverability as illustrated by equation 4.9.

$$O_{t,f,fpso}^w \leq Q_{t,f}^w \quad \forall t \quad \forall f \quad \forall fpso \quad (4.9)$$

The deliverability for each field is approximated by a third order polynomial in fraction of oil recovered, as done in the single-field model. It is assumed that each well in the field share the same production profile as given in equation 4.10.

$$Q_{t,f}^w = k_{1,f}^q f_{t-1,f}^3 + k_{2,f}^q f_{t-1,f}^2 + k_{3,f}^q f_{t-1,f} + k_{4,f}^q \quad \forall t \quad \forall f \quad (4.10)$$

The fraction of oil recovered from field f up until time t is given by equation 4.11.

$$f_{t,f} = \frac{\sum_{\tau=1}^t O_{\tau,f} \alpha}{O_f^{rec}} \quad \forall t \quad \forall f \quad (4.11)$$

Here O_f^{rec} is the recoverable amount of oil in field f , and $O_{t,f}$ is the total oil flow rate from field f in time step t . This oil flow rate must be the sum of all flows from the field in time step t , as illustrated by equation 4.12.

$$O_{t,f} = \sum_{fpso}^{N_{fpso}} O_{t,f,fpso} \quad \forall t \quad \forall f \quad (4.12)$$

A similar relation can be made for the total gas flow out from field f in time step t , as presented in equation 4.13

$$G_{t,f} = \sum_{fpso}^{N_{fpso}} G_{t,f,fpso} \quad \forall t \quad \forall f \quad (4.13)$$

The accumulated oil recovered from field f , can naturally not exceed the amount of recoverable oil in the field, which is ensured by equation 4.14.

$$\sum_{\tau=1}^t O_{\tau,f} \alpha \leq O_f^{rec} \quad \forall t \quad \forall f \quad (4.14)$$

The pressure decline for each field is assumed to be linear in the fraction of oil recovered from the field as implemented in the single-field model. The resulting pressure profile equations are presented in equation 4.15.

$$p_{t,f}^{res} = p_f^{init} - \beta_f f_{t,f} \quad \forall t \quad \forall f \quad (4.15)$$

In order to size the subsea equipment installed at each of the fields, the mass balances of each subsea system must be solved. This means setting up the mass balances for every unit and interconnection in the superstructure presented in figure 3.4 for each of the fields of the multifield superstructure shown in figure 2.4. The resulting set of equations take the form presented in equation 4.16.

$$\underline{\mathbf{A}} \underline{\mathbf{x}}_{t,f} = \underline{\mathbf{b}}_{t,f} \quad \forall t \quad \forall f \quad (4.16)$$

Here $\underline{\mathbf{A}}$ is the matrix defined in Chapter 3.2.2, $\underline{\mathbf{x}}_{t,f}$ is the vector of mass flows as denoted in figure 3.4 for field f in time step t and $\underline{\mathbf{b}}_{t,f}$ is the right hand side defined as follows:

$$\underline{\mathbf{b}}_{t,f} = \left[G_{t,f} \quad 0 \quad 0 \quad 0 \quad 0 \quad 0 \quad -O_{t,f} \quad 0 \quad 0 \quad 0 \quad 0 \quad 0 \quad 0 \quad 0 \quad 0 \right]^T \quad \forall t \quad \forall f \quad (4.17)$$

The mass flows to the unused subsea units must be set to zero, as previously done for the single-field model in Chapter 3. In this model, however, there are multiple fields, and the equipment can be installed at any time step of the horizon. This must be reflected by the constraints, as done in equation set 4.18

$$\left. \begin{aligned}
 x_{1,t,f} - U \sum_{\tau=1}^t y_{1,\tau,f} &\leq 0 & (4.18a) \\
 x_{2,t,f} - U \sum_{\tau=1}^t y_{2,\tau,f} &\leq 0 & (4.18b) \\
 x_{7,t,f} - U \sum_{\tau=1}^t y_{5,\tau,f} &\leq 0 & (4.18c) \\
 x_{10,t,f} - U \sum_{\tau=1}^t y_{5,\tau,f} &\leq 0 & (4.18d) \\
 x_{11,t,f} - U \sum_{\tau=1}^t y_{4,\tau,f} &\leq 0 & (4.18e) \\
 x_{5,t,f} - U \sum_{\tau=1}^t y_{6,\tau,f} &\leq 0 & (4.18f) \\
 x_{6,t,f} - U \sum_{\tau=1}^t y_{8,\tau,f} &\leq 0 & (4.18g) \\
 x_{15,t,f} - U \sum_{\tau=1}^t y_{11,\tau,f} &\leq 0 & (4.18h) \\
 x_{16,t,f} - U \sum_{\tau=1}^t y_{8,\tau,f} &\leq 0 & (4.18i)
 \end{aligned} \right\} \forall t \quad \forall f$$

If subsea unit j has not been installed in field f up until time step t , the mass flow to the subsea unit in time step t must be set to zero. However, if the unit is installed in time step t , the mass flow in this time step, and all following time steps are constrained by some upper limit U . The underlying logic presented in table 3.2 is still valid for equation set 4.18. In addition, the well flow from field f to FPSO f_{pso} should be zero if the relevant field and FPSO has not been connected up until time step t . This is ensured by equation 4.19.

$$O_{t,f,f_{pso}}^w - U \sum_{\tau=1}^t z_{\tau,f,f_{pso}}^c \leq 0 \quad \forall t \quad \forall f \quad \forall f_{pso} \quad (4.19)$$

4.2.3 Logical Conditions

The logical conditions related to the binary variables for the subsea equipment is similar to those presented for the single-field model in Chapter 3.2.3. However, in this model, these

conditions must hold for the entire time horizon and for all fields as well. In addition, if a field is not developed, no subsea equipment should be installed, which relaxes some of the equality constraints to inequality constraints. The resulting set of logical constraints is presented in equation 4.20 and 4.21.

$$\left. \begin{aligned} \sum_t^{N_t} (y_{3,t,f} + y_{5,t,f}) - 1 &\leq 0 & (4.20a) \end{aligned} \right\} \forall f$$

$$\left. \begin{aligned} \sum_t^{N_t} (y_{4,t,f} + y_{5,t,f}) - 1 &\leq 0 & (4.20b) \end{aligned} \right\} \forall f$$

$$\left. \begin{aligned} \sum_t^{N_t} (y_{6,t,f} + y_{8,t,f}) - 1 &\leq 0 & (4.20c) \end{aligned} \right\} \forall f$$

$$\left. \begin{aligned} \sum_t^{N_t} (y_{11,t,f} + y_{8,t,f}) - 1 &\leq 0 & (4.20d) \end{aligned} \right\} \forall f$$

$$y_{5,t,f} - y_{8,t,f} \leq 0 \quad (4.21a)$$

$$y_{8,t,f} = y_{9,t,f} = y_{10,t,f} \quad (4.21b)$$

$$y_{6,t,f} = y_{7,t,f} \quad (4.21c)$$

$$y_{11,t,f} = y_{12,t,f} \quad (4.21d)$$

The reasoning for including these constraints can be found in Chapter 3.2.3 for the single-field model. In addition, a piece of subsea equipment should not be installed multiple times in the same field during the time horizon, which is ensured by equation 4.22.

$$\sum_t^{N_t} y_{j,t,f} \leq 1 \quad \forall j \quad \forall f \quad (4.22)$$

Equation set 4.23 gives the logical conditions for the FPSOs and connections to the fields.

$$\sum_t^{N_t} z_{t,fpso} \leq 1 \quad \forall fpso \quad (4.23a)$$

$$\sum_{fpso}^{N_{fpso}} \sum_t^{N_t} z_{t,f,fpso}^c \leq 1 \quad \forall f \quad (4.23b)$$

$$z_{t,f,fpso}^c - \sum_{\tau}^{N_t} z_{\tau,fpso} \leq 0 \quad \forall t \quad \forall f \quad \forall fpso \quad (4.23c)$$

More specifically, equation 4.23a specifies that a FPSO can be installed only once during the time horizon. Equation 4.23b specifies that each field can produce to only a single FPSO during the time horizon. Equation 4.23c ensures that no connection between a field and a FPSO can be made before the corresponding FPSO has been installed. Equation set 4.24 gives the logical conditions for the drilling.

$$N_{t,f}^w = N_{t-1,f}^w + D_{t,f} \quad \forall t \quad \forall f \quad (4.24a)$$

$$N_{t,f}^w \leq N_f^{w,max} \quad \forall t \quad \forall f \quad (4.24b)$$

$$\sum_f^{N_f} D_{t,f} \leq D_t^{max} \quad \forall t \quad (4.24c)$$

$$\sum_f^{N_f} N_{t,f}^w \leq N^{w,max} \quad \forall t \quad (4.24d)$$

The number of producing wells for field f in time step t is equal to the number of producing wells in the previous time step plus the number of wells drilled in time step t , as ensured by equation 4.24a. Equation 4.24b constrains the total number of wells that can be drilled in field f to be less than some max-limit, $N_f^{w,max}$, for the field. Equation 4.24c specifies that there can only be drilled D_t^{max} wells over all fields per time step. Equation 4.24d limits the total number of wells that can be drilled during the time horizon.

4.2.4 Compressor and Pump Duties

All equations for duties and densities are identical to the ones presented for the single-field model in chapter 3.2.4, with the exception that each field now has its own set of equations as illustrated in equation set 4.25.

$$\left. \begin{aligned}
 P_{t,f}^k &= \frac{x_{3,t,f}}{\eta_k} \frac{R T_f}{M_m 3.6} \frac{\gamma}{\gamma - 1} \left(\frac{p_{2,f}}{p_{t,f}^{res}} \frac{\gamma-1}{\gamma} - 1 \right) \\
 P_{t,f}^p &= x_{11,t,f} \frac{p_{2,f} - p_{t,f}^{res}}{\rho_{oil} 3600 \eta_p} \\
 P_{t,f}^{MP} &= x_{10,t,f} \frac{g h_{t,f}}{3600 \eta_{MP}} \\
 \Delta P_{t,f} &= 0.0981 h_{t,f} \frac{\rho_{t,f}^{mix}}{\rho_{water}} \\
 \rho_{t,f}^{mix} &= \frac{O_{t,f} + G_{t,f}}{\frac{O_{t,f}}{\rho_{oil}} + \frac{G_{t,f}}{\rho_{t,f}^{gas}}} \\
 \rho_{t,f}^{gas} &= \frac{p_{t,f}^{res} M_m}{R T_f}
 \end{aligned} \right\} \forall t \quad \forall f \quad (4.25)$$

Note, however that it is assumed that the reservoir temperature is constant for each field.

4.2.5 Sizing and Cost Estimation

Since the subsea equipment can be installed at any time step of the horizon in any field, the cost of the equipment must include the time index as well as the field index. This means that each unit has its own cost variable for each field in each time step. Including this for the cost estimation equations given in section 3.2.5 gives the following set of cost correlations for the subsea equipment:

$$\left. \begin{aligned}
 C_{1,t,f} &= (24000 y_{1,t,f} + 46 A_{t,f}^{1.2}) f_{inst} f_{sub} f_I \\
 C_{2,t,f} &= (a_f^{sub} y_{2,t,f} + b_f^{sub} m_{t,f}^{sub,max}) f_{inst} f_{sub} f_I \\
 C_{3,t,f} &= (490000 y_{3,t,f} + 16800 (P_{t,f}^{k,max})^{0.6}) f_{inst} f_{sub} f_I \\
 C_{4,t,f} &= C_{pm,t,f} + \left(6900 y_4 + 206 \left(\frac{m_{t,f}^{p,max}}{\rho_o 3.6} \right)^{0.9} \right) f_{inst} f_{sub} f_I \\
 C_{pm,t,f} &= (-950 y_{4,t,f} + 1770 (P_{t,f}^{p,max})^{0.6}) f_{inst} f_{sub} f_I \\
 C_{5,t,f} &= 3000000 f_{inst} f_I y_5 \\
 C_{10,t,f} &= (a_{t,f}^{top} y_{10,t,f} + b_{t,f}^{top} m_{t,f}^{top,max}) f_{inst} f_I
 \end{aligned} \right\} \forall t \quad \forall f \quad (4.26)$$

Note that the model now includes a variable for the installed capacity for each unit in each field for each time step. This gives rise to an additional type of constraints presented in equation set 4.27.

$$\left. \begin{aligned} \sum_{\tau=1}^t P_{\tau,f}^{k,max} &\geq P_{t,f}^k \\ P_{t,f}^{k,max} - U y_{3,t,f} &\leq 0 \end{aligned} \right\} \quad \forall t \quad \forall f \quad (4.27a)$$

$$(4.27b)$$

Here 4.27a ensures that the power consumption rate of the compressor in field f in time step t does not exceed the capacity installed up until that time step. Equation 4.27b ensures that the capacity is installed only once, namely at the time step the compressor is installed in the system. Similar constraints are included for the pumps, separators and coolers, as presented in equation 4.28.

$$\left. \begin{aligned} \sum_{\tau=1}^t P_{\tau,f}^{p,max} &\geq P_{t,f}^p, & P_{t,f}^{p,max} - U y_{4,t,f} &\leq 0 \\ \sum_{\tau=1}^t m_{\tau,f}^{sub,max} &\geq x_{2,t,f}, & m_{t,f}^{sub,max} - U y_{2,t,f} &\leq 0 \\ \sum_{\tau=1}^t m_{\tau,f}^{top,max} &\geq x_{17,t,f}, & m_{t,f}^{top,max} - U y_{10,t,f} &\leq 0 \\ \sum_{\tau=1}^t m_{\tau,f}^{c,max} &\geq x_{1,t,f}, & m_{t,f}^{c,max} - U y_{1,t,f} &\leq 0 \end{aligned} \right\} \quad \forall t \quad \forall f \quad (4.28)$$

These equations combined with equation 4.22 ensures that the cost-variable for a unit in a given field can be nonzero only once in the time horizon. This cost is then dependent on the installed capacity and the installed capacity can not be exceeded during the time horizon. The cost of the transport lines and risers are given by equation 4.29a and 4.29b respectively.

$$C_{j,t,f} = (C_j^b f_j^s + C_j^{coat}) d_{f,fpso} y_{j,t,f} z_{t,f,fpso}^c \quad \forall j \in \{6, 8, 11\}, \quad \forall t, \quad \forall f, \quad \forall fpso \quad (4.29a)$$

$$C_{j,t,f} = (C_j^b f_j^s + C_j^{coat}) w_{fpso}^d y_{j,t,f} z_{t,f,fpso}^c \quad \forall j \in \{7, 9, 12\}, \quad \forall t, \quad \forall f, \quad \forall fpso \quad (4.29b)$$

Here, $C_j^b f_j^s$ and C_j^{coat} are the parameters presented in table 3.3. w_{fpso}^d is the water-depth and $d_{f,fpso}$ is the distance between field f and FPSO $fpso$. The costs are multiplied with the binary variable for installation of the unit in the field, $y_{j,t,f}$, and the binary variable for the connection of field f and FPSO $fpso$, $z_{t,f,fpso}^c$.

4.3 Case Studies

The multi-field model includes equation 4.1-4.29. The model was implemented in GAMS for two cases of different sizes, by adjusting the number of time steps in the horizon and the number of potential wells for the fields. Both cases included a system of three FPSOs and three potential fields. The resulting superstructure is given in figure 4.2. The implementation of case I in GAMS is given in appendix D.2.

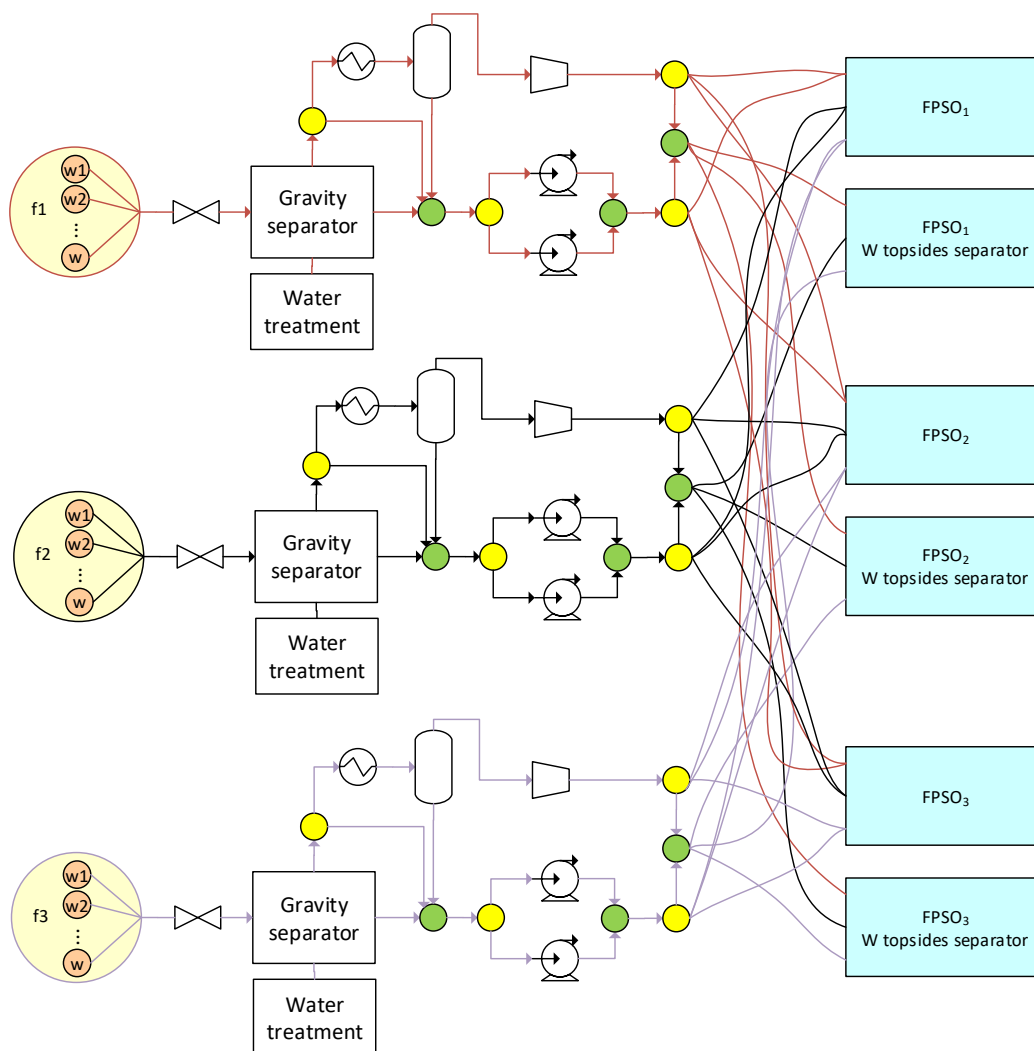


Figure 4.2: Superstructure for base case of multi-field model with three FPSOs and three fields.

4.3.1 Case I

Case I is a relatively small example, where the production from three fields to three potential FPSOs are optimized over a horizon of five time steps. The three fields have varying sizes, production profiles, gas ratios and initial pressures. A maximum of two wells can be drilled each time step for the system. The data for the fields is given in table 4.2.

Table 4.2: Parameters for the oil fields.

Parameter	Field			Unit
	1	2	3	
p_f^{init}	9000	6500	7000	[kPa]
O_f^{rec}	20	40	50	[Mton]
Q_f^0	5	10	20	[kbbl/day]
T_f	300	300	300	[K]
GOR_f	0.045	0.07	0.06	[-]
W_f^d	0.15	0.5	0.7	[km]
C_f^{drill}	50	75	90	[mill USD]
$N_f^{w,max}$	4	5	3	[-]

The distances from the proposed locations of the FPSOs and the fields are given in table 4.3.

Table 4.3: Distances between the proposed locations of the FPSOs and the fields of the base case.

		Field			Unit
		1	2	3	
	1	63.79	43.17	15.62	[km]
FPSO	2	20.03	24.00	30.26	[km]
	3	25.00	10.00	31.62	[km]

Table 4.4 shows the fixed cost of the proposed FPSOs and the water depth at each location.

Table 4.4: Fixed costs for FPSOs and water depths.

FPSO				
Parameter	1	2	3	Unit
C_{fpso}^{FPSO}	440	490	450	[Mill USD]
W_{fpso}^d	0.15	0.5	0.7	[km]

The size of the problem is given in table 4.5.

Table 4.5: Size of multi-field model for 3 FPSOs, 3 fields and 5 time steps (case I).

Number of equations	1,575
Number of variables	1,406
Number of discrete variables	270

The remaining parameters essential for the simulation is given in appendix B.

4.3.2 Case II

Case II is an extension of case I to a larger scale. The time horizon is now increased to 10 years, that is discretized into 10 time steps of 1 year duration. The number of wells that can be drilled per time step is increased to six, and the total number of wells that can be drilled during the entire time horizon is increased to 20. The number of potential wells for each field is increased as shown in table 4.6. All other parameters were unchanged from case I.

Table 4.6: Number of potential wells for the fields of case II.

Field			
	1	2	3
$N_f^{w,max}$	9	12	8

This increases the size of the problem as shown in table 4.7

Table 4.7: Size of multi-field model for three FPSOs, three fields and 10 time steps (case II).

Number of equations	3,095
Number of variables	2,811
Number of discrete variables	540

4.4 Results

This chapter presents the most significant results of the optimization of case I and case II for the multi-field model, including the calculated objective, computational time used, FPSO-installments, drilling schedule and subsea equipment installations. Additional output is presented in Appendix C. Both cases were run on the NEOS server for numerical optimization with a maximum time limit of eight hours. The cases were solved for two different solvers: DICOPT and BARON. The optimality gap for termination was set to 0.001 % for BARON.

4.4.1 Case I

The best solutions found by BARON and DICOPT for case I of the multi-field model is presented in table 4.8. Table 4.9 and 4.10 displays the overall best solution found by BARON. The former shows the scheduling for installation of FPSOs and drilling. The latter shows the installation of the subsea units for the fields.

Table 4.8: Best solutions found by DICOPT and BARON for case I.

	DICOPT	BARON
NPV [mill USD]	0	4090.2050
Optimality gap [-]	-	$\leq 1e-5$
Time [s]	0.048	1289.500

Table 4.9: Scheduling of drilling and installation of FPSOs for case I.

	$D_{t,f}$			$b_{t,fpso}$		
	Field 1	Field 2	Field 3	Fpso1	Fpso2	Fpso3
t1	0	0	2	0	0	1
t2	0	1	1	0	0	0
t3	0	2	0	0	0	0
t4	0	2	0	0	0	0
t5	1	1	0	0	0	0

Table 4.10: Installed subsea equipment for the fields of case I.

	Field 1	Field 2	Field 3
$y_{1,t,f}$	1	0	0
$y_{2,t,f}$	1	0	0
$y_{3,t,f}$	1	0	0
$y_{4,t,f}$	1	0	0
$y_{5,t,f}$	0	1	1
$y_{6,t,f}$	0	0	0
$y_{7,t,f}$	0	0	0
$y_{8,t,f}$	1	1	1
$y_{9,t,f}$	1	1	1
$y_{10,t,f}$	1	1	1
$y_{11,t,f}$	0	0	0
$y_{12,t,f}$	0	0	0
t	5	2	1

4.4.2 Case II

The best solutions found by DICOPT and BARON for case II is presented in table 4.11. The scheduling of drilling and FPSO-installations are displayed in table 4.12 for the best solution found by BARON. The installation of subsea units for the fields are illustrated in table 4.13.

Table 4.11: Best solutions found by DICOPT and BARON for case II.

	DICOPT	BARON
NPV [mill USD]	0	16184.87
Optimality gap [-]	-	0.294
Time [s]	0.396	28740

Table 4.12: Scheduling of drilling and installation of FPSOs for case II.

	$D_{t,f}$			$b_{t,fps0}$		
	Field 1	Field 2	Field 3	Fpso1	Fpso2	Fpso3
t1	0	0	6	0	0	1
t2	0	4	2	0	0	0
t3	0	6	0	0	0	0
t4	0	2	0	0	0	0
t5	0	0	0	0	0	0

Table 4.13: Installed subsea equipment for the fields of case II.

	Field 1	Field 2	Field 3
$y_{1,t,f}$	0	0	0
$y_{2,t,f}$	0	0	0
$y_{3,t,f}$	0	0	0
$y_{4,t,f}$	0	0	0
$y_{5,t,f}$	0	1	1
$y_{6,t,f}$	0	0	0
$y_{7,t,f}$	0	0	0
$y_{8,t,f}$	0	1	1
$y_{9,t,f}$	0	1	1
$y_{10,t,f}$	0	1	1
$y_{11,t,f}$	0	0	0
$y_{12,t,f}$	0	0	0
t	-	2	1

4.5 Discussion

As shown in table 4.8, the solution returned by DICOPT for case I has a NPV of zero, where all decision variables are set to zero. This is due to the fact that the relaxed NLP of the problem has a local maximum at zero, where all integer variables have integral values. The search performed by DICOPT is then terminated. A couple of different initial points and bounds were tested for the solver, without any improvement. The solution returned by BARON has an optimality gap at 0.001 %, which indicates that the solution is very close to, or at the global optimum. However, the computational time used by BARON is now considerably greater than compared to the single-field model. BARON uses close to half an hour to get the optimality gap at the specified limit of 0.001 %. Since a combinatorial problem of five time steps, three fields and three FPSOs is relatively small from a practical perspective, this indicates that the model formulation will be very hard to solve to global optimality for realistic cases. From table 4.5, the size of the optimization model for case I is significantly larger than the size of the single-field model in table 3.4. The time difference in computational time however, has increased disproportionately. This could be due to the fact that additional bilinear terms have been introduced in the model through constraints 4.8a and 4.29. This causes the multi-field model to include more non-convexities, which increases

the difficulty of obtaining the globally optimal solution. This could also be the reason why DICOPT does not perform as well for the multi-field model as for the single-field model. It should be noted however, that the optimal solution is found by BARON within the first two minutes of the search. The rest of the time is used to reduce the upper bound sufficiently to verify that the solution is indeed the global optimum.

Table 4.9 shows that FPSO3 is installed in time step 1 in the optimal solution found by BARON for case I. Since only one FPSO is installed during the time horizon, the only natural choice is to install it in the first time step to maximize the production over the time horizon. Although the fixed cost of the installed FPSO is higher than the fixed cost of FPSO1, the distances between the developed fields and the proposed location of FPSO3 are shorter on average, reducing the cost of the transport lines for the oil and the gas. From table 4.3 it can be seen that the distance from FPSO1 to field 3 is approximately half of the distance from FPSO3 to field 3. A possible solution could therefore have been to install both FPSOs and connect field 1 and 2 to FPSO 3, and field 3 to FPSO 1. However, the reduced cost of the pipelines does not outweigh the increased cost of an additional FPSO, as the distances are relatively short for the case. If the distance from field 3 to FPSO3 had been greater, the optimal solution might have been to install FPSO1 in time step 1 with a connection to field 3, and FPSO3 in time step 2 with connections to field 2 and field 1. This, however, would only be profitable if the production from field 3 alone could have supported the cost of the additional FPSO and the required subsea equipment in the short time horizon considered.

The optimal drilling schedule presented in table 4.9 shows that field 3 is the first field to be developed for case I. 2 wells are initially drilled in the first time step, before 1 extra well is drilled in time step 2. This is as expected since field 3 has significantly higher estimated well production profiles compared to the competing fields. The production is therefore maximized by ensuring that field 3 produces over the entire time horizon. In addition, table 4.2 shows that field 3 has the largest recoverable oil reserves. This means that the recovery factor will be generally lower for field 3 in the short time horizon considered, and the maximum deliverability for the field will therefore have a less steep descent. Although field 3 has the highest drilling cost of the fields, an additional well is drilled in time step 2, which means that the profit from increasing the number of wells still outweighs the fixed cost associated with drilling in the field, despite the production decline. The development of field 2 is also started in time step 2. The drilling continues here until the maximum limit for wells in the field is reached.

Table 4.10 shows that multiphase boosting with multiphase transport and rising were chosen

for both field 2 and field 3. For field 1, the optimal configuration of the subsea separation system was found to include separate phase compression and pumping for the gas and oil phase respectively, with multiphase transport and rising of the reservoir fluids. These results can be explained by several factors. First of all it should be noted that both field 2 and field 3 have high initial production rates from the well profile estimates. Table 4.2 also shows that the average gas oil ratio of the fields are high compared to the average gas oil ratio of field 1. When the number of wells drilled in field 2 and 3 in addition are higher than the number of wells drilled in field 1, this leads to significantly higher gas flow rates in the subsea systems of field 2 and 3. Since the cost of the subsea compressors are very sensitive to the installed capacity ($P_{t,f}^k$), multiphase boosting is chosen for these fields. It can also be seen from table 4.2 that the initial reservoir pressure of field 2 and 3 are lower than the initial reservoir pressure of field 1. The required pressure differential over the compressors would therefore have had to been greater for these fields to transport the gas to the FPSOs, which would require an even higher installed capacity for the potential subsea compressors. Since field 1 produces from a single well, has a low gas oil ratio, and a relatively high initial reservoir pressure, the installed capacity for the subsea compressor is low, and the total cost of the compressor is low compared to the fixed cost of the multiphase pump. Note, however, that the cost model used for the multiphase pump is highly uncertain as it is based on a very limited set of data, as discussed in Chapter 3.

Although field 1 is located fairly close to the installed FPSO, the reservoir fluids are transported through a multiphase transport line which requires the additional installation of a topside separator. The cost of the topside separator could have been avoided by transporting the gas and the oil separately over the short distance to the FPSO. However, from table 4.4, the water depth is at 700 meters, which gives a high cost for two separate sets of risers to the FPSO. In addition, the production rates from the field are relatively low, which reduces the cost of the required topside separator. The use of multiphase transport and rising is therefore optimal for the field, despite the fact that the phases are boosted separately. It should also be noted that all of the subsea equipment in table 4.10 are installed in the same time step as the development of the field takes place. The constraints in the model only specifies that the subsea equipment must be installed some time before production begins. However, since the NPV of the project is used as the objective function, the time value of money forces the investments and costs to be pushed back as far as possible without affecting the production.

It should be emphasized that case I is a relatively small example. The planning horizon of five time steps is not very realistic, and the operation should be optimized over the entire life

time of the fields. However, case I provides a simple base case that can be solved to global optimality, and the results from the case indicate that the model works as intended and gives solutions that seem reasonable. Case II is a more realistic case, where the planning horizon is set to 10 time steps of one year duration, and the number of potential wells in each field is increased. The number of fields and FPSOs are not changed, however. Still, table 4.7 shows that the size of the optimization problem has increased drastically from case I. Since the number of potential wells in each field is also increased, the amount of combinatorial possibilities of the system becomes even larger. BARON provides the best integer solution for the case. Table 4.12 shows that FPSO3 is installed in time step 1 as for case I. This makes sense as the reservoir parameters and costs are unchanged from the first case. The development of the fields also follow the same sequence as for case I, with the exception that field 1 is not developed during the time horizon. This can be explained from the fact that the number of potential wells are increased in each field, so that more wells can be placed in the profitable fields. Despite the fact that the production from field 2 and 3 declines over time, it is still more profitable to increase the number of wells in these large fields, than to invest in developing in field 1 for a smaller production. Especially since the maximum number of wells drilled over the time horizon is an active constraint (equation 4.24d). Table 4.13 shows that multiphase boosting, transport and rising still is chosen for both field 2 and 3 as for case I. This is to be expected as the number of producing wells are increased in each field, which lead to higher production rates that are favored by multiphase boosting as previously explained. This indicates that the obtained solution for case II of the multi-field model is a good integer solution for the problem. However, table 4.11 shows that the optimality gap of the problem is at 29% after the maximum computational time limit of eight hours was reached. This suggests that the obtained solution might be far from the global optimum of the problem. An optimality gap of this magnitude can be especially problematic due to the large values of the objective function. It seems that the model formulation creates too large and complex problems to be solved efficiently by a global solver like BARON when the number of time steps becomes large.

A suggestion for further work would therefore be to linearize the model. This could be done by applying piecewise linearization techniques, where the nonlinear functions are approximated by a series of linear segments. A MILP solver like CPLEX could then be applied to solve the linear formulation of the model. Since MILP solvers have reached a higher state of reliability and maturity than solvers used for MINLP-problems, the linear formulation would be solved much more efficiently. However, piecewise linearization requires additional binary variables to

represent the linear line segments. This could lead to a substantial increase in variables for the model. Adding more discretization points results in better approximations of the nonlinear functions, but also increases the computational time of the solver. The linearization procedure is therefore a trade-off between good approximations and computational effectiveness. After the MILP-model is solved, the solution could be used as an initial point for the MINLP-formulation to increase the possibility of identifying the true global optimum.

Chapter 5

Conclusion

The purpose of this thesis was to develop a MINLP-model for optimizing the planning and development of offshore oil field infrastructure with an integrated subsea separation system for each field. First, a MINLP-model was developed for a single field and FPSO-connection. The main objective of the model was to identify the set of subsea processing units that maximized the net present value of the operation over the given time horizon. The model was based on several assumptions regarding the field characteristics and required deterministic values for several parameters including initial reservoir pressure, the size of the reservoir and the average gas oil ratio over the time horizon.

A superstructure was generated for the system based on the different possibilities for boosting and transportation of the phases and was used as a basis for the formulation of the optimization model. The oil flowrate from the field was constrained by the maximum deliverability which was approximated by a third order polynomial in the fraction of oil recovered from the field. By solving the mass balances of the system for each time step, the capacity of the potential units were calculated and used to approximate the cost. The single-field model was implemented in GAMS and solved on the NEOS server for two cases with different reservoir sizes, production rates, pressures, tie-back distances and water depths. Both cases were solved to global optimality by BARON, and it was showed that different configurations of the flowsheet were optimal for the two cases, depending on the reservoir parameters. However, the model results do not provide good indicators for actual economic profitability of the project as the model only estimates the costs necessary for comparing the potential configurations. In addition, the results are highly dependent on the reliability of the cost equations, which makes the results somewhat questionable as there is limited data for cost correlations

of multiphase pumps.

The single-field model was extended to include multiple potential fields and FPSOs as well as scheduling of the installations and drilling over the time horizon. Additional binary and integer variables were introduced to represent the potential installation of FPSOs, field-connections and number of wells to be drilled in each field for each time step. The superstructure of the subsea separation system was included for each of the potential fields in the model. The resulting MINLP-model was implemented in GAMS and solved on the NEOS server for two different cases of three potential FPSOs and three fields. The first case was a relatively small example, with few potential wells, that was optimized over a time horizon of five steps. BARON was able to provide a solution with an optimality gap below 0.001 %, which indicated that the solution was very close to or at the global optimum. Case II was a more realistic case with more potential fields that was optimized over a time horizon of 10 time steps. After the maximum computational time limit of 8 hours was reached, the best solution returned had an optimality gap of 29%, which indicated that the solution found might be far from the global optimum, and that the model formulation produces too big and complex optimization problems to be efficiently solved by a global solver like BARON for a high number of time steps.

5.1 Future Work

To efficiently solve the model for a high number of time steps, the formulation could be linearized by appropriate linearization techniques including piecewise linearization. This would allow the model to be solved by powerful solvers developed for MILP problems such as CPLEX and GUROBI. The solution of the MILP problem could then be used as an initial point for the MINLP formulation. The operating conditions of the subsea separation systems should also be included in the model formulation as decision variables. This would allow for simultaneous optimization of process structure, scheduling and operating conditions. However, it would also require appropriate models for the processing units as well as an additional set of constraints to ensure efficient and safe production. This would complicate the model even further, which emphasizes the need for a linear formulation of the model. Lastly, a better cost estimation model for the multiphase pump should be developed to give more credence to the results of the model. Alternatively, uncertainty could be introduced in the cost of the multiphase pump to produce a stochastic programming problem.

List of Symbols

Symbol	Unit	Description
a_j	[-]	Constant cost coefficient for subsea unit j
$A_{t,f}$	[m ²]	Installed heat transfer area in field f in time step t
$\underline{\mathbf{A}}$	[-]	Mass balance matrix
b_j	[-]	Cost coefficient for variable cost of subsea unit j
$\underline{\mathbf{b}}_{t,f}$	[ton/h]	RHS for mass balance in field f for time step t
C_0	[mill USD]	Investment cost
C_j	[mill USD]	Cost of subsea unit j
$C_{j,t,f}$	[mill USD]	Cost of installing subsea unit j in field f in time step t
C_f^{drill}	[mill USD]	Drilling cost for field f
C_t^F	[mill USD]	Cash flow in time step t
C_{fpso}^{FPSO}	[mill USD]	Installation cost of $fpso$
$CAPEX_t$	[mill USD]	Capital expenditure for time step t
$COST_t$	[mill USD]	Total cost in time step t
C_p	[J/kgK]	Heat capacity
$d_{f,fpso}$	[km]	Distance from field to $fpso$
$D_{t,f}$	[-]	Number of wells drilled in field f in time step t
f_{inst}	[-]	Cost factor for installation
f_{sub}	[-]	Cost factor for subsea operation
f_I	[-]	Cost factor for price changes in time
$f_{t,f}$	[-]	Fraction of oil recovered from field f by time t
g	[m/s ²]	Gravitational acceleration
$G_{t,f}$	[ton/h]	Gas flow rate from field f in time step t
$G_{t,fpso}$	[ton/h]	Total gas flow rate to $fpso$ in time step t
$G_{t,f,fpso}$	[ton/h]	Gas flow rate from field f to $fpso$ in time step t

GOR_f	[ton/ton]	Gas oil ratio for field f
$h_{t,f}$	[m]	Head for MP pump in field f in time step t
j	[-]	Index for subsea equipment
k_f^q	[ton/h]	Coefficients for polynomial used for Q_t
$m_{t,f}^{max}$	[ton/h]	Maximum installed flow capacity for unit in field f for time step t
M	[ton/kmol]	Molar mass
n	[-]	Exponential cost factor
N_t	[-]	Number of time steps in time horizon
N_j	[-]	Number of equipment pieces in subsea system
$N_{t,f}^w$	[-]	Number of producing wells in field f in time step t
NPV	[mill USD]	Net present value
$O_{t,f}$	[ton/h]	Oil flow rate from field f in time step t
$O_{t,fpso}$	[ton/h]	Total oil flow rate to $fpso$ in time step t
$O_{t,f,fpso}$	[ton/h]	Oil flow rate from field f to $fpso$ in time step t
$O_{t,f,fpso}^w$	[ton/h]	Oil flow rate per well from field f to $fpso$ in time step t
O_f^{rec}	[ton/h]	Total amount of recoverable oil from field f
$OPEX_t$	[mill USD]	Operating expenses for time step t
$p_{t,f}^{res}$	[kPa]	Reservoir pressure for field f in time step t
p_f^{init}	[kPa]	Initial reservoir pressure for field f
$P_{t,f}$	[kW]	Power consumption rate of subsea unit in field f in time step t
$P_{t,f}^{max}$	[kW]	Maximum power capacity installed for unit in field f in time step t
$Q_{t,f}^w$	[ton/h]	Deliverability of oil per well in field f for time step t
r	[-]	Interest rate
R	[kJ/kmolK]	Universal gas constant
REV_t	[mill USD]	Revenue in time step t
t	[-]	Index for time step
T_f	[K]	Reservoir temperature of field f
ΔT_{lm}	[K]	Logarithmic mean temperature difference
U	[ton/h]	Upper limit for mass flows
U_h	[W/m ² K]	Heat transfer coefficient
W_{fpso}^d	[km]	Water depth for $fpso$
$\underline{\mathbf{x}}_{t,f}$	[ton/h]	Total mass flow vector for field f in time step t
$y_{j,f,t}$	[-]	Binary variable for installing subsea unit j in field f in time step t
$z_{t,fpso}$	[-]	Binary variable for installing $fpso$ at time step t
$z_{t,f,fpso}^c$	[-]	Binary variable for connecting field f to $fpso$ in time step t

CHAPTER 5. CONCLUSION

α	[h]	Operating hours per time step
β_f	[-]	Proportionality constant for pressure decline of field f
γ	[-]	heat capacity ratio
η	[-]	Efficiency
ρ	[ton/m ³]	Density

Bibliography

- [1] Carlos A. Henao. *A superstructure modeling framework for process synthesis using surrogate models*. Thesis, The University of Wisconsin-Madison, 2012.
- [2] Vijay Gupta and Ignacio E. Grossmann. An efficient multiperiod minlp model for optimal planning of offshore oil and gas field infrastructure. *Industrial & Engineering Chemistry Research*, 51(19):6823–6840, 2012.
- [3] A. S. Lee and J. S. Aronofsky. A linear programming model for scheduling crude oil production. *Journal of Petroleum Technology*, 10(07):51–54, 1958.
- [4] Lester Claud Frair. *Economic optimization of offshore oil field development*. Thesis, The University of Oklahoma., 1973.
- [5] Rob Perry and Reda Akdim. Reviewing trends in subsea processing. *Offshore*, 71(5):116, 2011.
- [6] Jorge Moreno-Trejo, Rajesh Kumar, and Tore Markeset. Mapping factors influencing the selection of subsea petroleum production systems: a case study. *International Journal of System Assurance Engineering and Management*, 3(1):6–16, 2012.
- [7] J.C. Jones. *Hydrocarbon Process Safety - A Text for Students and Professionals (2nd Edition)*. Whittles Publishing, 2014.
- [8] Naeim Nouri Samie. *Practical engineering management of offshore oil and gas platforms*. Gulf Professional Publishing, 2016.
- [9] Denis Babusiaux. *Oil and Gas Exploration and Production - Reserves, Costs, Contracts (3rd Edition Revised and Updated)*. Editions Technip, 2011.
- [10] R Fantoft. Subsea gas compression-challenges and solutions. In *Offshore Technology Conference*, 2005.

- [11] O.T McClimans, R Fantoft, et al. Status and new developments in subsea processing. In *Offshore Technology Conference*, 2006.
- [12] Simon R.H. Davies, William Bakke, Rune Mode Ramberg, Roger Oen Jensen, et al. Experience to date and future opportunities for subsea processing in statoilhydro. In *Offshore Technology Conference*, 2010.
- [13] Van Khoi Vu, Rune Fantoft, Chris K Shaw, Henning Gruehagen, et al. Comparison of subsea separation systems. In *Offshore Technology Conference*, 2009.
- [14] Ole Økland, Simon R. Davies, Rune M. Ramberg, and Hege Rognø. Steps to the subsea factory. In *Offshore Technology Conference Brasil*, 2013.
- [15] Eivind Flatlandsmo, Mari Brænden Bordal, and John-Haakon Krøke Medby. Subsea gas boosting laboratory: Design and construction. Master’s thesis, NTNU, 2016.
- [16] Torstein Vinterstø, Bjørn Birkeland, Rune Mode Ramberg, Simon Davies, Pål Eirik Hedne, et al. Subsea compression–project overview. In *Offshore Technology Conference*, 2016.
- [17] Bernt Bjerkreim, Snorre Frydenlund, John Arild Lie, Knut Ola Staver, Karl Olav Haram, Bjørn Nystad, Håkon Skofteland, Hans Gedde, Alberto Tesei, Michel Postic, et al. Ormen lange subsea compression pilot system. In *Offshore Technology Conference*, 2009.
- [18] Hector Yeomans and Ignacio E. Grossmann. A systematic modeling framework of superstructure optimization in process synthesis. *Computers & Chemical Engineering*, 23(6):709–731, 1999.
- [19] Lingxun Kong, S. Murat Sen, Carlos A. Henao, James A. Dumesic, and Christos T. Maravelias. A superstructure-based framework for simultaneous process synthesis, heat integration, and utility plant design. *Computers & Chemical Engineering*, 91:68–84, 2016.
- [20] Gary R. Kocis and Ignacio E. Grossmann. A modelling and decomposition strategy for the minlp optimization of process flowsheets. *Computers & Chemical Engineering*, 13(7):797–819, 1989.
- [21] Jorge Nocedal and Stephen J. Wright. *Numerical Optimization*. Springer Series in Operations Research and Financial Engineering. Springer New York, 1999.

BIBLIOGRAPHY

- [22] GAMS Development Corporation, Washington, DC, USA. *GAMS - The Solver Manuals, GAMS Release 24.8*, 2018.
- [23] Lorenz T. Biegler, Ignacio E. Grossmann, and Arthur W. Westerberg. *Systematic methods of chemical process design*. Prentice Hall PTR, 1997.
- [24] Frederick S. Hillier and Gerald J. Lieberman. *Introduction to operations research*. McGraw-Hill Education, 2015.
- [25] Pietro Belotti, Christian Kirches, Sven Leyffer, Jeff Linderoth, James Luedtke, and Ashutosh Mahajan. Mixed-integer nonlinear optimization. *Acta Numerica*, 22:1–131, 2013.
- [26] Marco A. Duran and Ignacio E. Grossmann. An outer-approximation algorithm for a class of mixed-integer nonlinear programs. *Mathematical programming*, 36(3):307–339, 1986.
- [27] Arthur M. Geoffrion. Generalized benders decomposition. *Journal of optimization theory and applications*, 10(4):237–260, 1972.
- [28] Leo Liberti. Introduction to global optimization. *Lecture of Ecole Polytechnique, Palaiseau F*, 91128:12, 2008.
- [29] R. Sinnott and G. Towler. *Chemical Engineering Design 5th edition*. Elsevier Ltd., Oxford, 2009.
- [30] Manoochehr Bozorgmehrian. *Sizing and Selection Criteria for Subsea Multiphase Pumps*. Thesis, University of Houston, 2013.
- [31] Håvard Brandt, Bjørn Nilberg, and Robin Pitblado. Life cycle cost analysis of subsea multiphase booster pumps. Technical report, Det Norske Veritas, 2001.
- [32] Bai Yong. *Subsea engineering handbook*. Elsevier Science, 2010.
- [33] Joseph Czyzyk, Michael P. Mesnier, and Jorge J. Moré. "The NEOS Server". *IEEE Journal on Computational Science and Engineering*, 5(3):68 — 75, 1998.
- [34] Factpages Norwegian Petroleum Directorate (NPD). <http://factpages.npd.no/factpages/>. Accessed: 25.05.2018.
- [35] Crude oil & natural gas prices. <https://www.bloomberg.com/energy>. Accessed: 08.05.2018.

BIBLIOGRAPHY

- [36] M. Thombre, M. Lund, and H. Betten. *Subsea Separation*. Process design project, NTNU, 2015.

Appendix A

Cost Estimation of Separators

This chapter shows how the simplified cost equations 3.32a and 3.32b are derived to approximate separator cost as a function of total mass flow. The basis for the approximations are the more rigorous cost estimation models shown in equation A.1a and A.1b [29].

$$C_{s,vertical} = (10000 + 29 m_{shell}^{0.85}) \quad (\text{A.1a})$$

$$C_{s,horizontal} = (8800 + 27 m_{shell}^{0.85}) \quad (\text{A.1b})$$

Here m_{shell} is the shell mass of the vessel, given by equation A.2

$$m_{shell} = \pi D_v L_v \tau_w \rho \quad (\text{A.2})$$

D_v and L_v are the diameter and length of the vessel respectively. τ_w is the wall thickness and ρ is the material density. In order to find the shell mass, the diameter and the length of the separator must be estimated. This is done for the topside separator and the subsea separator in the following two sections.

A.1 Topside Separator

The topside separator should be designed as a horizontal separator as the liquid content is high in the multiphase flow. The settling velocity of the droplets is estimated by equation A.3

$$u_s = 0.07 \left(\frac{\rho_L - \rho_v}{\rho_v} \right)^{0.5} \quad (\text{A.3})$$

where ρ_L is the density of the oil and ρ_v is the density of the gas. The required vapor residence time for the droplets to settle is then given by equation A.4.

$$\tau_g^{req} = \frac{h_v}{u_s} = \frac{D_v}{u_s} \quad (\text{A.4})$$

h_v is the liquid height, here assumed to be half of the vessel diameter. However, the actual residence time of the vapour is given by the fraction of the vessel length and the vapour velocity, as illustrated in equation A.5.

$$\tau_g = \frac{L}{u_v} = \frac{L}{q_v} \frac{Ac}{8} = \frac{\pi D_v^2 L_v}{8 q_v}, \quad (\text{A.5})$$

where q_v is the volumetric vapour flow rate and L_v is the vessel length. Since the operating pressure is high, the vessel length is set 5 times the vessel diameter as a general guideline. The vessel diameter can then be solved by combining equation A.4 and A.5 which produces equation A.6

$$D_v = \sqrt{\frac{4 q_v}{5 \pi u_s}} \quad (\text{A.6})$$

The hold up time for the liquid can be calculated by equation A.7.

$$\tau_l = \frac{\text{Liquid volume}}{\text{Liquid flowrate}} = \frac{\pi D_v^2 L}{8 q_l} \quad (\text{A.7})$$

For this model, a minimum holdup-time of 10 minutes is assumed (τ_l^{req}). If the calculated hold-up time from equation A.7 is unsatisfactory, the diameter is increased by the factor:

$$f = \sqrt{\left(\frac{\tau_l^{req}}{\tau_l} \right)} \quad (\text{A.8})$$

For the average GOR, oil density and gas density of the field, the separator cost can be calculated for a set of total mass flows in the relevant range. The constants a_{top} and b_{top} can then found from regression. This simplifies the optimization model significantly which leads to a more efficient solution process. Figure A.1 shows the data set of costs calculated

for various total mass flows for the conditions of the field in case I of the single-field model. Linear regression was performed for the log-transformed data in the region of interest, which yielded a power regression model. Similar regression was done for all fields in both the single-field and the multi-field model. The resulting coefficients are presented in table B.3 and B.5.

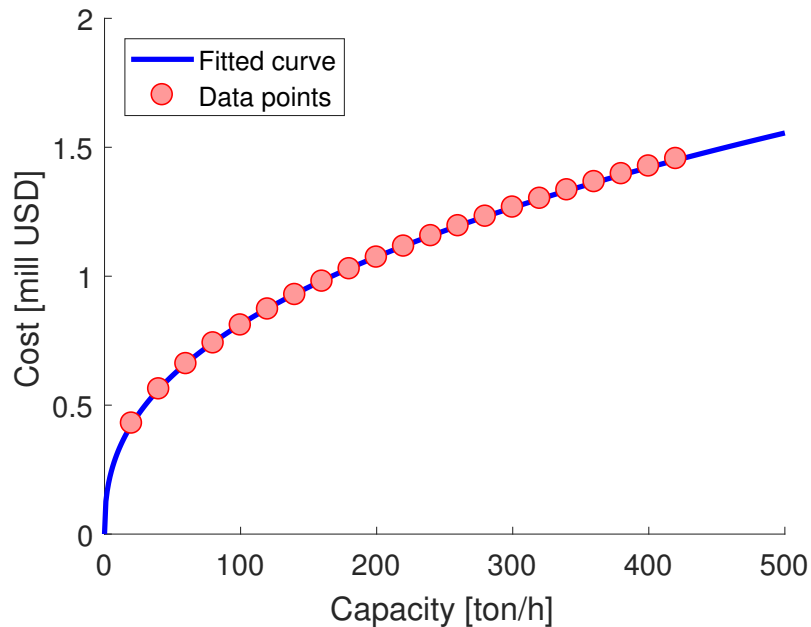


Figure A.1: Cost of topside separator for case I of the single-field model as a function of total multiphase mass flow.

A.2 Subsea Separator

The subsea separator is designed as a vertical separator due to the low liquid content in the flow. The settling velocity is given by equation A.3. The diameter of the vessel must be large enough for the droplets to settle out, which produces equation A.9.

$$D_v = \sqrt{\frac{4 q_v}{\pi u_s}} \quad (\text{A.9})$$

The height of the vessel is approximated by equation A.10

$$L = L_h + \max\{0.5 D_v, 0.6\text{m}\} + \max\{D_v, 1\text{m}\} + 0.4 \quad (\text{A.10})$$

where L_h is the liquid height, which can be calculated by equation A.11

$$L_h = \frac{qt \tau_{holdup}}{A_c} \quad (\text{A.11})$$

τ_{holdup} is the hold up time in the vessel, assumed to be 10 minutes for the purpose of this model. Similar to the previous section, the cost of the subsea separator can be calculated for a variety of total mass flows for the conditions of a field. The cost coefficients a_{sub} and b_{sub} for that specific field can then be obtained by regression over the region of interest. Figure A.1 shows the data set of costs calculated for a set of total mass flows for the conditions of the field in case I of the single-field model. Linear regression was performed on the region of interest to obtain the cost coefficients. Similiar regression was performed on all other fields from both the single-field and the multi-field model to obtain the cost correlation. The resulting coefficients are presented in table B.3 and B.5.

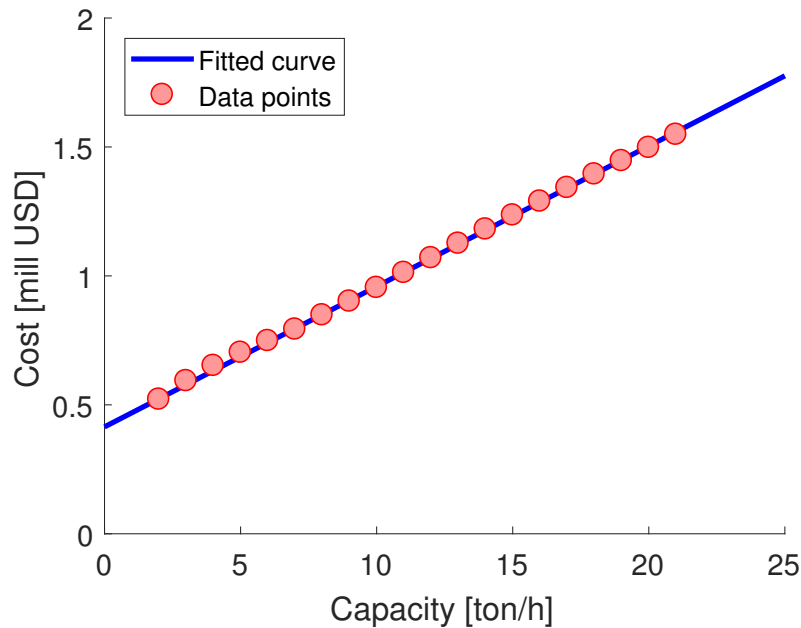


Figure A.2: Cost of subsea separator for case I of the single-field model as a function of total mass flow.

Appendix B

Simulation Parameters

This chapter presents the parameters used for the simulation of the case studies. The parameters that were common for all simulations are presented in table B.1.

Table B.1: Simulation parameters common for all cases.

Parameter	Value	Unit
p_{oil} [35]	69.86	[USD/bbl]
p_{gas} [35]	2.76	[USD/MMBTU]
p_e [29]	0.12	[USD/kWh]
r	0.10	[-]
α	8000	[h/year]
η_k	0.75	[-]
η_p	0.75	[-]
η_{MP}	0.75	[-]
f_{inst} [29]	4.208	[-]
f_I [29]	1.1035	[-]
f_{sub} [36]	3	[-]
U_h [29]	20	[W/m ² K]
ΔT_{lm}	20	[K]
ΔT	2.5	[K]

B.1 Single-Field Model

The coefficients for maximum oil deliverability and pressure decline for case I & II of the single-field model is presented in table B.2.

Table B.2: Coefficients for oil deliverability and pressure decline for case I & II (single-field model).

Parameter	Case I	Case II	Unit
k_1^q	-250	-1500	[ton/h]
k_2^q	375	2250	[ton/h]
k_3^q	-215	-1200	[ton/h]
k_4^q	90	450	[ton/h]
β	6000	4000	[kPa]
P_{boost}	12000	15000	[kPa]

The cost coefficients of the separators are given in table B.3 in accordance with the derivation procedure presented in appendix A.

Table B.3: Cost coefficients for separators case I & II (single-field model).

Parameter	Case I	Case II
a_{sub}	0.414	0.421
b_{sub}	0.054	0.065
a_{top}	0.127	0.127
b_{top}	0.403	0.403

B.2 Multi-Field Model

The parameters for maximum oil deliverability and pressure decline for the cases in the multi-field model is presented in table B.4. The cost coefficients for the separators of the fields of case I and II of the multi-field model is given in table B.5, in accordance with the derivation procedure shown in appendix A.

Table B.4: Coefficients for oil deliverability and pressure decline for case I & II (multi-field model).

Parameter	Field			Unit
	1	2	3	
k_1^q	-100	-80	-400	[ton/h]
k_2^q	150	120	600	[ton/h]
k_3^q	-78	-96.25	-312.5	[ton/h]
k_4^q	28.125	56.25	112.5	[ton/h]
β	6000	3500	4200	[kPa]
p_{boost}	11000	12000	14000	[kPa]

Table B.5: Cost coefficients for separators case I & II (multi-field model).

Parameter	Field		
	1	2	3
a_f^{sub}	0.414	0.419	0.417
b_f^{sub}	0.054	0.062	0.060
a_f^{top}	0.143	0.119	0.127
b_f^{top}	0.406	0.401	0.403

Appendix C

Simulation Output Data

C.1 Single-Field Model

Table C.1: Installed equipment costs for the single-field model (case I & case II).

Unit cost	Case I	Case II
	[Mill USD]	[Mill USD]
C_1	0.33	0
C_2	0.71	0
C_3	10.26	0
C_4	0.58	0
C_5	0	13.93
C_6	1.48	0
C_7	0.26	0
C_8	0	41.30
C_9	0	2.56
C_{10}	0	1.525
C_{11}	3.65	0
C_{12}	0.56	0

Table C.2: Installed equipment capacities for the single-field model (case I & case II).

Parameter	Case I	Case II	Unit
P_{max}^k	87.78	0	[kW]
P_{max}^p	118.84	0	[kW]
m_{max}^p	93.05	0	[ton/h]
m_{max}^{sub}	5.40	0	[ton/h]
m_{max}^{top}	0	477	[ton/h]
A	25.65	0	[m ²]

C.2 Multi-Field Model

Table C.3: Installed equipment costs for the multi-field model (case I & case II).

Eq. cost Mill USD	Case I			Case II		
	Field 1	Field 2	Field 3	Field 1	Field 2	Field 3
C ₁	0.340	0	0	0	0	0
C ₂	0.482	0	0	0	0	0
C ₃	7.954	0	0	0	0	0
C ₄	0.273	0	0	0	0	0
C ₅	0	13.931	13.931	0	13.931	13.931
C ₆	0	0	0	0	0	0
C ₇	0	0	0	0	0	0
C ₈	14.750	5.900	18.656	0	5.900	18.656
C ₉	2.989	2.989	2.989	0	2.989	2.989
C ₁₀	0.555	1.185	1.305	0	1.514	1.803
C ₁₁	0	0	0	0	0	0
C ₁₂	0	0	0	0	0	0

Table C.4: Installed equipment capacities for the multi-field model (case I & case II).

Parameter	Case I			Case II			
	Field 1	Field 2	Field 3	Field 1	Field 2	Field 3	
P_{max}^k	13.752	0	0	0	0	0	[kW]
P_{max}^p	24.740	0	0	0	0	0	[kW]
m_{max}^p	28.188	0	0	0	0	0	[ton/h]
m_{max}^{sub}	1.266	0	0	0	0	0	[ton/h]
m_{max}^{top}	28.188	308.175	324.388	0	568.657	722.873	[ton/h]
A	6.011	0	0	0	0	0	[m ²]

Appendix D

GAMS Code

This chapter presents the source code for the implemented optimization models in GAMS. Section D.1 gives the implementation of case I of the single-field model. Section D.2 gives the implementation of case I of the multi-field model.

D.1 Single-Field Model

```
1  $Title Single field MINLLP model.

3  $OnText
4  MINLP-model for identifying the optimal set of subsea process units and
5  production for a single field connected to a FPSO.
6  CASE I
7  $OffText

9  *Defining symbol for end of line comment.
10 $eolcom ->

12 *Declaring sets.
13 Sets
14     t "steps in time horizon" /t1*t10/
15     i "index for mass flows of subsea separation system" /i1*i17/
16     j "index for subsea equipment in system" /j1*j12/
17     k "index for mass balances"/k1*k13/
18     l(k) "subset of mass balance indices with zero-elements on RHS"
19     /k2,k3,k4,k5,k6,k8,k9,k10,k11,k12,k13/
```

APPENDIX D. GAMS CODE

```
20      s(t) "years following year 1";

22  *Defining sets
23      s(t) = yes$(ord(t) gt 1);
24      alias(tau,t);          -> additional alias set for the time steps.

26  *Defining parameters for the model
27  Parameters

29  *Upper bound for mass flows
30      U "upper limit for mass flows" /1000/

32  *Reservoir parameters
33      d "distance to field from FPSO in km" /8/
34      w_d "water depth in km" /0.2/
35      O_REC "Recoverable oil in ton" /25500000/
36      p_init "Initial pressure kPa" /9000/
37      gor "gas oil ratio" /0.06/
38      beta "proportionality constant for pressure decline" /6000/
39      -> coefficients for production decline curve.
40      k1 /-250/
41      k2 /375/
42      k3 /-215/
43      k4 /90/

46  *Economic factors
47      r "discount rate" /0.1/
48      p_bbl "price per barrel oil" /57.30/
49      p_g "price natural gas" /2.61/
50      alfa "operating hours per year" /8000/
51      p_e "price for electricity" /0.09/
52      f_inst "installation factor" /4.208/
53      f_sub "factor for installation subsea" /3/
54      f_I "scaling economics for inflation" /1.1035/
55      f_I_MP "scaling economics for MP pump" /1.3738/
56      f_s_fm "economic size factor for multiphase flowline" /1.00/
57      f_s_rm "economic size factor for multiphase riser" /1.70/
58      f_s_fo "economic size factor for oil flowline" /0.72/
59      f_s_ro "economic size factor for oil riser" /1.1/
60      f_s_fg "economic size factor for gas flowline" /0.15/
61      f_s_rg "economic size factor for gas riser" /0.5/
```

APPENDIX D. GAMS CODE

```

62      c.b.rigid "base cost for rigid pipe lines" /0.230/
63      c.b.flex "base cost for flexible pipe lines" /2.300/
64      c.MP.coat "coating cost multiphase pipes" /0.360/
65      c.o.coat "coating cost oil pipes" /0.290/
66      c.g.coat "coating cost gas pipes" /0.150/
67      a.sub "cost factor for subsea separator" /0.414/
68      b.sub "cost factor for subsea separator" /0.054/
69      b.top "cost factor for subsea separator" /0.127/
70      n.top "cost factor for subsea separator" /0.403/

72  *compressor
73      p2 "pressure out kPa" /12000/
74      gamma "Cp over Cv" /1.557488545/
75      eff.k "effectivity" /0.75/
76      Te "Temperature" /300/

78  *oil pump
79      d.oil "density of oil" /0.844/
80      eff.p "adiabatic efficiency pump" /0.75/

82  *Multiphase pump
83      eff.MP "multiphase pump efficiency" /0.75/
84      d.water "density of water tonne per m3" /1/

86  *Heat exchanger
87      LMTD "logarithmic mean temp difference" /19.6/
88      dT "temperature difference (out-in)" /2.5/
89      Cp.g "Heat capacity of gas" /2681/
90      U.h "heat transfer coefficient" /20/

92  *Other factors and constans
93      Rc "gas constant J|molK" /8.314/
94      Mm "molar mass natural gas" /16.8036/
95      bbl.m3 "barrels per cubic meter" /6.29/
96      MMBTU.m3 "MMBTU per cubic meter" /0.0354/
97      d.gas.std "density of gas (std conditions) [ton|m3]" /0.000712/;

99  Table A(k,i) "Mass balance matrix"
100      i1  i2  i3  i4  i5  i6  i7  i8  i9  i10  i11  i12  i13  i14  i15  i16  i17
101  k1      1   0   0   0   0   0   1   0   0   0   0   0   0   0   0   0
102  k2      1  -1   0   0   0   0   0   0   0   0   0   0   0   0   0   0
103  k3      0  0.05  0   0   0   0   0  -1   0   0   0   0   0   0   0   0

```

APPENDIX D. GAMS CODE

```

104 k4      0 -1  1  0  0  0  0  1  0  0  0  0  0  0  0  0  0
105 k5      0  0 -1  1  0  0  0  0  0  0  0  0  0  0  0  0  0
106 k6      0  0  0 -1  1  1  0  0  0  0  0  0  0  0  0  0  0
107 k7      0  0  0  0  0  0  1  1 -1  0  0  0  0  0  0  0  0
108 k8      0  0  0  0  0  0  0  0 -1  1  1  0  0  0  0  0  0
109 k9      0  0  0  0  0  0  0  0  0 -1  0  1  0  0  0  0  0
110 k10     0  0  0  0  0  0  0  0  0  0 -1  0  1  0  0  0  0
111 k11     0  0  0  0  0  0  0  0  0  0  0  1  1 -1  0  0  0
112 k12     0  0  0  0  0  0  0  0  0  0  0  0  0 -1  1  1  0
113 k13     0  0  0  0  0  1  0  0  0  0  0  0  0  0  0  1 -1;

```

115 **Defining variables*

116 **Positive variables**

```

117      x(i,t)  "Mass flow i in time t"
118      O(t)    "Oil production rate of field in time step t [ton|h]"
119      G(t)    "Gas production rate of field in time step t [ton|h]"
120      f(t)    "Fraction of oil recovered [-]"
121      Q(t)    "Maximum deliverability of oil [ton|h]"
122      c0      "Investment cost"
123      CF(t)   "Cash flow"
124      C_k     "Cost of compressor"
125      C_p     "Cost of pump"
126      C_pmo   "Cost of pump motor"
127      C_MP    "Cost of multiphase pump"
128      C_c     "Cost of cooler"
129      C_tss  "Cost of topside separator"
130      C_s     "Cost of subsea seperator"
131      C_fg    "Cost for flowline gas"
132      C_rg    "Cost for riser gas"
133      C_fo    "Cost for flowline oil"
134      C_ro    "Cost for riser oil"
135      C_fm    "Cost for flowline multiphase"
136      C_rm    "Cost for riser multiphase"
137      P_k_m   "Max power consumption of compressor [ton|h]"
138      P_p_m   "Max power consumption of pump [ton|h]"
139      U_p     "Max flow capacity oil pump [ton|h]"
140      m_max_1 "Max flow capacity of subsea sep [ton|h]"
141      m_max_2 "Max flow capacity of topsides sep [ton|h]"
142      U_hx    "Max cooler capacity [ton|h]"
143      P_k(t)  "Power consumption of compressor"
144      P_p(t)  "Power consumption of pump"
145      P_MP(t) "Power consumption multiphase pump"

```

APPENDIX D. GAMS CODE

```
146      P_MP_m    "Max power consumption multiphase pump"
147      Area      "Heat exchange area"
148      p1(t)     "Reservoir pressure"
149      d_gas(t)  "Density of gas at reservoir pressure"
150      d_mix(t)  "Density of oil-gas mixture"
151      head(t)   "Pressure head MP pump";

153 Binary variables
154      y(j)      "Binvar for installment of subsea unit j";

156 Variables
157      NPV       "Net present value"
158      b(k,t)    "Right handside of mass balances in time t";

160 *Declaring equations
161 Equations
162      eq3_1     "Objective function"
163      eq3_3     "Investment costs"
164      eq3_4(t)  "Cash flow"
165      eq3_5(t)  "Oil profile"
166      eq3_6(t)  "Gas profile"
167      eq3_7(t)  "Maximum production rate"
168      eq3_8(t)  "Fraction of oil recovered"
169      eq3_9(t)  "Accumulated oil constraint"
170      eq3_10(t) "Pressure profile"
171      eq3_11(k,t) "Mass balances"
172      eq3_12a(t) "Right hand side for mass balances"
173      eq3_12b(t) "Right hand side for mass balances"
174      eq3_12c(k,t) "Right hand side for mass balances"
175      eq3_13a(t) "Set flow of unused unit to zero"
176      eq3_13b(t) "Set flow of unused unit to zero"
177      eq3_13c(t) "Set flow of unused unit to zero"
178      eq3_13d(t) "Set flow of unused unit to zero"
179      eq3_13e(t) "Set flow of unused unit to zero"
180      eq3_13f(t) "Set flow of unused unit to zero"
181      eq3_13g(t) "Set flow of unused unit to zero"
182      eq3_13h(t) "Set flow of unused unit to zero"
183      eq3_13i(t) "Set flow of unused unit to zero"
184      eq3_16a(t) "Logic equation for subsea system"
185      eq3_16b(t) "Logic equation for subsea system"
186      eq3_16c(t) "Logic equation for subsea system"
187      eq3_16d(t) "Logic equation for subsea system"
```

APPENDIX D. GAMS CODE

```

188      eq3_16e(t)      "Logic equation for subsea system"
189      eq3_16f(t)      "Logic equation for subsea system"
190      eq3_16g(t)      "Logic equation for subsea system"
191      eq3_16h(t)      "Logic equation for subsea system"
192      eq3_16i(t)      "Logic equation for subsea system"
193      eq3_17(t)       "Power consumption rate compressor"
194      eq3_18(t)       "Power consumption rate oil pump"
195      eq3_19(t)       "Power consumption rate MP pump"
196      eq3_20(t)       "Pressure head for MP pump"
197      eq3_21(t)       "Density for MP flow"
198      eq3_22(t)       "Density for natural gas"
199      eq3_23(t)       "Cost of compressor"
200      eq3_24(t)       "Capacity equation for compressor (power)"
201      eq3_25(t)       "Cost of oil pump"
202      eq3_26(t)       "Capacity equation for oil pump (flow)"
203      eq3_27(t)       "Cost of explosion proof motor"
204      eq3_28(t)       "Capacity equation for motor (power)"
205      eq3_29(t)       "Cost equation for MP pump"
206      eq3_30(t)       "Cost equation for cooler"
207      eq3_31a(t)      "Heat exchange area"
208      eq3_31b(t)      "Capacity equation for cooler"
209      eq3_32a(t)      "Cost equation for subsea separator"
210      eq3_32b(t)      "Cost equation for topside separator"
211      eq3_33a(t)      "Capacity equation for subsea separator"
212      eq3_33b(t)      "Capacity equation for topside separator"
213      eq3_34a(t)      "Cost equation for gas transport line"
214      eq3_34b(t)      "Cost equation for gas riser"
215      eq3_34c(t)      "Cost equation for MP transport line"
216      eq3_34d(t)      "Cost equation for MP riser"
217      eq3_34e(t)      "Cost equation for oil transport line"
218      eq3_34f(t)      "Cost equation for oil riser";

```

220 **Defining the equations*

222 **OBJECTIVE FUNCTION*

```

223 eq3_1..      NPV =e= -C0/(1+r) + sum(t,CF(t)/((1+r)**ord(t)));
224 eq3_3..      C0 =e= C_c + C_s + C_k + C_p + C_MP + C_fg
225              + C_rg + C_fm + C_rm + C_ts + C_fo + C_ro;
226 eq3_4(t)..   CF(t) =e= (1/1000000)*((O(t)*bbl_m3*p_bbl/d_oil +
227              G(t)*MMBTU_m3*p_g/d_gas_std)*alfa
228              - (P_k(t)+P_p(t)+P_MP(t))*alfa*p_e);

```


APPENDIX D. GAMS CODE

```

230 *MASS BALANCES AND PRESSURE DECLINE
231 eq3_5(t)..      O(t) =l= Q(t);
232 eq3_6(t)..      G(t) =e= gor*O(t);
233 eq3_7(t)..      Q(t) =e= k1*f(t-1)**3 + k2*f(t-1)**2 + k3*f(t-1) + k4;
234 eq3_8(t)..      f(t) =e= sum(tau$(ord(tau) le ord(t)),O(tau)*alfa)/O_REC;
235 eq3_9(t)..      sum(tau$(ord(tau) le ord(t)),O(tau)*alfa) =l= O_REC;
236 eq3_10(t)..     p1(t) =e= p_init-beta*f(t-1);
237 eq3_11(k,t)..   sum(i,A(k,i)*x(i,t)) =e= b(k,t);
238 eq3_12a(t)..   b('k1',t) =e= G(t);
239 eq3_12b(t)..   b('k7',t) =e= -O(t);
240 eq3_12c(k,t)$l(k)..b(k,t) =e= 0;
241 eq3_13a(t)..   x('i1',t) - U*y('j1') =l= 0;
242 eq3_13b(t)..   x('i2',t) - U*y('j2') =l= 0;
243 eq3_13c(t)..   x('i7',t) - U*y('j5') =l= 0;
244 eq3_13d(t)..   x('i10',t) - U*y('j5') =l= 0;
245 eq3_13e(t)..   x('i11',t) - U*y('j4') =l= 0;
246 eq3_13f(t)..   x('i5',t) - U*y('j6') =l= 0;
247 eq3_13g(t)..   x('i6',t) - U*y('j8') =l= 0;
248 eq3_13h(t)..   x('i15',t) - U*y('j11') =l= 0;
249 eq3_13i(t)..   x('i16',t) - U*y('j8') =l= 0;

252 *LOGICAL CONDITIONS
253 eq3_16a(t)..   y('j4') + y('j5') =e= 1;
254 eq3_16b(t)..   y('j3') + y('j5') =e= 1;
255 eq3_16c(t)..   y('j8') + y('j11') =e= 1;
256 eq3_16d(t)..   y('j8') + y('j6') =e= 1;
257 eq3_16e(t)..   y('j5') - y('j8') =l= 0;
258 eq3_16f(t)..   y('j8') - y('j9') =e= 0;;
259 eq3_16g(t)..   y('j8') - y('j10') =e= 0;
260 eq3_16h(t)..   y('j6') - y('j7') =e= 0;
261 eq3_16i(t)..   y('j11') - y('j12')=e= 0;

263 *COMPRESSOR AND PUMP DUTIES
264 eq3_17(t)..     P_k(t) =e= x('i3',t)*(Rc*Te/(Mm*3.6))*(gamma/(gamma-1))*
265                ((p2/p1(t))**((gamma-1)/gamma)-1)/eff_k;
266 eq3_18(t)..     P_p(t) =e= (p2-p1(t))*x('i11',t)/(d_oil*3600*eff_p);
267 eq3_19(t)..     P_MP(t) =e= x('i10',t)*9.81*head(t)/(3600*eff_MP);
268 eq3_20(t)..     head(t) =e= (p2-p1(t))/(0.0981*(d_mix(t)/d_water)*100+0.01);
269 eq3_21(t)..     d_mix(t) =e= (x('i7',t) + O(t))/(x('i7',t)/d_gas(t) +
270                O(t)/d_oil+0.01);
271 eq3_22(t)..     d_gas(t) =e= p1(t)*Mm/(Rc*Te*1000);

```

APPENDIX D. GAMS CODE

```

273  *SIZING AND CAPACITIES
274  eq3_24(t)..      P_k_m =g= P_k(t);
275  eq3_26(t)..      x('i11',t) =l= U_p;
276  eq3_28(t)..      P_p_m =g= P_p(t);
277  eq3_31a(t)..     Area =e= U_hx*dT*Cp_g/(3.6*U_h*LMTD);
278  eq3_31b(t)..     x('i1',t) =l= U_hx;
279  eq3_33a(t)..     m_max_1 =g= x('i2',t);
280  eq3_33b(t)..     m_max_2 =g= x('i17',t);

282  *COST ESTIMATIONS
283  eq3_23(t)..      C_k =e= (0.49*y('j3') + 0.0168*P_k_m**0.6)*
284                  f_inst*f_sub*f_I;
285  eq3_25(t)..      C_p =e= C_pmo + (0.0069*y('j4') +
286                  0.000206*(U_p/(d_oil*3.6))**0.9)*f_inst*f_sub*f_I;
287  eq3_27(t)..      C_pmo =e= (-0.00095*y('j4') + 0.00177*P_p_m**0.6)*
288                  f_inst*f_sub*f_I;
289  eq3_29(t)..      C_MP =e= 3*f_inst*f_I*y('j5');
290  eq3_30(t)..      C_c =e= (0.024000*y('j1')+0.000046*Area**1.2)*f_inst*f_sub;
291  eq3_32a(t)..     C_s =e= (a_sub*y('j2')+b_sub*m_max_1);
292  eq3_32b(t)..     C_ts =e= (b_top*m_max_2**n_top);
293  eq3_34a(t)..     C_fg =e= (c_b_rigid*f_s_fg + c_g_coat)*d*y('j6');
294  eq3_34b(t)..     C_rg =e= (c_b_flex*f_s_rg + c_g_coat)*w_d*y('j7');
295  eq3_34c(t)..     C_fm =e= (c_b_rigid*f_s_fm + c_MP_coat)*d*y('j8');
296  eq3_34d(t)..     C_rm =e= (c_b_flex*f_s_rm + c_MP_coat)*w_d*y('j9');
297  eq3_34e(t)..     C_fo =e= (c_b_rigid*f_s_fo + c_o_coat)*d*y('j11');
298  eq3_34f(t)..     C_ro =e= (c_b_flex*f_s_ro + c_o_coat)*w_d*y('j12');

301  *STARTING VALUES
302  p1.L(t) = 65000;          -> AVOID DIVISION BY ZERO.
303  d_gas.L(t) = 0.05;
304  O.L(t) = k4;

306  *Bounds DICOPT
307  C_k.up = 100;
308  C_MP.up = 100;

311  *Generating model
312  Model mod /all/;

```

```

314 *Options for simulation
315 Option optcr=0.00001;      ->Relative optimality gap.
316 Option reslim=28740;     ->Increased time limit.
317 option domlim = 500;

319 *Choosing subsolvers for milp and nlp problems
320 option mip = cplex;
321 option nlp = conopt;

323 *Choosing solver for MINLP
324 *option minlp = DICOPT;
325 option minlp = BARON;

327 *Solving the model
328 Solve mod using MINLP maximizing NPV;

330 *Displaying optimal set of binary variables
331 display y.l;

```

D.2 Multi-Field Model

```

1  $Title Multifield MINLP model.

3  $OnText
4  MINLP-model for optimizing the planning and development of multiple oil
5  reservoirs with the additional optimization of a subsea separation system for
6  each field.
7  $OffText

9  *Defining symbol for end of line comment.
10 $eolcom ->

12 *Declaring sets.
13 Sets
14     f "field" /f1*f3/
15     fpsy "floating production storage & offloading" /fpsy1*fpso3/
16     t "time steps in planning horizon" /t1*t5/
17     tf(t) "years following year 1"
18     i "index for mass flows for standard subsea system" /i1*i17/

```

APPENDIX D. GAMS CODE

```
19     j "index for subsea equipment in system" /j1*j12/
20     k "index for mass balances" /k1*k13/
21     l(k) "subset of mass balance indices with zero-elements on RHS"
22     /k2,k3,k4,k5,k6,k8,k9,k10,k11,k12,k13/;

24 *Defining sets
25     tf(t)= yes$(ord(t) gt 1);
26     alias (tau,t);           -> additional alias set for the time steps.

28 *Defining parameters for the model
29 Parameters

31 *Upper bound for mass flows
32     U "upper limit for mass flows" /5000/

34 *Reservoir parameters
35     p.res.init(f) "initial reservoir pressure in kPa"
36     /f1=9000,f2=6500,f3=7000/
37     O.REC(f) "total recoverable oil in ton"
38     /f1=20000000, f2=40000000, f3=50000000/
39     C.fpso(fpso) "fixed installment cost of fpso"
40     /fpso1=440, fpso2=490, fpso3=450/
41     C.drill(f) "fixed drilling cost of fields in mill USD"
42     /f1=50, f2=75, f3=90/
43     N.max(f) "Maximum wells for each field" /f1=4, f2=6, f3=3/
44     D.max "Maximum number of wells drilled per time step" /2/
45     w.d(fpso) "water depth in km" /fpso1=0.15, fpso2=0.5, fpso3=0.7/
46     -> Production decline curves for fields.
47     a.q(f) /f1=-100, f2=-80, f3=-400/
48     b.q(f) /f1=150, f2=120, f3=600/
49     c.q(f) /f1=-78.125, f2=-96.25, f3=-312.5/
50     d.q(f) /f1=28.125, f2=56.25, f3=112.5/
51     gor(f) /f1=0.045, f2=0.07, f3=0.06/
52     beta(f) "proportionality constant for pressure decline" /f1=6000, f2=3500,f3=4200/
53     Te "Reservoir temperature" /300/

55 *Economic factors
56     r "discount rate" /0.1/
57     p.bbl "price per barrel oil" /57.30/
58     p.g "price natural gas" /2.61/
59     alfa "operating hours per year" /8000/
60     p.e "price for electricity" /0.09/
```

APPENDIX D. GAMS CODE

```
61     f_inst "installation factor" /4.208/
62     f_sub "factor for installation subsea" /3/
63     f_I "scaling economics for inflation" /1.1035/
64     f_s_fm "economic size factor for multiphase flowline" /1.00/
65     f_s_rm "economic size factor for multiphase riser" /1.70/
66     f_s_fo "economic size factor for oil flowline" /0.72/
67     f_s_ro "economic size factor for oil riser" /1.1/
68     f_s_fg "economic size factor for gas flowline" /0.15/
69     f_s_rg "economic size factor for gas riser" /0.5/
70     c_b_rigid "base cost for rigid pipe lines" /0.230/
71     c_b_flex "base cost for flexible pipe lines" /2.300/
72     c_MP_coat "coating cost multiphase pipes" /0.360/
73     c_o_coat "coating cost oil pipes" /0.290/
74     c_g_coat "coating cost gas pipes" /0.150/
75     a_sub(f) "cost coeff for subsea sep" /f1=0.414, f2=0.419, f3=0.417/
76     b_sub(f) "cost coeff for top sep" /f1=0.054, f2=0.062, f3=0.060/
77     b_top(f) "cost coeff for subsea sep" /f1=0.143, f2=0.119, f3=0.127/
78     n_top(f) "cost coeff for top sep" /f1=0.406, f2=0.401, f3=0.403/

80 *compressor
81     p_boost(f) "pressure out kPa" /f1=11000, f2=12000, f3=14000/
82     gamma "Cp over Cv" /1.557488545/
83     d_gas "density" /0.05344791051/
84     eff_k "effectivity" /0.75/

86 *oil pump
87     d_oil "density of oil" /0.844/
88     eff_p "adiabatic efficiency pump" /0.75/

90 *Multiphase pump
91     eff_MP "multiphase pump efficiency" /0.75/

93 *Heat exchanger
94     LMTD "logarithmic mean temp difference" /19.6/
95     dT "temperature difference (out-in)" /2.5/
96     Cp_g "Heat capacity of gas" /2681/
97     U_h "heat transfer coefficient" /20/

100 *Other constants
101     Rc "gas constant J|molK" /8.314/
102     Mm "Molar mass natural gas" /16.8036/
```

APPENDIX D. GAMS CODE

```

103         bbl_m3 "barrels per standard cubic meter" /6.29/
104         MMBTU_m3 "MMBTU per standard cubic meter" /0.0354/;

106 Table A(k,i) "Mass balance matrix"
107         i1  i2  i3  i4  i5  i6  i7  i8  i9  i10 i11 i12 i13 i14 i15 i16 i17
108 k1         1   0   0   0   0   0   1   0   0   0   0   0   0   0   0   0   0
109 k2         1  -1   0   0   0   0   0   0   0   0   0   0   0   0   0   0   0
110 k3         0  0.05 0   0   0   0   0  -1   0   0   0   0   0   0   0   0   0
111 k4         0  -1   1   0   0   0   0   1   0   0   0   0   0   0   0   0   0
112 k5         0   0  -1   1   0   0   0   0   0   0   0   0   0   0   0   0   0
113 k6         0   0   0  -1   1   1   0   0   0   0   0   0   0   0   0   0   0
114 k7         0   0   0   0   0   0   1   1  -1   0   0   0   0   0   0   0   0
115 k8         0   0   0   0   0   0   0   0  -1   1   1   0   0   0   0   0   0
116 k9         0   0   0   0   0   0   0   0   0  -1   0   1   0   0   0   0   0
117 k10        0   0   0   0   0   0   0   0   0   0  -1   0   1   0   0   0   0
118 k11        0   0   0   0   0   0   0   0   0   0   0   1   1  -1   0   0   0
119 k12        0   0   0   0   0   0   0   0   0   0   0   0   0  -1   1   1   0
120 k13        0   0   0   0   0   1   0   0   0   0   0   0   0   0   0   1  -1;

122 Table d(f,fpso) "Distances"
123         fpso1  fpso2  fpso3
124 f1          63.79  20.03  25.00
125 f2          43.17  24.00  10.00
126 f3          15.62  30.26  31.62;

130 *Defining variables
131 Positive Variables
132 O_f(f,t) "Oil production rate from field f in time step t [ton|h]"
133 G_f(f,t) "Gas production rate from field f in time step t [ton|h]"
134 O_fpso(fpso,t) "Oil production rate in FPSO fpso in time step t [ton|h]"
135 G_fpso(fpso,t) "Gas production rate in FPSO fpso in time step t [ton|h]"
136 O(f,fpso,t) "Oil production rate from f to fpso in time step t [ton|h]"
137 G(f,fpso,t) "Gas production rate from f to fpso in time step t [ton|h]"
138 O_w(f,fpso,t) "Well production rate from f to fpso in t [ton|h]"
139 Q_w(f,fpso,t) "Maximum deliverability of oil [ton|h]"
140 f_c(f,t) "Recoverd oil [-]"
141 p_res(f,t) "Reservoir pressure in field f in time step t [kPa]"
142 rho_gas(f,t) "Density of natural gas in field f in time step t [ton|m3]"
143 rho_mix(f,t) "Density of MP flow in field f in time step t [ton|m3]"
144 head(f,t) "Pressure head for MP pump for field f in time step t [m]"

```

APPENDIX D. GAMS CODE

```
145     CF(t) "Cash flow in time step t [mill USD]"
146     REV(t) "Total revenue in time step t [mill USD]"
147     COST(t) "Total cost in time step t [mill USD]"
148     CAP(t) "Total CAPEX in time step t [mill USD]"
149     OPER(t) "Total OPEX in time step t [mill USD]"
150     c_eq(f,t,j) "Equipment cost of unit j in field f in t [mill USD]"
151     Area(f,t) "Installed heat transfer area for field f in time step t [m2]"
152     P_k_m(f,t) "Installed compressor capacity for field f in t [kW]"
153     P_p_m(f,t) "Installed oil pump capacity for field f in time step t [kW]"
154     C_pmo(f,t) "Cost for explosive proof electrical pump motor [mill USD]"
155     U_p(f,t) "Installed oil pump capacity for field f in t [ton|h]"
156     U_c(f,t) "Installed cooler capacity for field f in t [ton|h]"
157     U_sub(f,tau) "Installed cap for subsea sep in field f in t [ton|h]"
158     U_top(f,tau) "Installed cap for topside sep for field f in t [ton|h]"
159     x(f,t,i) "Mass flow i in field f in time step t [ton|h]"
160     P_k(f,t) "Power consumption rate of compressor in field f in t [kW]"
161     P_p(f,t) "Power consumption rate of oil pump in field f in t [kW]"
162     P_MP(f,t) "Power consumption rate of MP pump in field f in t [kW];
```

165 Integer Variables

```
166     N(f,t) "Number of producing wells for field f in time step t"
167     D_w(f,t) "Number of wells drilled in field f in time step t";
```

169 Binary Variables

```
170     z(fpso,t) "binvar for installing fpso in time step t"
171     z_c(f,fpso,t) "binvar for connecting f to fpso in time step t"
172     y(f,t,j) "binvar for installing subsea unit j in field f in time t";
```

174 Variables

```
175     NPV "Net present value of the project"
176     rhs(f,t,k) "Right handside of mass balances for field f in time t";
```

178 **declaring equations*

179 Equations

```
180     eq4_1 "Objective function"
181     eq4_2(t) "Cash flow"
182     eq4_3(t) "Revenue"
183     eq4_4(t) "Cost"
184     eq4_5(t) "Capex"
185     eq4_6(t) "Opex"
186     eq4_7a(fpso,t) "Oil production rate FPSO"
```

APPENDIX D. GAMS CODE

187	eq4_7b(fpso,t)	"Gas production rate FPSO"
188	eq4_8a(f,fpso,t)	"Oil production rate from f to fpso"
189	eq4_8b(f,fpso,t)	"Gas production rate from f to fpso"
190	eq4_9(f,fpso,t)	"Maximum deliverability constraint"
191	eq4_10a(f,fpso,t)	"Aprrx of max deliverability"
192	eq4_10b(f,fpso)	"Initial production rate"
193	eq4_11(f,t)	"Fraction oil recovered from f"
194	eq4_12(f,t)	"Oil production rate from f"
195	eq4_13(f,t)	"Gas production rate from f"
196	eq4_14(f,t)	"Accumulated oil constraint"
197	eq4_15(f,t)	"Reservoir pressure profiles"
198	eq4_16(f,t,k)	"Mass balances for subsea superstructures"
199	eq4_17a(f,t)	"RHS of mass balances"
200	eq4_17b(f,t)	"RHS of mass balances"
201	eq4_17c(f,t,k)	"RHS of mass balances"
202	eq4_18a(f,t)	"Set flow of unused unit to zero"
203	eq4_18b(f,t)	"Set flow of unused unit to zero"
204	eq4_18c(f,t)	"Set flow of unused unit to zero"
205	eq4_18d(f,t)	"Set flow of unused unit to zero"
206	eq4_18e(f,t)	"Set flow of unused unit to zero"
207	eq4_18f(f,t)	"Set flow of unused unit to zero"
208	eq4_18g(f,t)	"Set flow of unused unit to zero"
209	eq4_18h(f,t)	"Set flow of unused unit to zero"
210	eq4_18i(f,t)	"Set flow of unused unit to zero"
211	eq4_19(f,fpso,t)	"Well flow is zero if no connection is made"
212	eq4_20a(f)	"Logic equation for subsea system"
213	eq4_20b(f)	"Logic equation for subsea system"
214	eq4_20c(f)	"Logic equation for subsea system"
215	eq4_20d(f)	"Logic equation for subsea system"
216	eq4_21a(f,t)	"Logic equation for subsea system"
217	eq4_21b1(f,t)	"Logic equation for subsea system"
218	eq4_21b2(f,t)	"Logic equation for subsea system"
219	eq4_21c(f,t)	"Logic equation for subsea system"
220	eq4_21d(f,t)	"Logic equation for subsea system"
221	eq4_22(f,j)	"Logic equation for subsea system"
222	eq4_23a(fpso)	"Logic equation for fpsos and field connections"
223	eq4_23b(f)	"Logic equation for fpsos and field connections"
224	eq4_23c(f,fpso,t)	"Logic equation for fpsos and field connections"
225	eq4_24a1(f,t)	"Logic equation for drilling and wells"
226	eq4_24a2(f)	"Logic equation for drilling and wells"
227	eq4_24b(f,t)	"Logic equation for drilling and wells"
228	eq4_24c(t)	"Logic equation for drilling and wells"

APPENDIX D. GAMS CODE

```

229      eq4_24d(t)          "Logic equation for drilling and wells"
230      eq4_25a(f,t)      "Compressor power consumption rate"
231      eq4_25b(f,t)      "Oil pump power consumption rate"
232      eq4_25c(f,t)      "MP pump power consumption rate"
233      eq4_25d(f,t)      "Pressure head for MP pump"
234      eq4_25e(f,t)      "Density of MP flow"
235      eq4_25f(f,t)      "Density of natural gas"
236      eq4_26a(f,t)      "Cost of coolers"
237      eq4_26b(f,t)      "Cost of subsea separators"
238      eq4_26c(f,t)      "Cost of compressors"
239      eq4_26d(f,t)      "Cost of oil pumps"
240      eq4_26e(f,t)      "Cost of explosive proof motors"
241      eq4_26f(f,t)      "Cost of MP pumps"
242      eq4_26g(f,t)      "Cost of topside separator"
243      eq4_27a(f,t)      "Capacity equation for compressor (power)"
244      eq4_27b(f,t)      "Capacity equation for compressor (power)"
245      eq4_28a(f,t)      "Capacity equation for oil pump (power)"
246      eq4_28b(f,t)      "Capacity equation for oil pump (power)"
247      eq4_28c(f,t)      "Capacity equation for oil pump (flow)"
248      eq4_28d(f,t)      "Capacity equation for oil pump (flow)"
249      eq4_28e(f,t)      "Capacity equation for subsea separator"
250      eq4_28f(f,t)      "Capacity equation for subsea separator"
251      eq4_28g(f,t)      "Capacity equation for topside separator"
252      eq4_28h(f,t)      "Capacity equation for topside separator"
253      eq4_28i(f,t)      "Capacity equation for cooler"
254      eq4_28j(f,t)      "Capacity equation for cooler"
255      eq4_28k(f,t)      "Required heat transfer area"
256      eq4_29a1(f,t)     "Cost of oil transport line"
257      eq4_29a2(f,t)     "Cost of MP transport line"
258      eq4_29a3(f,t)     "Cost of gas transport line"
259      eq4_29b1(f,t)     "Cost of oil riser"
260      eq4_29b2(f,t)     "Cost of MP riser"
261      eq4_29b3(f,t)     "Cost of gas riser";

```

```

265  *defining equations

```

```

267  *OBJECTIVE FUNCTION

```

```

268  eq4_1..      NPV =e= sum(t, (CF(t))/((1+r)**ord(t)));
269  eq4_2(t)..   CF(t) =e= REV(t)-COST(t);
270  eq4_3(t)..   REV(t) =e= (1/1000000)*(sum(fpso, O_fpso(fpso,t))*

```

APPENDIX D. GAMS CODE

```

271          bbl_m3*p_bbl/d_oil + sum(fps0, G_fps0(fps0,t))
272          *MMBTU_m3*p_g/d_gas)*alfa;
273 eq4_4(t)..          COST(t) =e= CAP(t)+OPER(t);
274 eq4_5(t)..          CAP(t) =e= sum(fps0, C_fps0(fps0)*z(fps0,t)) +
275          sum(f,C_drill(f)*D_w(f,t)) + sum(f, sum(j,c_eq(f,t,j)));
276 eq4_6(t)..          OPER(t) =e= (1/1000000)*sum(f,(P_k(f,t)+P_p(f,t)
277          +P_MP(f,t))*alfa*p_e);

279 *MASS BALANCES AND PRESSURE DECLINE
280 eq4_7a(fps0,t)..          O_fps0(fps0,t) =e= sum(f,O(f,fps0,t));
281 eq4_7b(fps0,t)..          G_fps0(fps0,t) =e= sum(f,G(f,fps0,t));
282 eq4_8a(f,fps0,t)..          O(f,fps0,t) =e= N(f,t)*O_w(f,fps0,t);
283 eq4_8b(f,fps0,t)..          G(f,fps0,t) =e= gor(f)*O(f,fps0,t);
284 eq4_9(f,fps0,t)..          O_w(f,fps0,t) =l= Q_w(f,fps0,t);
285 eq4_10a(f,fps0,t)$tf(t).. Q_w(f,fps0,t) =e= a_q(f)*power((f_c(f,t-1)),3) +
286          b_q(f)*power((f_c(f,t-1)),2) + c_q(f)*(f_c(f,t-1)) +
287          d_q(f);
288 eq4_10b(f,fps0)..          Q_w(f,fps0,'t1') =e= d_q(f);
289 eq4_11(f,t)..          f_c(f,t) =e= sum(tau$(ord(tau) le ord(t)),
290          O_f(f,tau)*alfa)/O_REC(f);
291 eq4_12(f,t)..          O_f(f,t) =e= sum(fps0, O(f,fps0,t));
292 eq4_13(f,t)..          G_f(f,t) =e= sum(fps0, G(f,fps0,t));
293 eq4_14(f,t)..          sum(tau$(ord(tau) le ord(t)),O_f(f,tau)*alfa) =l=
294          O_REC(f);
295 eq4_15(f,t)..          p_res(f,t) =e= p_res_init(f) - beta(f)*f_c(f,t-1);
296 eq4_16(f,t,k)..          sum(i,A(k,i)*x(f,t,i)) =e= rhs(f,t,k);
297 eq4_17a(f,t)..          rhs(f,t,'k1') =e= G_f(f,t);
298 eq4_17b(f,t)..          rhs(f,t,'k7') =e= -O_f(f,t);
299 eq4_17c(f,t,k)$l(k)..          rhs(f,t,k) =e= 0;

302 *Setting flows to zero
303 eq4_18a(f,t)..          x(f,t,'i1') - U*sum(tau$(ord(tau) le ord(t)),
304          y(f,tau,'j1')) =l= 0;
305 eq4_18b(f,t)..          x(f,t,'i2') - U*sum(tau$(ord(tau) le ord(t)),
306          y(f,tau,'j2')) =l= 0;
307 eq4_18c(f,t)..          x(f,t,'i7') - U*sum(tau$(ord(tau) le ord(t)),
308          y(f,tau,'j5')) =l= 0;
309 eq4_18d(f,t)..          x(f,t,'i10') - U*sum(tau$(ord(tau) le ord(t)),
310          y(f,tau,'j5')) =l= 0;
311 eq4_18e(f,t)..          x(f,t,'i11') - U*sum(tau$(ord(tau) le ord(t)),
312          y(f,tau,'j4')) =l= 0;

```

APPENDIX D. GAMS CODE

```

313 eq4_18f(f,t)..      x(f,t,'i15') - U*sum(tau$(ord(tau) le ord(t)),
314                    y(f,tau,'j6')) =l= 0;
315 eq4_18g(f,t)..      x(f,t,'i6') - U*sum(tau$(ord(tau) le ord(t)),
316                    y(f,tau,'j8')) =l= 0;
317 eq4_18h(f,t)..      x(f,t,'i15') - U*sum(tau$(ord(tau) le ord(t)),
318                    y(f,tau,'j11')) =l= 0;
319 eq4_18i(f,t)..      x(f,t,'i16') - U*sum(tau$(ord(tau) le ord(t)),
320                    y(f,tau,'j8')) =l= 0;
321 eq4_19(f,fpso,t)..   O_w(f,fpso,t) - U*sum(tau$(ord(tau) le ord(t)),
322                    z_c(f,fpso,tau)) =l= 0;

324 *LOGICAL CONDITIONS
325 *Subsea equipment
326 eq4_20a(f)..          sum(t,y(f,t,'j3') + y(f,t,'j5')) =l= 1;
327 eq4_20b(f)..          sum(t,y(f,t,'j4') + y(f,t,'j5')) =l= 1;
328 eq4_20c(f)..          sum(t,y(f,t,'j6') + y(f,t,'j8')) =l= 1;
329 eq4_20d(f)..          sum(t,y(f,t,'j11') + y(f,t,'j8')) =l= 1;
330 eq4_21a(f,t)..        y(f,t,'j5') - y(f,t,'j8') =l= 0;
331 eq4_21b1(f,t)..       y(f,t,'j8') - y(f,t,'j9') =e= 0;
332 eq4_21b2(f,t)..       y(f,t,'j9') - y(f,t,'j10') =e= 0;
333 eq4_21c(f,t)..        y(f,t,'j6') - y(f,t,'j7') =e= 0;
334 eq4_21d(f,t)..        y(f,t,'j11') - y(f,t,'j12') =e= 0;
335 eq4_22(f,j)..         sum(t,y(f,t,j)) =L= 1;

337 *FPSOs and connections
338 eq4_23a(fpso)..        sum(t,z(fpso,t)) =l= 1;
339 eq4_23b(f)..          sum(t,sum(fpso,z_c(f,fpso,t))) =l= 1;
340 eq4_23c(f,fpso,t)..   z_c(f,fpso,t) =l= sum(tau$(ord(tau) le ord(t)), z(fpso,tau));
341 *Well drilling
342 eq4_24a1(f,t)$tf(t).. N(f,t) =e= N(f,t-1) + D_w(f,t);
343 eq4_24a2(f)..          N(f,'t1') =e= D_w(f,'t1');
344 eq4_24b(f,t)..        N(f,t) =l= N_max(f);
345 eq4_24c(t)..          sum(f,D_w(f,t)) =l= D_max;
346 eq4_24d(t)..          sum(f,N(f,t)) =l= 10;

350 *COMPRESSOR AND PUMP DUTIES
351 eq4_25a(f,t)..        P_k(f,t) =e= x(f,t,'i3')*(Rc*Te/(Mm*3.6))*(gamma/(gamma-1))*
352                    ((p_boost(f)/p_res(f,t))**(gamma-1)/gamma-1)/eff_k;
353 eq4_25b(f,t)..        P_p(f,t) =e= (p_boost(f)-p_res(f,t))*x(f,t,'i11')/
354                    (d_oil*3600*eff_p);

```

APPENDIX D. GAMS CODE

```

355 eq4_25c(f,t).. P_MP(f,t) =e= x(f,t,'i10')*9.81*head(f,t)/(3600*eff_MP);
356 eq4_25d(f,t).. head(f,t) =e= (p_boost(f)-p_res(f,t))/(0.0981*rho_mix(f,t)
357 *100+0.1);
358 eq4_25e(f,t).. rho_mix(f,t) =e= (1-sum(tau$(ord(tau) le ord(t)),
359 y(f,tau,'j5')))+(x(f,t,'i7') + O_f(f,t))/(x(f,t,'i7')/
360 rho_gas(f,t) + O_f(f,t)/d_oil + 0.01);
361 -> first is added to avoid div by zero in eq 4.25d.
362 eq4_25f(f,t).. rho_gas(f,t) =e= p_res(f,t)*Mm/(Rc*Te*1000);

366 *COST ESTIMATION SUBSEA UNITS
367 eq4_26a(f,t).. c_eq(f,t,'j1') =e= (0.024000*y(f,t,'j1') + 0.000046*
368 Area(f,t)**1.2)*f_inst*f_sub*f_I;
369 eq4_26b(f,t).. c_eq(f,t,'j2') =e= (a_sub(f)*y(f,t,'j2')+b_sub(f)*U_sub(f,t));
370 eq4_26c(f,t).. c_eq(f,t,'j3') =e= (0.49*y(f,t,'j3') + 0.0168*P_k_m(f,t)**0.6)
371 *f_inst*f_sub*f_I;
372 eq4_26d(f,t).. c_eq(f,t,'j4') =e= C_pmo(f,t) + (0.0069*y(f,t,'j4') +
373 0.000206*(U_p(f,t)/(d_oil*3.6))**0.9)*f_inst*f_sub*f_I;
374 eq4_26e(f,t).. C_pmo(f,t) =e= (-0.00095*y(f,t,'j4') + 0.00177*
375 P_p_m(f,t)**0.6)*f_inst*f_sub*f_I;
376 eq4_26f(f,t).. c_eq(f,t,'j5') =e= 3*f_inst*f_I*y(f,t,'j5');
377 eq4_26g(f,t).. c_eq(f,t,'j10') =e= b_top(f)*U_top(f,t)**n_top(f);

379 *SIZING AND CAPACITIES
380 eq4_27a(f,t).. sum(tau$(ord(tau) le ord(t)), P_k_m(f,tau)) =g= P_k(f,t);
381 eq4_27b(f,t).. P_k_m(f,t) - 15000*y(f,t,'j3') =L= 0;
382 eq4_28a(f,t).. sum(tau$(ord(tau) le ord(t)), P_p_m(f,tau)) =g= P_p(f,t);
383 eq4_28b(f,t).. P_p_m(f,t) - 15000*y(f,t,'j4') =L= 0;
384 eq4_28c(f,t).. x(f,t,'i11') - sum(tau,U_p(f,tau)) =L= 0;
385 eq4_28d(f,t).. U_p(f,t) - U*y(f,t,'j4') =L= 0;
386 eq4_28e(f,t).. sum(tau,U_sub(f,tau)) =g= x(f,t,'i2');
387 eq4_28f(f,t).. U_sub(f,t) - U*y(f,t,'j2') =L= 0;
388 eq4_28g(f,t).. sum(tau,U_top(f,tau)) =g= x(f,t,'i17');
389 eq4_28h(f,t).. U_top(f,t) - U*y(f,t,'j10') =L= 0;
390 eq4_28i(f,t).. x(f,t,'i1') - sum(tau,U_c(f,tau)) =L= 0;
391 eq4_28j(f,t).. U_c(f,t) - U*y(f,t,'j1') =L= 0;
392 eq4_28k(f,t).. Area(f,t) =e= U_c(f,t)*dT*Cp_g/(3.6*U_h*LMTD);

```

```

396 *COST ESTIMATION FLOWLINES AND RISERS

```

APPENDIX D. GAMS CODE

```

397 eq4_29a1(f,t).. c.eq(f,t,'j6') =e= sum(fpso,(c.b_rigid*f.s_fg +c.g_coat)
398                *d(f,fpso)* y(f,t,'j6')*sum(tau,z_c(f,fpso,tau)));
399 eq4_29a2(f,t).. c.eq(f,t,'j8') =e= sum(fpso,(c.b_rigid*f.s_fm + c.MP_coat)
400                *d(f,fpso)* y(f,t,'j8')*sum(tau,z_c(f,fpso,tau)));
401 eq4_29a3(f,t).. c.eq(f,t,'j11') =e= sum(fpso,(c.b_rigid*f.s_fo + c.o_coat)
402                *d(f,fpso)* y(f,t,'j11')*sum(tau,z_c(f,fpso,tau)));
403 eq4_29b1(f,t).. c.eq(f,t,'j7') =e= sum(fpso,(c.b_flex*f.s_rg + c.g_coat)
404                *w_d(fpso)* y(f,t,'j7')*sum(tau,z_c(f,fpso,tau)));
405 eq4_29b2(f,t).. c.eq(f,t,'j9') =e= sum(fpso,(c.b_flex*f.s_rm + c.MP_coat)
406                *w_d(fpso)* y(f,t,'j9')*sum(tau,z_c(f,fpso,tau)));
407 eq4_29b3(f,t).. c.eq(f,t,'j12') =e= sum(fpso,(c.b_flex*f.s_ro + c.o_coat)
408                *w_d(fpso)*y(f,t,'j12')*sum(tau,z_c(f,fpso,tau)));

```

```

414 *INITIAL GUESSES TO AVOID DIVISION BY ZERO

```

```

415 p_res.L(f,t) = p_res.init(f);
416 rho_gas.L(f,t) = 0.05;
417 rho_mix.L(f,t) = 1000;

```

```

420 *Bounds DICOPT

```

```

421 c_eq.up(f,t,'j3') = 100;

```

```

423 *Upper variable bounds

```

```

424 $OnText

```

```

425 Area.up(f,t) = 500;
426 P_k_m.up(f,t) = 5000;
427 P_p_m.up(f,t) = 5000;
428 C_pmo.up(f,t) = 10;
429 U_p.up(f,t) = 500;
430 U_c.up(f,t) = 500;
431 x.up(f,t,i) = 5000;
432 P_k.up(f,t) = 5000;
433 P_p.up(f,t) = 5000;
434 P_MP.up(f,t) = 5000;
435 G_f.up(f,t) = 500;
436 OPER.up(t) = 10;
437 p_res.up(f,t) = 15000;
438 rho_gas.up(f,t) = 500;

```

APPENDIX D. GAMS CODE

```
439 rho_mix.up(f,t) = 1000;
440 head.up(f,t) = 9000;
441 U_sub.up(f,tau) = 1000;
442 U_top.up(f,tau) = 1000;
443 O_fpso.up(fpso,t) = 5000;
444 G_fpso.up(fpso,t) = 5000;
445 O.up(f,fpso,t) = 1000;
446 O_w.up(f,fpso,t) = 1000;
447 Q_w.up(f,fpso,t) = 1000;
448 O_f.up(f,t) = 1000;
449 c_eq.up(f,t,j) = 500;
450 N.up(f,t) = 15;
451 D_w.up(f,t) = 15;
452 $OffText

455 *Generating model
456 model mod /all/;

458 *Options for simulation
459 Option optcr=0.00001;           ->Relative optimality gap.
460 Option reslim=28740;          ->Max computational time.

463 *Choosing subsolvers for milp and nlp problems
464 option mip = cplex;
465 option nlp = conopt;

467 *Choosing solver for MINLP
468 *option minlp = DICOPT;
469 option minlp = BARON;

471 *Solving the model
472 solve mod us minlp max NPV;
```
